

# COUPLING A FINITE ELEMENT STORM SURGE MODEL OF THE NORTH CAROLINA SOUNDS WITH OPERATIONAL OCEAN AND WEATHER PREDICTION MODELS

Silver Spring, Maryland  
October 2010



**noaa** National Oceanic and Atmospheric Administration

---

U.S. DEPARTMENT OF COMMERCE  
National Ocean Service  
Coast Survey Development Laboratory

**Office of Coast Survey  
National Ocean Service  
National Oceanic and Atmospheric Administration  
U.S. Department of Commerce**

**The Office of Coast Survey (OCS) is the Nation's only official chartmaker. As the oldest United States scientific organization, dating from 1807, this office has a long history. Today it promotes safe navigation by managing the National Oceanic and Atmospheric Administration's (NOAA) nautical chart and oceanographic data collection and information programs.**

**There are four components of OCS:**

**The Coast Survey Development Laboratory develops new and efficient techniques to accomplish Coast Survey missions and to produce new and improved products and services for the maritime community and other coastal users.**

**The Marine Chart Division acquires marine navigational data to construct and maintain nautical charts, Coast Pilots, and related marine products for the United States.**

**The Hydrographic Surveys Division directs programs for ship and shore-based hydrographic survey units and conducts general hydrographic survey operations.**

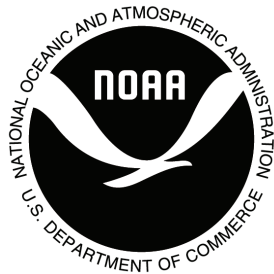
**The Navigational Services Division is the focal point for Coast Survey customer service activities, concentrating predominately on charting issues, fast-response hydrographic surveys, and Coast Pilot updates.**

# COUPLING A FINITE ELEMENT STORM SURGE MODEL OF THE NORTH CAROLINA SOUNDS WITH OPERATIONAL OCEAN AND WEATHER PREDICTION MODELS

Yuji Funakoshi, Jesse C. Feyen, and Frank Aikman III  
Office of Coast Survey, Coast Survey Development Laboratory,  
Silver Spring, MD

Carlos Lozano and Hendrik Tolman  
National Centers for Environmental Prediction,  
Environmental Modeling Center, Camp Springs, MD

October 2010



**noaa** National Oceanic and Atmospheric Administration

---

U. S. DEPARTMENT  
OF COMMERCE  
Gary Locke, Secretary

National Oceanic and  
Atmospheric Administration  
Jane Lubchenco, Ph.D.  
Under Secretary

National Ocean Service  
John H. Dunnigan  
Assistant Administrator

Office of Coast Survey  
Captain Steven R. Barnum, NOAA

Coast Survey Development Laboratory  
Mary Erickson

## **NOTICE**

**Mention of a commercial company or product does not constitute an endorsement by NOAA. Use for publicity or advertising purposes of information from this publication concerning proprietary products or the tests of such products is not authorized.**

## TABLE OF CONTENTS

LIST OF FIGURES .....	v
LIST OF TABLES .....	ix
LIST OF ACRONYMS AND ABBREVIATIONS .....	x
EXECUTIVE SUMMARY .....	xi
1. INTRODUCTION .....	1
2. DATA SOURCES .....	3
2.1. Bathymetry Data .....	3
2.2. Topographic Data .....	4
2.3. Digital Elevation Model .....	4
2.4. Meteorological Data .....	5
2.5. Water Surface Elevation Data .....	6
2.6. High Water Marks .....	7
3. COASTAL FLOODING AND HYDRODYNAMIC MODELING .....	9
3.1. The ADCIRC Model .....	9
3.2. Model Grid Development .....	10
3.3. Bathymetric and Topographic data for the Regional CFM .....	11
3.4. Tidal Forcing of the Regional and Basin-Scale CFM .....	12
4. HURRICANE ISABEL AND METEOROLOGICAL MODELS .....	15
4.1. Hurricane Isabel .....	15
4.2. Meteorological Models .....	17
4.3. Adjustment of Wind Average Time Period and Height .....	18
4.4. Adjustment of Wind Forcing Interval .....	20
4.5. Blending Meteorological Models .....	20
5. LATERAL BOUNDARY CONDITION .....	23
5.1. The Lateral Boundary Condition from Basin-Scale CFM .....	23
5.2. Real-Time Ocean Forecast System .....	23
5.3. The Lateral Boundary Condition from RTOFS .....	25
6. RESULTS AND DISCUSSION .....	23
6.1. Validation of Hurricane Isabel Wind Fields .....	27
6.2. Validation of Water Surface Elevation .....	38
6.3. Validation of High Water Marks .....	41
6.4. Validation of Blended Meteorological Models .....	44
6.5. Validation of Lateral Boundary Conditions .....	53
6.6. Skill Assessment .....	60
6.7. Water Surface Elevation Skill Assessment .....	60
7. SUMMARY AND CONCLUSIONS .....	67
ACKNOWLEDGMENTS .....	69
REFERENCES .....	69
APPENDIX A. FEMA Coastal High Water Marks .....	73

APPENDIX B. HYDRODYNAMIC MODEL PARAMETERS .....	77
B.1. Wind Stress .....	77
B.2. Atmospheric Pressure Gradient.....	77
B.3. ADCIRC Input File (fort.15).....	77

## LIST OF FIGURES

Figure 1.	North Carolina Albemarle-Pamlico sound system. ....	2
Figure 2.	Construction of the continuous bathy/topo DEM application. ....	5
Figure 3.	Locations of NDBC stations (red triangles) in the study area. ....	6
Figure 4.	Locations of NOS stations (red squares) in the study area. Only the last four digits of the station numbers are shown; the first three digits are 865 for all stations (see Table 2). ....	7
Figure 5.	Locations of FEMA CHWMs (red circles) in the study area. ....	8
Figure 6.	The regional CFM in the North Carolina region; the MHW shoreline is shown in green and the sample point of the lateral boundary condition as a red circle in Section 5.3. ....	10
Figure 7.	The regional CFM of Pamlico Sound and surrounding areas; the MHW shoreline is shown in green. ....	11
Figure 8.	The basin-scale CFM grid. ....	12
Figure 9.	National Hurricane Center best track positions for Hurricane Isabel, 6 – 19 September 2003 (Beven and Cobb 2004). ....	15
Figure 10.	Wind speed (m/s) from meteorological models on September 18 2003 before Hurricane Isabel made land fall on the North Carolina’s Outer Banks from H*Wind (a), GFDL (b), and GFS (c). Red box in the GFDL panel shows the boundary of its nested grid. ....	19
Figure 11.	RTOFS orthogonal grid with approximate grid spacing contours (a) and bathymetry (b). ....	24
Figure 12.	The lateral boundary condition at the sample location along outer boundary of the regional CFM (see Figure 6); 1) Tide (black), 2) the basin-scale CFM (red), 3) RTOFS (blue), and 4) detrended RTOFS (green). ....	25
Figure 13.	The comparison of wind speed (a) and direction (b) provided by H*Wind (red triangle), GFDL (blue asterisk), and GFS (green cross) with observation of NDBC continuous wind data (black dot) at NDBC location 41001. ....	29
Figure 14.	The comparison of wind speed (a) and direction (b) provided by H*Wind (red triangle), GFDL (blue asterisk), and GFS (green cross) with observation of NDBC continuous wind data (black dot) at NDBC location 41002. ....	30

Figure 15. The comparison of wind speed (a) and direction (b) provided by H*Wind (red triangle), GFDL (blue asterisk), and GFS (green cross) with observation of NDBC continuous wind data (black dot) at NDBC location 44014. ....	31
Figure 16. The comparison of wind speed (a) and direction (b) provided by H*Wind (red triangle), GFDL (blue asterisk), and GFS (green cross) with observation of NDBC continuous wind data (black dot) at NDBC location DUCN7. ....	32
Figure 17. The comparison of wind speed (a) and direction (b) provided by H*Wind (red triangle), GFDL (blue asterisk), and GFS (green cross) with observation of NDBC continuous wind data (black dot) at NDBC location CLKN7. ....	33
Figure 18. Track of Isabel (solid black line) and wind speeds at 10 m height in $\text{ms}^{-1}$ for Isabel: H*Wind (a), GFDL (b), and GFS (c) at 1200 UTC September 17, and H*Wind (d), GFDL (e), and GFS (f) at 1800 UTC September 17. ....	34
Figure 19. Track of Isabel (solid black line) and wind speeds at 10 m height in $\text{ms}^{-1}$ for Isabel: H*Wind (a), GFDL (b), and GFS (c) at 0000 UTC September 18, and H*Wind (d), GFDL (e), and GFS (f) at 0600 UTC September 18. ....	35
Figure 20. Track of Isabel (solid black line) and wind speeds at 10 m height in $\text{ms}^{-1}$ for Isabel: H*Wind (a), GFDL (b), and GFS (c) at 1200 UTC September 18, and H*Wind (d), GFDL (e), and GFS (f) at 1500 UTC September 18. ....	36
Figure 21. Track of Isabel (solid black line) and wind speeds at 10 m height in $\text{ms}^{-1}$ for Isabel: H*Wind (a), GFDL (b), and GFS (c) at 1800 UTC September 18, and H*Wind (d), GFDL (e), and GFS (f) at 2100 UTC September 18. ....	37
Figure 22. The comparison of water surface elevations provided by H*Wind (red), GFDL (blue), and GFS (green) with observations (black) at Duck FRF Pier (a) and Oregon Inlet Marine Pamlico Sound (b). ....	39
Figure 23. The comparison of water surface elevations provided by H*Wind (red), GFDL (blue), and GFS (green) with observations (black) at Cape Hatteras Fishing Pier (a) and Beaufort Duke Marine Lab (b). ....	40
Figure 24. The distribution of maximum storm surge (m NAVD 88) in the basin-scale CFM from each meteorological model (from left to right H*Wind, GFDL, and GFS); circles denote FEMA CHWMs; (a) – (c) illustrates the entire North Carolina sound system, and (d) – (f) show the enlargement of west side of Pamlico Sound including the Neuse and Pamlico Rivers. ....	41
Figure 25. The HWMs from H*Wind (a) and GFDL (b) forcing minus observed FEMA HWMs for Hurricane Isabel (excluding marks that were not flooded in each simulation). ....	43
Figure 26. The HWMs from GFS forcing minus observed FEMA HWMs for Hurricane Isabel (excluding marks that were not flooded in the simulation). ....	44

Figure 27. The comparison of wind speed (a) and direction (b) provided by the blended models (red asterisk) with observations of NDBC continuous wind data (black dot) at NDBC location 41001. ....	45
Figure 28. The comparison of wind speed (a) and direction (b) provided by the blended models (red asterisk) with observations of NDBC continuous wind data (black dot) at NDBC location 41002. ....	46
Figure 29. The comparison of wind speed (a) and direction (b) provided by the blended models (red asterisk) with observations of NDBC continuous wind data (black dot) at NDBC location 44014. ....	47
Figure 30. The comparison of wind speed (a) and direction (b) provided by the blended models (red asterisk) with observations of NDBC continuous wind data (black dot) at NDBC location DUCN7. ....	48
Figure 31. The comparison of wind speed (a) and direction (b) provided by the blended models (red asterisk) with observations of NDBC continuous wind data (black dot) at NDBC location CLKN7. ....	49
Figure 32. The comparison of water surface elevations provided by the blended meteorological forcing (red) against observations (black) at Duck FRF Pier (a) and Oregon Inlet Marine Pamlico Sound (b). ....	50
Figure 33. The comparison of water surface elevations provided by the blended meteorological forcing (red) against observations (black) at Cape Hatteras Fishing Pier (a) and Beaufort Duke Marine Lab (b). ....	51
Figure 34. The distribution of maximum storm surge (m NAVD88) in the North Carolina sound system from the blended meteorological forcing; circles denote FEMA CHWMs. ....	52
Figure 35. The HWMs from the blended meteorological forcing minus observed FEMA HWMs for Hurricane Isabel (excluding marks that were not flooded in the simulation). ....	52
Figure 36. The comparison of water surface elevations forced by tide (red), basin-scale CFM (blue), and RTOFS (green) lateral boundary conditions with observations (black) at Duck FRF Pier (a) and Oregon Inlet Marine Pamlico Sound (b). ....	54
Figure 37. The comparison of water surface elevations forced by tide (red), basin-scale CFM (blue), and RTOFS (green) lateral boundary conditions with observations (black) at Cape Hatteras Fishing Pier (a) and Beaufort Duke Marine Lab (b). ....	55
Figure 38. The comparison of water surface elevations forced by basin-scale CFM (red), RTOFS (blue), and detrended RTOFS (green) lateral boundary conditions with	

observations (black) at Duck FRF Pier (a) and Oregon Inlet Marine Pamlico Sound (b).....	56
Figure 39. The comparison of water surface elevations forced by basin-scale CFM (red), RTOFS (blue), and detrended RTOFS (green) lateral boundary conditions with observations (black) at Cape Hatteras Fishing Pier (a) and Beaufort Duke Marine Lab (b).....	57
Figure 40. The comparison of subtidal water surface elevation forced by basin-scale CFM (red), RTOFS (blue), and detrended RTOFS (green) lateral boundary conditions with observations (black) at Duck FRF Pier (a) and Oregon Inlet Marine Pamlico Sound (b).....	58
Figure 41. The comparison of subtidal water surface elevation forced by basin-scale CFM (red), RTOFS (blue), and detrended RTOFS (green) lateral boundary conditions with observations (black) at Cape Hatteras Fishing Pier (a) and Beaufort Duke Marine Lab (b).....	59

## LIST OF TABLES

Table 1. NDBC stations in the study area.....	5
Table 2. NOS stations in the study area.....	6
Table 3. Sample of the tidal constituents and harmonic constants used for the regional CFM.....	13
Table 4. The best track positions and intensities (Beven and Cobb 2004).....	16
Table 5. Wind fields for Hurricane Isabel interpolation onto the basin-scale CFM.....	27
Table 6. Skill assessment statistics (from Hess et al., 2003). .....	60
Table 7. Skill assessment statistics of different meteorological forcings in the basin-scale CFM. ....	62
Table 8. The comparison of peak storm surge heights and times of occurrence in both observations and simulations in the basin-scale CFM.....	63
Table 9. Skill assessment statistics of different lateral boundary condition forcings in the regional CFM.....	64
Table 10. The comparison of peak storm surge heights and times of occurrence in both observations and simulations in the regional CFM.....	65

## LIST OF ACRONYMS AND ABBREVIATIONS

ADCIRC	ADvanced CIRCulation model
AOML	Atlantic Oceanographic and Meteorological Laboratory
CFM	Coastal Flooding Model
CHWM	Coastal High Water Mark
C-MAN	Coastal-Marine Automated Network
CO-OPS	Center for Operational Oceanographic Products and Services
CSDL	Costal Survey Development Laboratory
DEM	Digital Elevation Model
EC95	East Coast 1995 modeled tidal database
EC2001	East Coast 2001 modeled tidal database
EMC	Environmental Modeling Center
FEMA	Federal Emergency Management Agency
GEODAS	GEophysical DATA System
GFDL	Geophysical Fluid Dynamics Laboratory Hurricane Model
GFS	Global Forecast System
GPS	Global Positioning System
HWM	High Water Mark
HRD	Hurricane Research Division
HWRF	Hurricane Weather and Research Forecasting model
H*Wind	Hurricane Wind analysis system
HYCOM	HYbrid Coordinate Ocean Model
LIDAR	LIght Detection And Ranging
LWD	Low Water Datum
MLW	Mean Low Water
MLLW	Mean Lower Low Water
MSL	Mean Sea Level
NCCOS	National Centers for Coastal Ocean Science
NCEP	National Centers for Environmental Prediction
NDBC	National Data Buoy Center
NED	National Elevation Dataset
NGDC	National Geophysical Data Center
NOS	National Ocean Service
NOAA	National Oceanic and Atmospheric Administration
NWS	National Weather Service
NAD 83	North American Datum of 1983
NAVD 88	North American Vertical Datum of 1988
POM	Princeton Ocean Model
RTOFS	Real-Time Ocean Forecast System
RHWM	Riverine High Water Mark
SSH	Sea Surface Height
TPC	Tropical Prediction Center
USACE	United States Army Corps of Engineers
USGS	United States Geological Survey
UTC	Coordinated Universal Time
WSE	Water Surface Elevation

## **EXECUTIVE SUMMARY**

The National Ocean Service (NOS) of the National Oceanic and Atmospheric Administration (NOAA) is studying the impacts of storm surge on the coastal region in the sounds and estuaries of North Carolina. NOS' Coast Survey Development Laboratory and the National Centers for Environmental Prediction (NCEP) of the NOAA's National Weather Service are cooperating to develop advanced storm surge modeling capability that will be useful to emergency managers.

The approach is to simulate storm surge for the coastal region using a high resolution Coastal Flooding Model (CFM) of the North Carolina sound system. In addition, the approach also examines the impact of boundary and meteorological forcing from a suite of NCEP models. Boundary conditions are provided to the CFM in the North Carolina region both by a basin-scale ADvanced CIRCulation (ADCIRC) model and by the NCEP Real-Time Ocean Forecast System (which is based on a HYbrid Coordinate Model basin-scale ocean circulation model). The meteorological forcing fields (e.g. the hurricane wind and pressure fields) being tested include the Hurricane Wind analysis system (H\*Wind), the Geophysical Fluid Dynamics Laboratory Hurricane Model, and the Global Forecast System. Our test period focuses on Hurricane Isabel (2003).

The coupled system may provide products with which coastal inundation can be predicted via the inclusion of the high resolution ADCIRC coastal model. Furthermore, the outcomes of the coupled system will guide the direction of more accurate prediction, and new decision support tools. Using the expertise in several parts of NOS and NOAA as well as having partners in other federal and state agencies, will ensure that a variety of needs are addressed and that the outcomes are based on an integrated approach that makes the best use of data, modeling approaches, displaying results, and outreach.

**Key Words:** hydrodynamic model, storm surge, coastal flooding model, Hurricane Isabel.



## 1. INTRODUCTION

The National Ocean Service (NOS) of the National Oceanic and Atmospheric Administration (NOAA) is studying the impacts of storm surge on the coastal region in the sounds and estuaries of North Carolina (see Figure 1). NOS' Coastal Survey Development Laboratory (CSDL) and the National Weather Service's (NWS) National Centers for Environmental Prediction (NCEP) are cooperating to develop advanced hurricane storm surge modeling capability as part of a coupled atmosphere-ocean modeling system.

The approach is to simulate storm surge for the coastal region using a high resolution Coastal Flooding Model (CFM) of the North Carolina sound system. The finite element ADvanced CIRCulation (ADCIRC) model is the basis for the CFM, applying an unstructured grid to compute the water surface elevation and barotropic depth-averaged currents. The CFM is used to examine the impact of boundary and meteorological forcing by coupling to a suite of NCEP models. Hurricane storm surge height and coastal inundation distribution are strongly influenced by the geometry of the shelf and coast (especially for features which act as hydrodynamic controls) and by meteorological conditions. Hydrodynamic numerical models must represent the basin geometry in order to predict accurately the storm surge and the skill of these models is governed by the quality of their forcing at the surface and at open ocean boundaries. Therefore, NCEP is partnering with CSDL to investigate predictions of storm surge height by combining a coupled atmosphere-ocean modeling system with the high resolution CFM.

As a preliminary step in simulating storm surge, CSDL has developed a predictive hydrodynamic CFM of North Carolina's coastal areas that integrates bathymetry and topography using the VDatum vertical datum transformation tool (Spargo et al., 2005, 2006) in a combined modeling process. Using a digital elevation model (DEM) as well as the United States Geological Survey (USGS) National Elevation Dataset (NED), CSDL has integrated land areas with a hydrodynamic tidal model developed for VDatum to produce the CFM. This model is able to simulate not only the tidal response but also wind-driven (including hurricane) circulation within the system, including the resulting inundation. The purpose of the CFM is to study how storm surge will affect the coastal region, and the CFM is advantageous because it treats the landward and seaward areas as a single, continuous environment.

Boundary conditions are provided to the CFM in the North Carolina region by two large-scale basin models: (1) a basin-scale version of the ADCIRC model, and (2) the NCEP Real-Time Ocean Forecast System (RTOFS), which is based on a Hybrid Coordinate Model (HYCOM) basin-scale ocean circulation model. The meteorological forcing fields (e.g. the hurricane wind and pressure fields) being tested include the Hurricane Wind analysis system (H\*Wind), the Geophysical Fluid Dynamics Laboratory (GFDL) Hurricane Model, and the Global Forecast System (GFS) model. Our test period focuses on Hurricane Isabel (2003). Hurricane Isabel was the most powerful hurricane of the 2003 season and the first hurricane to make landfall on the east coast of the United States since 1999. After coming ashore on the Outer Banks of North Carolina on 18 September as a Category 2 hurricane, Isabel took a northward track into Virginia, causing high winds, storm surge flooding, and extensive property damage around Chesapeake Bay.

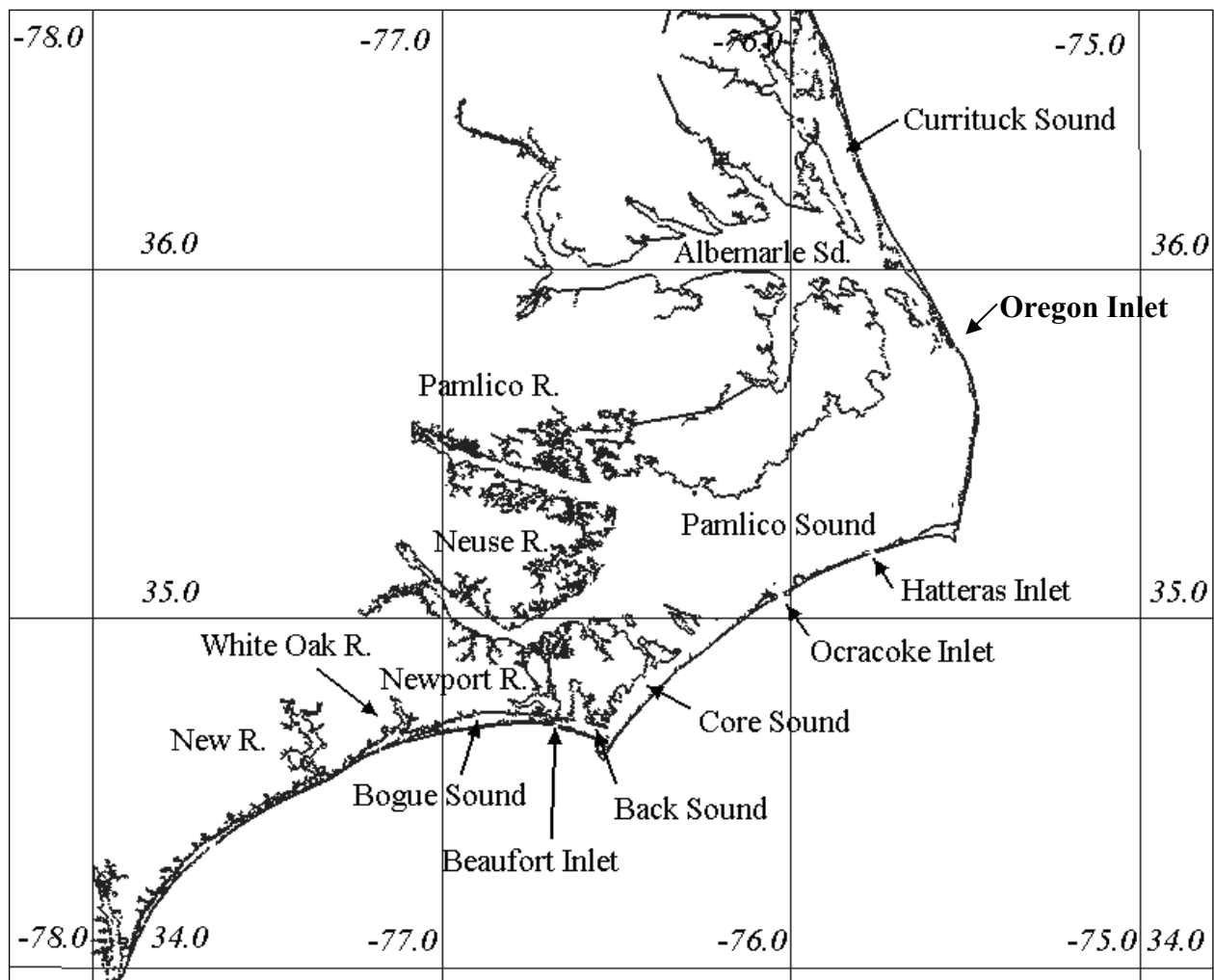


**Figure 1. North Carolina Albemarle-Pamlico sound system.**

The following sections describe the technical approach in executing the major components of the study:

- Creation of the DEM and development of the CFM
- Meteorological models and wind forcing adjustment
- NCEP RTOFS and lateral boundary conditions
- Results and discussion

## **2. DATA SOURCES**

In order to conduct this coastal inundation study several different types of data sources are required to build and validate the model. The CFM for the Pamlico Sound region of North Carolina was developed as part of a project to study the ecological effects of sea level rise (Feyen et al., 2006). This project was funded by NOS' National Center for Coastal Ocean Science (NCCOS), and resulted in construction of a bathymetric/topographic DEM, a tidal model, and a regional VDatum application. These products provide the basis for the CFM, and require several types of source data, which are described here. Bathymetric data comes from NOS hydrographic soundings and United States Army Corps of Engineers (USACE) surveys of dredged areas, which are primarily tidal inlets. Two different data sources, Federal Emergency Management Agency (FEMA) Light Detection And Ranging (LIDAR) data and the USGS NED, are used for topographic data. The DEM built by NOS' National Geodetic Survey/Remote Sensing Division (White and Sellars, 2004) combines the bathymetric data with the topographic data using VDatum to create a continuous bathy/topo dataset adjusted to a common vertical datum (i.e., the North American Vertical Datum of 1988 (NAVD 88)). The process of model validation, including Hurricane Isabel forcing, depends on the comparison with observations: meteorological data observed by the National Data Buoy Center (NDBC), observed water surface elevation from the Center for Operational Oceanographic Products and Services (CO-OPS) gauge stations, and High Water Marks (HWMs) measured by FEMA.

### **2.1. Bathymetry Data**

Water depths from historic NOS bathymetric surveys of the North Carolina coast are selected from the GEophysical DATA System (GEODAS) created by NOAA's National Geophysical Data Center (NGDC); information on this dataset is available at <http://www.ngdc.noaa.gov/mgg/geodas/geodas.html/>. About 90% of the study area is covered by NOS sounding data. Bathymetric data sets were processed during development of the tidal model in support of VDatum (Hess et al., 2005) This processing involved transformation of all surveys to common horizontal and vertical datums: the North American Datum of 1983 (NAD 83) for horizontal referencing, and NAVD 88 for vertical referencing. The surveys were also sorted chronologically so that the most recent data was used across the domain. According to NGDC, the horizontal accuracy of NOS soundings is generally 30 m, although accuracy has improved with recent surveys that employ a differential Global Positioning System (GPS). Vertical accuracy of the NOS soundings conforms to the international hydrographic standard: 0.30 m in 0 to 20 m of water, 1.0 m in 20 to 100 m of water, and 1% of the water depth in waters of 100 m depth or deeper.

The USACE has the responsibility to maintain navigational channels to design depths through its dredging program. Therefore these regions are subject to concentrated, repeated, highly refined hydrographic surveys to ensure bathymetric depths are sufficient. A suite of these surveys for the CFM region was obtained and applied to supersede NOS surveys because of their generally recent collection and high resolution. These surveys were also transformed to the common datum references (i.e., NAD 83 and NAVD 88).

## **2.2. Topographic Data**

Topographic data for floodplains were obtained from FEMA sponsored LIDAR collection to support the flood insurance mapping program, and USGS's NED. These two datasets were combined in creation of the high resolution DEM.

The raw FEMA LIDAR data has a horizontal resolution of 4 to 6 m and a vertical accuracy of 0.20 m in coastal counties and 0.25 m in inland counties. The available elevations consist of the original LIDAR returns and a post-processed bare earth dataset. The bare earth data have been thinned from the original returns to consist of only the LIDAR returns that represent the ground surface. This includes removing LIDAR returns capturing vegetation, buildings, power lines, birds, and so forth. (more information is available at [http://www.fema.gov/plan/prevent/fhm/lidar\\_4b.shtm](http://www.fema.gov/plan/prevent/fhm/lidar_4b.shtm)).

The USGS NED is a raster product assembled to provide a national elevation DEM that tries to use the latest topographic observation. The NED is designed to provide national elevation data in a seamless form with a consistent datum, elevation unit, and projection. The NED has a resolution of approximately 30 m for the conterminous United States. NAD 83 and NAVD 88 are consistently used as the horizontal and vertical datum, respectively (more information is available at <http://seamless.usgs.gov/products/3arc.php/>).

## **2.3. Digital Elevation Model**

A high resolution DEM was constructed for the western Pamlico Sound portion of North Carolina. The DEM was built for this region as input to a study of sea level rise impact (Feyen et al., 2006). The DEM primarily utilizes high resolution FEMA LIDAR elevation data for topographic information and NOAA soundings for bathymetric information. The DEM was constructed with 6 m resolution in the horizontal direction. Any small gaps in topographic data were filled by other sources such as the USGS NED. Vertical accuracy depends on the source data (e.g., 0.20 to 0.25 m where FEMA LIDAR data is utilized, 0.30 m for hydrographic soundings in less than 20 m of water).

The bathymetric data comes from NOS hydrographic soundings are referenced to Mean Low Water (MLW), Mean Lower Low Water (MLLW), or Low Water Datum (LWD). Using the vertical datum transformations from the VDatum software, these bathymetric data are first adjusted to Mean Sea Level (MSL) and then to NAVD 88. These converted bathymetric data are combined with topographic data relative to NAVD 88 to create a continuous bathy/topo dataset. The methodology for construction of the continuous bathy/topo DEM model application is shown in Figure 2.

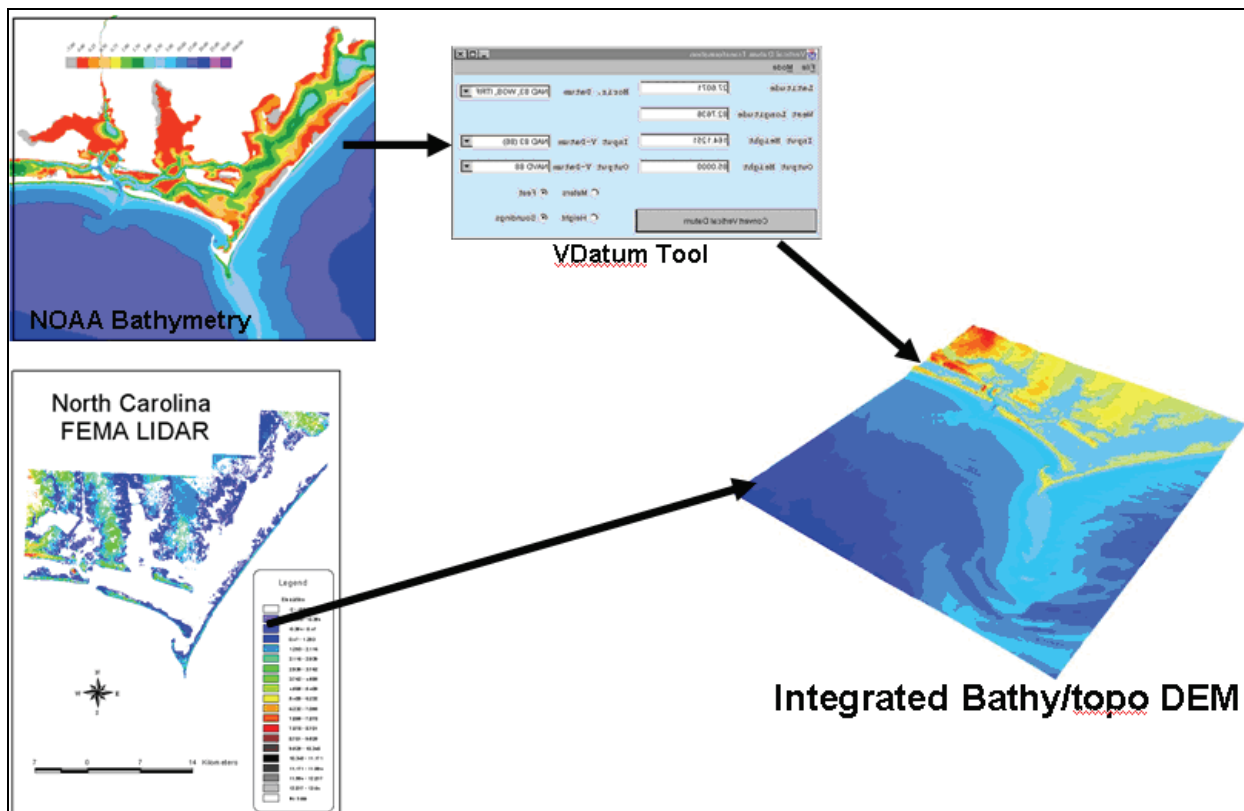


Figure 2. Construction of the continuous bathy/topo DEM application.

## 2.4. Meteorological Data

Meteorological data are obtained from NDBC buoys and Coastal-Marine Automated Network (C-MAN) stations in continuous winds format; more information is available at <http://www.ndbc.noaa.gov/>. NDBC locations and descriptions in the study area are shown in Figure 3 and Table 1. Ten-minute averaged wind speed (m/s) and wind direction measurements in degrees clockwise from true north, quality controlled and processed by NDBC, are used to validate Hurricane Isabel wind fields.

Table 1. NDBC stations in the study area.

No.	Station ID	Latitude	Longitude	Station Name (Location)
1	41001	34.68	-72.66	150 NM East of Cape Hatteras
2	41002	34.62	-76.52	S Hatteras - 250 NM East of Charleston, SC
3	44014	36.61	-74.84	Virginia Beach 64 NM East of Virginia Beach, VA
4	DUCN7	36.18	-75.75	Duck, NC
5	CLKN7	32.31	-75.35	Cape Lookout, NC

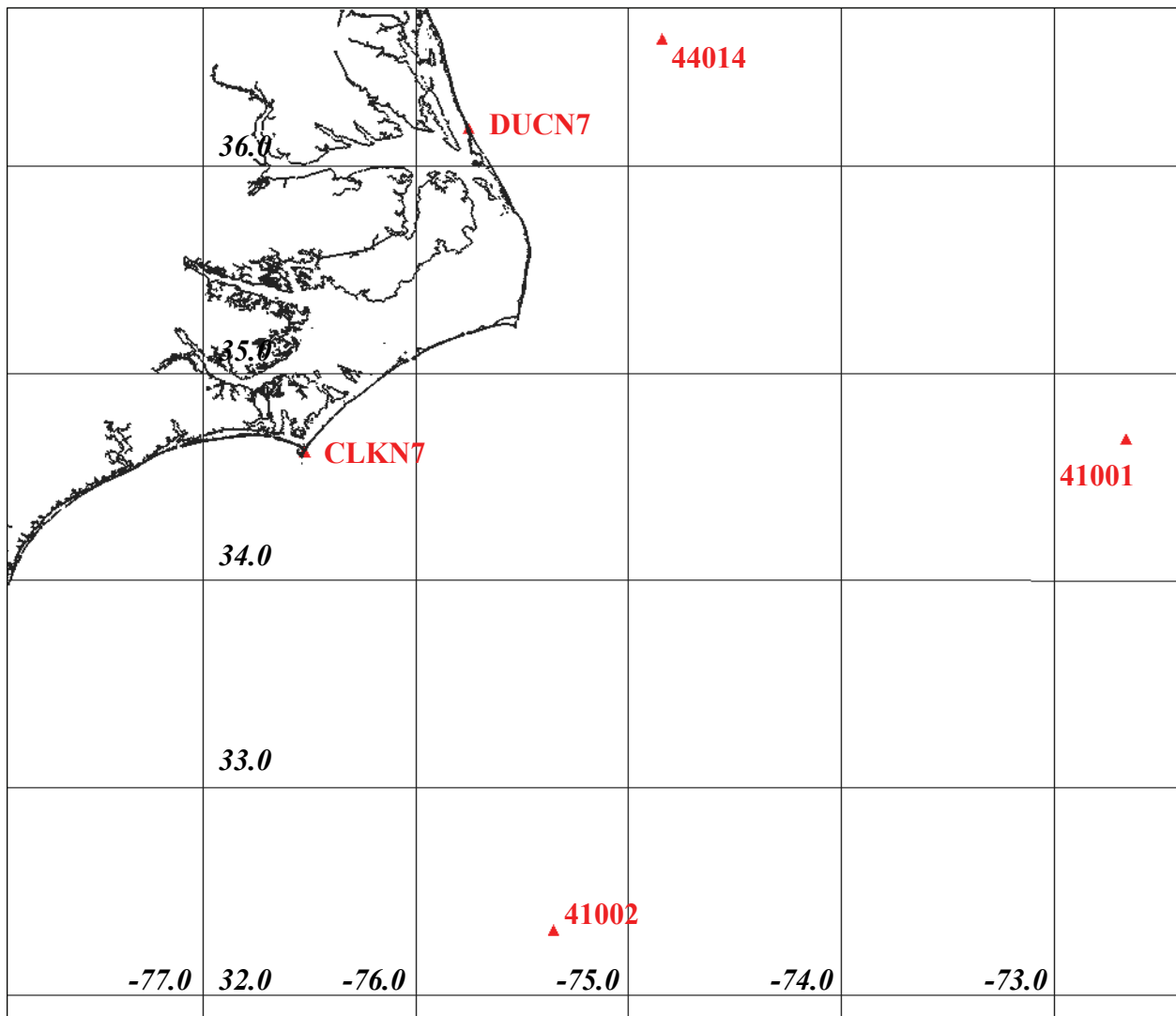


Figure 3. Locations of NDBC stations (red triangles) in the study area.

## 2.5. Water Surface Elevation Data

Time series of water surface elevation are available from NOS for four stations around the region, as shown in Figure 4; more information is available at <http://tidesonline.nos.noaa.gov/>. These are used for comparison with the CFM output. Station locations are given in Table 2. Six-minute interval water surface elevation data from the quality-controlled CO-OPS database are adjusted to NAVD 88 and used for comparison with modeled water surface elevation.

Table 2. NOS stations in the study area.

No.	Station ID	Latitude	Longitude	Station Name (Location)
1	8651370	36.183	-75.747	Duck FRF Pier
2	8652587	35.795	-75.548	Oregon Inlet Marina NC
3	8654400	35.223	-75.635	Cape Hatteras Fishing Pie
4	8656483	34.720	-76.670	Beaufort Duke Marine Lab

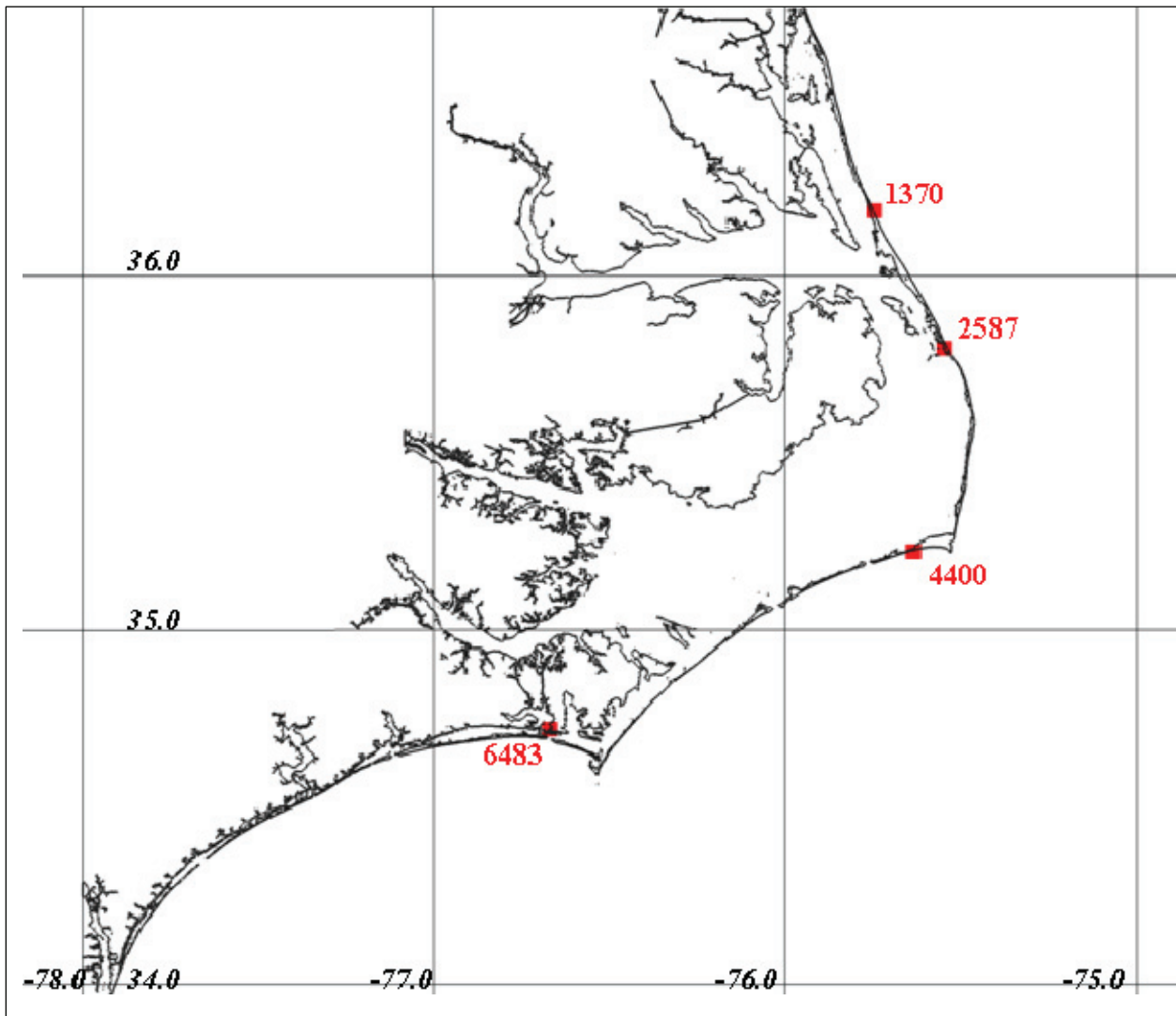


**Figure 4. Locations of NOS stations (red squares) in the study area. Only the last four digits of the station numbers are shown; the first three digits are 865 for all stations (see Table 2).**

## **2.6. High Water Marks**

HWMs are available from FEMA’s Hurricane Isabel rapid response coastal high water mark collection (FEMA 2003). FEMA categorizes a HWM as either Coastal (CHWM) or Riverine (RHWM) based on an evaluation of the type of flooding (coastal surge or riverine) at each location. The CHWMs, used for model validation, are obtained by field surveys and through interviews with local residents and witnesses. The CHWMs are identified based on general guidelines for HWM spacing (approximately 1 CHWM per 1.6 km of affected shoreline) using GPS. CHWM locations are surveyed horizontally in NAD 83 and vertically in NAVD 88. CHWM locations have been surveyed to within accuracies of 0.07 m vertically and 3 m horizontally with a 95% confidence level.

CHWMs are also classified as either Storm Surge or Stillwater CHWMs. The classification is based on a combination of the physical flood evidence and interviews with witnesses. Coastal Storm Surge HWMs are associated with flooded areas where there is evidence of damage from the wave action associated with a storm surge. Typically, Coastal Stillwater HWMs are associated with a slow rising flood that causes more water damage than structural damage. The approximate locations of the FEMA CHWMs used in this study are shown in Figure 5 and Table A.1 in Appendix A (FEMA 2003).

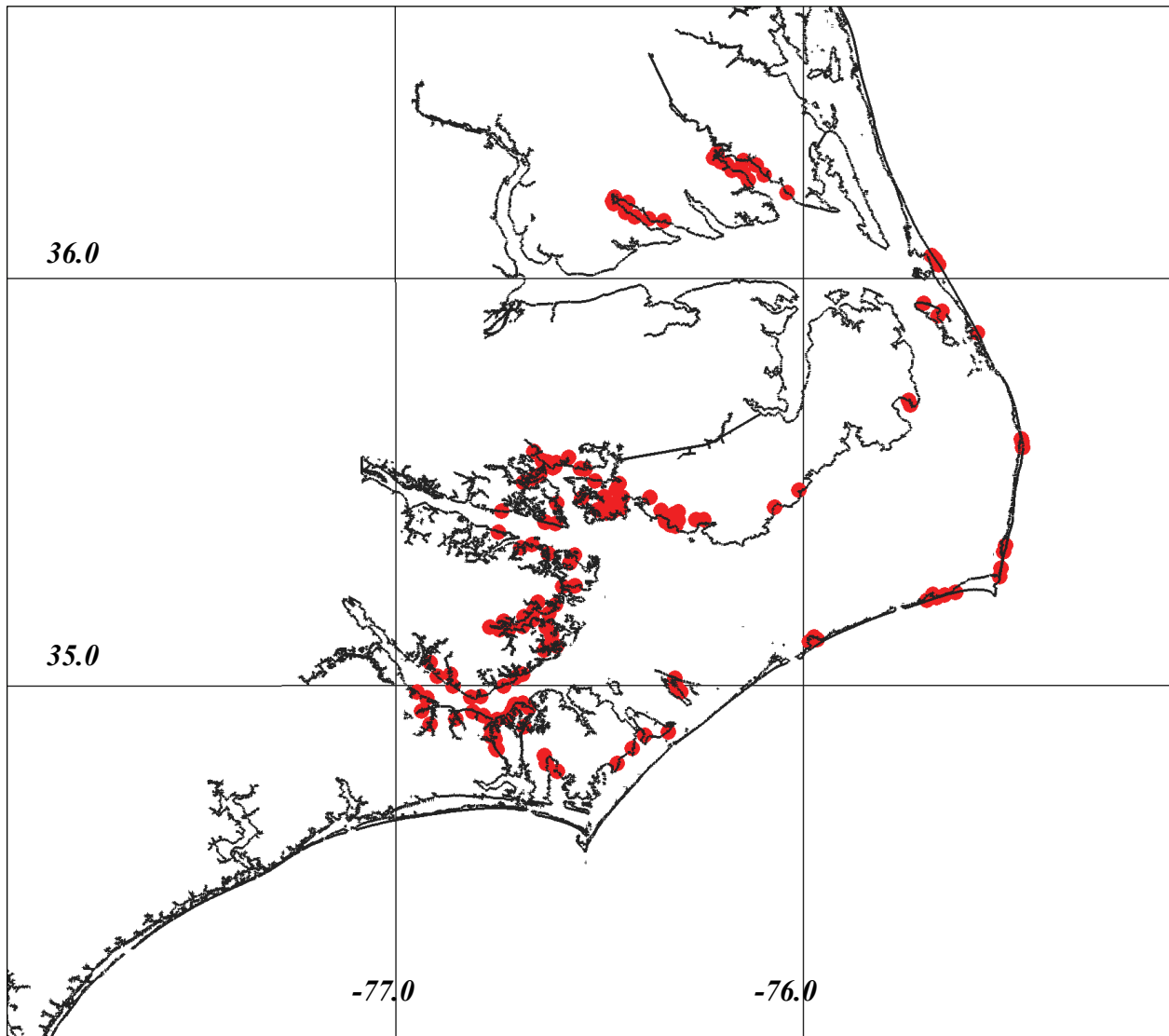


**Figure 5. Locations of FEMA CHWMs (red circles) in the study area.**

### **3. COASTAL FLOODING AND HYDRODYNAMIC MODELING**

As part of the CFM development, a high-resolution finite element hydrodynamic model was constructed for the study area. Bathymetry and topography data referenced to NAVD 88 were used to populate the grid with depths and land elevations. The model was originally developed as a tidal model which extended up to the MHW shoreline in order to support the development of the VDatum tool (Hess et al., 2005). This tidal model was run to simulate astronomical tides, and revised and calibrated until it produced sufficiently accurate tidal datum information for VDatum. The CFM was then built from the tidal model by adding additional grid resolution over low-lying coastal land. The storm surge simulations were run on this CFM.

#### **3.1. The ADCIRC Model**

The CFM is an application of ADCIRC, the ADvanced CIRCulation model for oceanic, coastal and estuarine waters. The CFM runs in two-dimensional (i.e., barotropic) mode on an unstructured grid composed of triangular elements; this type of grid is ideally suitable for representing complex coastlines to any desired resolution, and can be easily modified to add spatial resolution in any geographic area with little effort. The grid must then be populated by bathymetry and topography to represent the region, and boundary forcing must be added to simulate astronomical tides, storm surge, and other causes of water level variability.

The ADCIRC model was developed by Rick Luetlich at the University of North Carolina at Chapel Hill, Institute of Marine Sciences, and Joannes Westerink at the University of Notre Dame, Department of Civil Engineering and Geologic Sciences (Luetlich et al., 1992; Luetlich and Westerink 2004). This model is a system of computational algorithms that solve time-dependent, free surface circulation and transport problems in two and three dimensions. The ADCIRC Two-Dimensional Depth Integrated (2DDI) version, used for the North Carolina area studies, is the barotropic version of the model. ADCIRC utilizes the finite element method in space, taking advantage of highly flexible, irregularly spaced grids. Numerous studies have shown this model to be robust throughout the Western North Atlantic and Gulf of Mexico regions (Luetlich et al., 1994; Mukai et al., 2001; Westerink et al., 2008)

ADCIRC has a wetting and drying algorithm for modeling inundation that works as follows. When the water surface elevation at any node is less than a user-specified depth (here 0.10 m), that node becomes temporarily inactive (i.e., dry). When surrounding water surface elevation is sufficiently high to push water into the nodal area to make the water surface elevation rise above the 0.10 m value, the node is activated (i.e., wet). During the model runs, some nodes become 'ponded' when their depths are at or near 0.10 m, because the surrounding nodes are inactive and there is not a sufficient gradient for the water to flow out of them. For further information on the wetting and drying algorithm see Westerink et al. (2008).

The modeling of wind stress formulation and other parameters are discussed in detail in Appendix B.

### 3.2. Model Grid Development

The modeling strategy is to create a regional grid of central coastal North Carolina by using a portion of a larger scale grid, in this case, a Western North Atlantic Ocean grid (Luettich et al., 1994). Then, grid elements covering Pamlico and Albemarle Sounds and Beaufort Inlet developed by Luettich et al. (1999) were incorporated. Finally, additional elements were added by NOS to parts of the region within the DEM area where more resolution was needed, including the Intracoastal Waterway. The grid contains 36,409 nodes, and the smallest elements in that area had node spacing on the order of 13 m (Hess et al., 2005).

Based on this regional model grid, the CFM adds land areas and continuous contours of bathymetric and topographic data relative to a single referenced datum (i.e., NAVD 88). A 15 m topographic contour (relative to NAVD 88) was generated from the 30 m horizontal resolution USGS NED and used as the landward boundary. Computational mesh has been added between the prior MHW shoreline and this land boundary, including all island areas, as shown in Figure 6. The 15 m contour was chosen since this will allow the CFM to model severe storm surge conditions. Resolution ranges from 5 km offshore down to 20 m within narrow channels such as the Intracoastal Waterway. Resolution of inlets is generally from 100 to 200 m, with more than 10 elements across these inlets. Mesh size within sounds ranges between several hundred meters to nearly two kilometers, and rivers are discretized ranging from many nodes across to a pair of elements only 50 m in size. The regional CFM grid is shown in Figures 6 and 7.

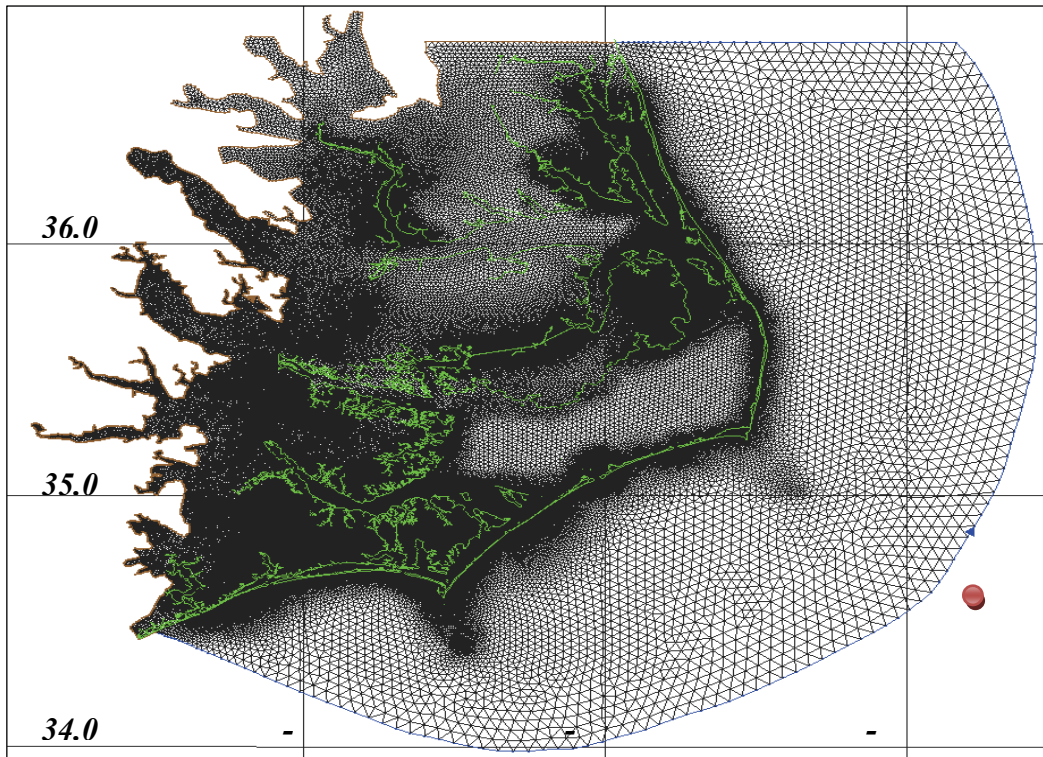


**Figure 6. The regional CFM in the North Carolina region; the MHW shoreline is shown in green and the sample point of the lateral boundary condition as a red circle in Section 5.3.**

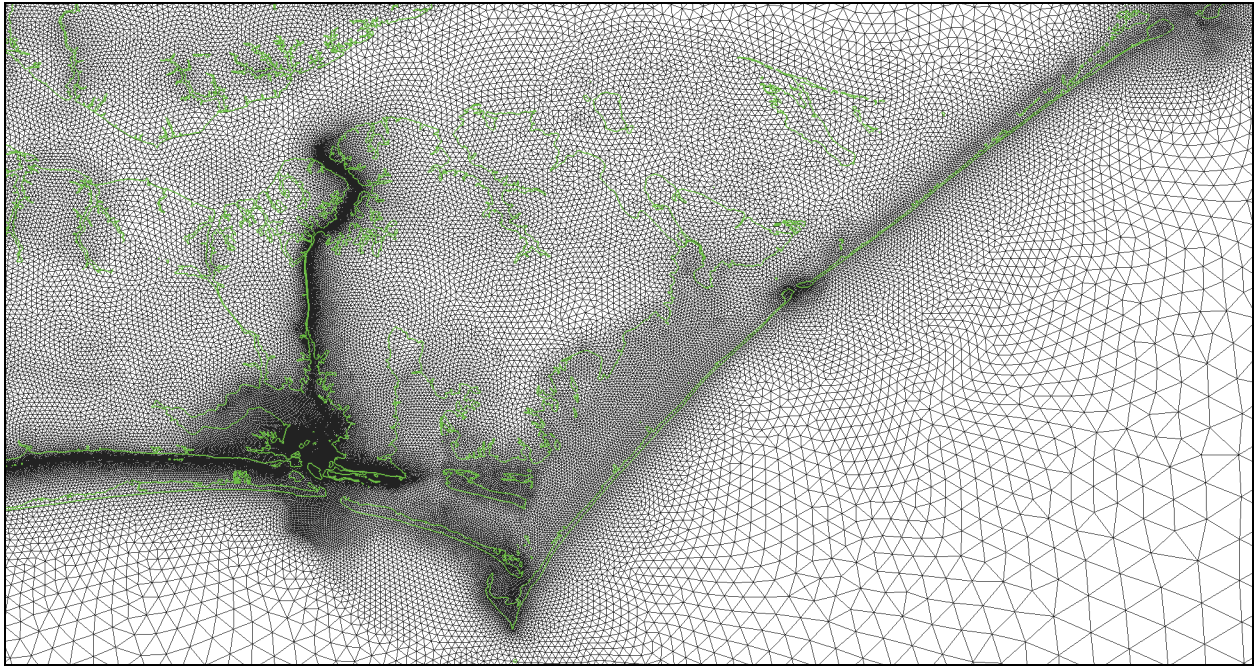


**Figure 7. The regional CFM of Pamlico Sound and surrounding areas; the MHW shoreline is shown in green.**

A basin-scale grid (Figure 8) was also created by incorporating the regional CFM into a Western North Atlantic grid developed for a 1995 East Coast (EC95) tidal database (Luettich et al., 1994). The resolution of the EC95 grid is rather coarse due to the limited computing resources available at the time, resulting in a domain of 31,435 nodes and resolution of approximately 75 km in the open ocean. However, it has been shown to effectively model tides and predict storm surge when integrated with a high resolution regional model grid (Westerink et al., 2008). While the EC95 grid has been used previously for tidal simulation, a solely tidally forced simulation is first run to successfully validate this combined CFM and EC95 domain application.

### **3.3. Bathymetric and Topographic data for the Regional CFM**

The regional CFM grid was populated by depths and elevations in a consistent vertical datum (NAVD 88). In order to produce accurate predictions of storm surge, it is necessary to have accurate and continuous elevation (bathymetric and topographic) information. The VDatum software was used to transform bathymetric sounding data from tidal datums (e.g., relative to MLW or MLLW) to the same orthometric datum (NAVD 88) used for topographic data. The regional CFM elevations were derived directly from the DEM where it provided coverage. The DEM does not cover all of the regional CFM mesh, however; it is limited to the area that ranges from southwest of the White Oak River to northeast of Hatteras Inlet. In areas the DEM does not cover, NOS sounding data was used for bathymetric depths and the USGS NED for topographic heights. All bathymetric and topographic data were applied to the computational mesh by interpolating at the local mesh scale. This was done by averaging all data points within the cluster of elements surrounding each node.

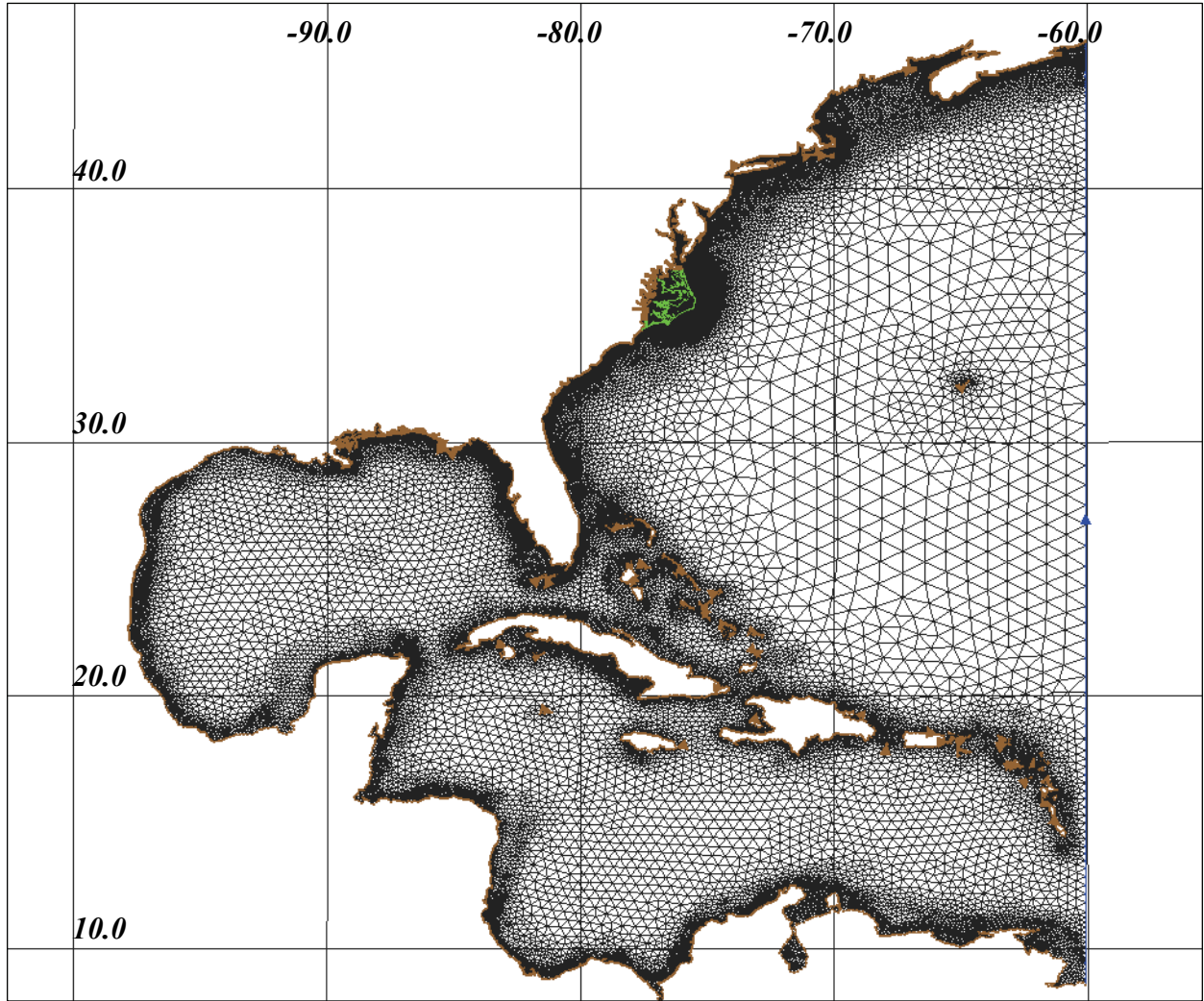


Figure 8. The basin-scale CFM grid.

### 3.4. Tidal Forcing of the Regional and Basin-Scale CFM

The outer coastal boundary of each ADCIRC grid is forced with periodic water level variations to simulate astronomical tides (Schureman 1958). The water surface elevation, relative to the model's zero elevation, at each node along the outer boundary is

$$H = h_0 + \sum f_n A_n \cos(\omega_n t + [V_0 + u]_n - \kappa_n)$$

where  $H$  is the total water surface elevation (m),  $h_0$  represents a constant offset, and the remaining terms represent the astronomical tide.  $A_n$  is the constituent amplitude (m),  $\omega_n$  is the constituent speed (degrees/hr),  $t$  is the time relative to Coordinated Universal Time (UTC),  $[V_0 + u]_n$  is the equilibrium angle (degrees), and  $\kappa_n$  is the phase relative to UTC (degrees). Therefore a unique set of harmonic constants is required at each grid node along the coastal boundary; a sample is shown in Table 3.

**Table 3. Sample of the tidal constituents and harmonic constants used for the regional CFM.**

Constituent	Amplitude (m)	Phase (deg)
	$A_n$	$\kappa_n$
K <sub>1</sub>	0.091433	177.978
O <sub>1</sub>	0.068979	191.636
M <sub>2</sub>	0.408000	351.313
S <sub>2</sub>	0.074515	10.154
N <sub>2</sub>	0.096141	336.247

The open boundary of the regional CFM grid (Figure 6) is located roughly along an arc approximately 100 km of the coast. An updated version of the Western North Atlantic tidal database was created for the East Coast in 2001 (EC2001; Mukai et al., 2001). This tidal database is used to provide the set of harmonic constants for forcing the tidal signal in the regional CFM.

The open boundary of the basin-scale CFM grid (Figure 8) is located along the 60° W longitude. A unique set of harmonic constants, M<sub>2</sub>, N<sub>2</sub>, S<sub>2</sub>, K<sub>1</sub>, and O<sub>1</sub> tidal constituents from Schwiderski's global tidal model (Schwiderski 1980) were used at each grid node along the open ocean boundary. This forcing dataset matches that used for the EC95 model grid, from which the basin-scale CFM is built.

Tidal forcing is normally imposed in ADCIRC via time and space varying conditions along the open boundaries of the model domain. However, ADCIRC also includes terms representing the Newtonian tidal potential and the corrections due to the effect of the Earth tides. The tidal potential term forces tides within the model domain. This term appears in the momentum equations, as spatial gradients that are subtracted from the spatial gradient of the free surface elevation. In continental shelf areas, the free surface elevation gradient is typically larger than the tidal potential term and therefore they are safely neglected. However, the free surface gradient can be very small in the deep ocean, and therefore, when significant areas of the deep ocean are included in the model domain, this tidal potential term may be significant. The Newtonian tidal potential and Earth tides are expressed as (Reid 1990):

$$\eta(\lambda, \phi, t) = \sum_{n,j} \alpha_{jn} C_{jn} f_{jn}(t_0) L_j(\phi) \cos \left[ \frac{2\pi(t - t_0)}{T_{jn} + j\lambda + \nu_{jn}(t_0)} \right]$$

where  $t_0$  is reference time,  $\alpha_{jn}$  is reduction in the field of gravity due to Earth tide,  $C_{jn}$  is Newtonian equilibrium tidal potential amplitude,  $f_{jn}$  is time-dependent nodal factor,  $T_{jn}$  is tidal period,  $\nu_{jn}$  is time-dependent astronomical argument,  $j$  ( $j = 0, 1, 2$ ) is tidal species, in which  $j = 0$  (declinational),  $j = 1$  (diurnal), and  $j = 2$  (semidiurnal):  $L_0 = 3 \sin^2(\phi) - 1$ ,  $L_1 = \sin(2\phi)$  and  $L_2 = \cos^2(\phi)$ . In addition, Reid (1990) consolidated the value of the effective earth elasticity factor,  $\alpha_{jn}$ , which is typically applied as 0.69 for all tidal constituents (Schwiderski 1980) even

though the value has been shown to be slightly constituent dependent. Tidal potential forcing was included for all ADCIRC simulations produced for this report.

## 4. HURRICANE ISABEL AND METEOROLOGICAL MODELS

Hurricane Isabel was chosen to evaluate the performance of the CFM because it was a recent well-documented hurricane that made a direct hit to the central North Carolina coast. The history of Hurricane Isabel is briefly described below. Meteorological conditions for Hurricane Isabel are provided by the Hurricane Wind analysis system (H\*Wind) from the Hurricane Research Division (HRD) of the Atlantic Oceanographic and Meteorological Laboratory (AOML), the Geophysical Fluid Dynamics Laboratory (GFDL) Hurricane Model, and the Global Forecast System (GFS) from NCEP. Adjustment of wind average time period, height, and time interval, including blending meteorological models, is discussed to define appropriate meteorological forcing for storm surge modeling.

### 4.1. Hurricane Isabel

Hurricane Isabel was the most powerful hurricane of the 2003 season and the first hurricane to make landfall on the east coast of the United States since 1999. After coming ashore on the Outer Banks of North Carolina on 18 September as a Category 2 hurricane (Saffir-Simpson Hurricane Scale), Isabel took a northward track through Virginia, causing high winds, storm surge flooding, and extensive property damage. Isabel produced a devastating storm surge to the North Carolina Outer Banks and Virginia coastline and a record-breaking storm surge in the Chesapeake Bay because of its strong wind toward inland. Figure 9 shows the best track chart of Isabel (<http://www.nhc.noaa.gov/2003isabel.shtml/>).

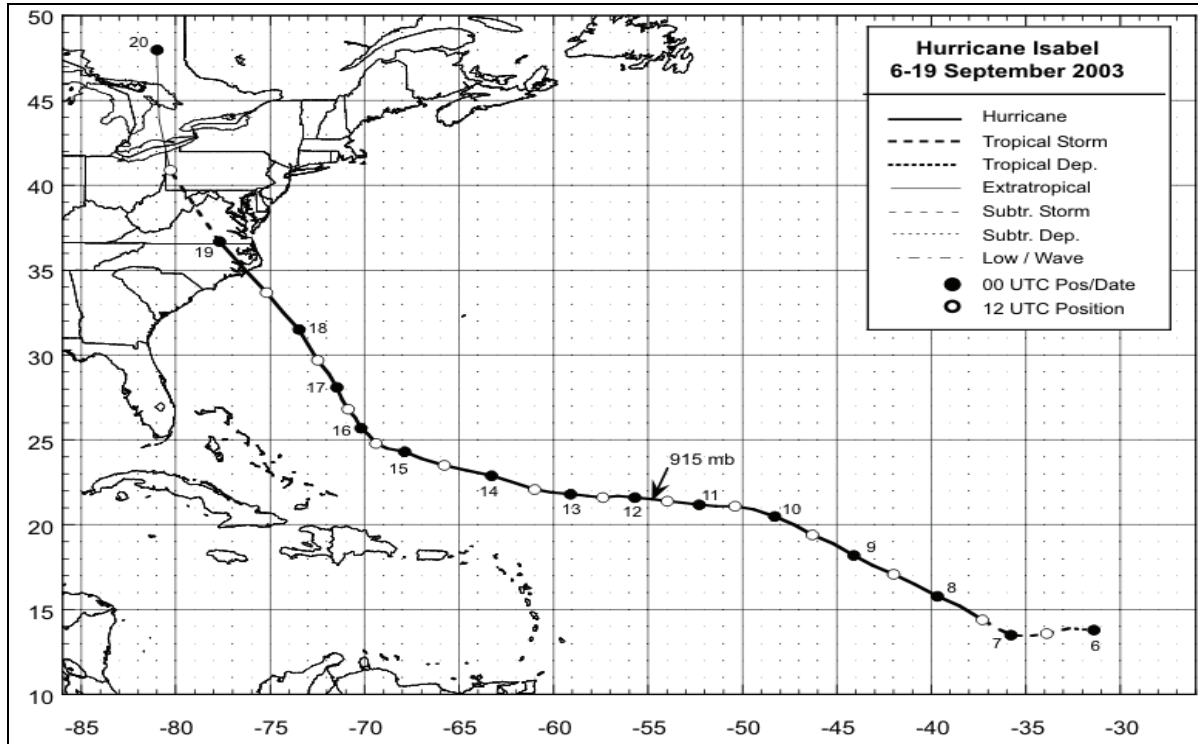


Figure 9. National Hurricane Center best track positions for Hurricane Isabel, 6 – 19 September 2003 (Beven and Cobb 2004).

Isabel reached a major hurricane in a few days after its formation in the western tropical Atlantic Ocean, about 7 September 2003. The best track positions and intensities are listed in Table 4. According to advisories published subsequently by the Tropical Prediction Center (TPC), at 1500 UTC on September 7, Isabel had become a Category 1 hurricane. Over the next few days Isabel gradually gained strength, reaching Category 5 status at 2100 UTC on September 11 with maximum sustained winds of 72 m/s. Isabel retained this strength through early September 15. Thereafter it gradually weakened, dropping to Category 2 strength with sustained winds of 46 m/s on 1500 UTC September 16. When landfall occurred on early September 19, Isabel retained this strength (NOAA, USACE, and FEMA 2005).

**Table 4. The best track positions and intensities (Beven and Cobb 2004).**

Date/Time (UTC)	Position		Pressure (hPa)	Wind Speed (m/s)	Stage
	Lat. (°N)	Lon. (°W)			
06 / 0000	13.8	31.4	1009	15	tropical depression
06 / 1200	13.6	33.9	1003	21	"
07 / 0000	13.5	35.8	994	28	"
07 / 1200	14.4	37.3	987	33	hurricane
08 / 0000	15.8	39.7	976	41	"
08 / 1200	17.1	42.0	952	57	"
09 / 0000	18.2	44.1	948	59	"
09 / 1200	19.4	46.3	948	59	"
10 / 0000	20.5	48.3	952	57	"
10 / 1200	21.1	50.4	948	59	"
11 / 0000	21.2	52.3	935	64	"
11 / 1200	21.4	54.0	925	69	"
12 / 0000	21.6	55.7	920	72	"
12 / 1200	21.6	57.4	920	72	"
13 / 0000	21.8	59.1	925	69	"
13 / 1200	22.1	61.0	935	69	"
14 / 0000	22.9	63.3	935	69	"
14 / 1200	23.5	65.8	935	69	"
15 / 0000	24.3	67.9	937	67	"
15 / 1200	24.8	69.4	946	62	"
16 / 0000	25.7	70.2	952	54	"
16 / 1200	26.8	70.9	959	49	"
17 / 0000	28.1	71.5	957	49	"
17 / 1200	29.7	72.5	957	46	"
18 / 0000	31.5	73.5	953	46	"
18 / 1200	33.7	75.2	956	46	"
19 / 0000	36.7	77.7	969	33	"
19 / 1200	40.9	80.3	997	18	extratropical
20 / 0000	48.0	81.0	1000	13	"
11 / 1800	21.5	54.8	915	75	<b>minimum pressure</b>
18 / 1700	34.9	76.2	957	46	landfall at Drum Inlet, North Carolina

## 4.2. Meteorological Models

Three different types of atmospheric models are employed in order to provide meteorological forcing to the CFM. One is an analytical model, H\*Wind, which integrates all available surface weather observations to analyze tropical cyclones. The others are dynamical forecast models (called the GFDL and GFS models) which solve a set of basic laws of physics to predict the atmosphere. Although the resolution, coverage, and accuracy are different between the models, each model is used as meteorological forcing, and their performances are evaluated.

The H\*Wind analysis system developed by AOML (Powell et al., 1996a) is an integrated tropical cyclone observing system that enables real-time interaction with, and analysis of, observations gathered in tropical cyclones. All available surface weather observations (e.g., ships, buoys, coastal platforms, surface aviation reports, reconnaissance aircraft data adjusted to the surface, etc.) are used to produce high-quality wind snapshots. All data are quality controlled and processed to conform to a common framework for height (10 m), exposure (marine or open terrain over land), and averaging period (maximum sustained 1 minute wind speed) using accepted methods from micrometeorology and wind engineering. H\*Wind is available for tropical storms and hurricanes at 3 to 6 hour intervals.

The GFDL hurricane model is an operational hurricane forecast model applying a nested grid system with an outermost domain and 2 nested grids with resolutions of 55, 27 and 9 km respectively; it uses 42 vertical levels. A spin-up vortex initialization is used with an axisymmetric version of the forecast model forced by intensity and structure parameters provided operationally by the NHC. The GFDL hurricane model is coupled to a high-resolution version of the Princeton Ocean Model (POM) for the Atlantic Basin. The ocean initialization system uses observed altimeter observations to provide a more realistic Loop Current and Gulf Stream condition. Hurricane forecasts are produced on demand every 6 hours at 00, 06, 12, and 18 UTC for up to 4 tropical storms at a time and provide hourly output.

The GFS operated by NCEP is a global spectral data assimilation and forecast model system. GFS forecasts are produced every six hours at 00, 06, 12 and 18 UTC. The GFS are based on a 70 km grid and are available at six hour increments out to 384 hours. NCEP implemented major changes to GFS on May 31, 2005, so the Isabel results were completed on the earlier version of the model. The GFS contains a full suite of parameterized physics as well as accompanying sea-ice and land-surface models.

The specification of grid resolution and wind field snapshot time interval from these meteorological models is important for model accuracy due to its significant contribution to the storm surge generation. Figure 10 illustrates the comparison of wind fields from the meteorological models H\*Wind (panel a), GFDL (panel b, red box shows the boundary of its nested grid), and GFS (panel c), on September 18, 2003 just before Hurricane Isabel made landfall on the North Carolina Outer Banks. H\*Wind has the highest resolution, as it's 1000 km square domain has a resolution of 6 km, although it has a limited domain size. GFDL has a 9 km inner nested grid that is constantly following the hurricane eye, and an outermost domain to capture far-field dynamics. GFS, with resolution of approximately 50 km for Hurricane Isabel, doesn't specifically resolve the hurricane dynamics; however, GFS is the only system with both observation-based reanalysis and model-generated forecast products.

H\*Wind records for Hurricane Isabel are composited for the storm over a 3 to 6 hour interval (25 analyses of Isabel's surface wind, starting at 1730 UTC on September 11 and ending 1630 UTC on September 18). GFDL produces hourly predictions of wind and atmospheric pressure reduced to MSL (from 0000 UTC September 7 to 1200 UTC September 18) which based on simulations start every 6 hours. GFS provides wind field and atmospheric pressure reduced to MSL at every 6-hour intervals from 0000 UTC September 7 to 0000 UTC September 21.

Two issues arise when applying H\*Wind to hurricane storm surge modeling. First, H\*Wind doesn't provide atmospheric pressure predictions. Since a water surface elevation response is associated with the atmospheric pressure deficit, it is one of the important components in storm surge generation. This is termed the inverted barometer effect; the rise is approximately 0.01 m for each hPa drop in pressure. Second, the H\*Wind grid is limited in size to produce wind snapshots of the main storm. H\*Wind has enough grid size to cover the entire hurricane, locating the center of the grid on the hurricane eye; however, it doesn't provide the far-field wind that generates set-up outside the H\*Wind domain. In order to resolve these issues it is necessary to blend H\*Wind with other meteorological models.

### **4.3. Adjustment of Wind Average Time Period and Height**

When dealing with hurricane storm surge modeling, the issue of the appropriate wind averaging time period has not been clearly defined. The length of the wind averaging time period will affect the reported wind speed and thus the surface stress applied to the water column of the storm surge model. This is because the shorter the averaging period, the higher the reported wind speed. Therefore, any time averaging should consider the time scale of the conditions being simulated in order to account for this factor.

It is important to recognize that wind averaging time period varies depending upon the application. Calculating wind impact on structures is generally based on a short wind duration (gust or peak sustained 1 minute average) due to their failure mechanism. However, wave generation is controlled by the fetch length, which would define the wind averaging time period. For inland lakes and rivers this can be as short as 1 to 5 minutes; over the open ocean this response time is reported to be 10 to 30 minutes.

Since the drag coefficient is controlled by sea surface roughness (i.e., wave conditions), it could be theorized that storm surge models should use the same wind averaging time period as used by the wave modeling community (i.e., 10 to 30 minutes). Thus, it is suggested that a time average between 10 and 30 minutes is acceptable for storm surge modeling. The winds produced by many parametric models most likely correspond to values within this time range (e.g., a 10 minute average is common). However, it is important to adjust observations and meteorological forcing to a common sampling period for comparison. In practice, use of a 10 minute averaging period has been found to be accurate in storm surge modeling (W. Shaffer pers. comm.) and can be used for direct comparison with continuous winds data collected at many NOAA observational platforms (i.e., NDBC buoy data). Furthermore, Powell and Reinhold (2007) report that hurricane winds over a 10 minute period are relatively stable (for computing a mean) while considerable changes occur over a longer time period such as an hour.

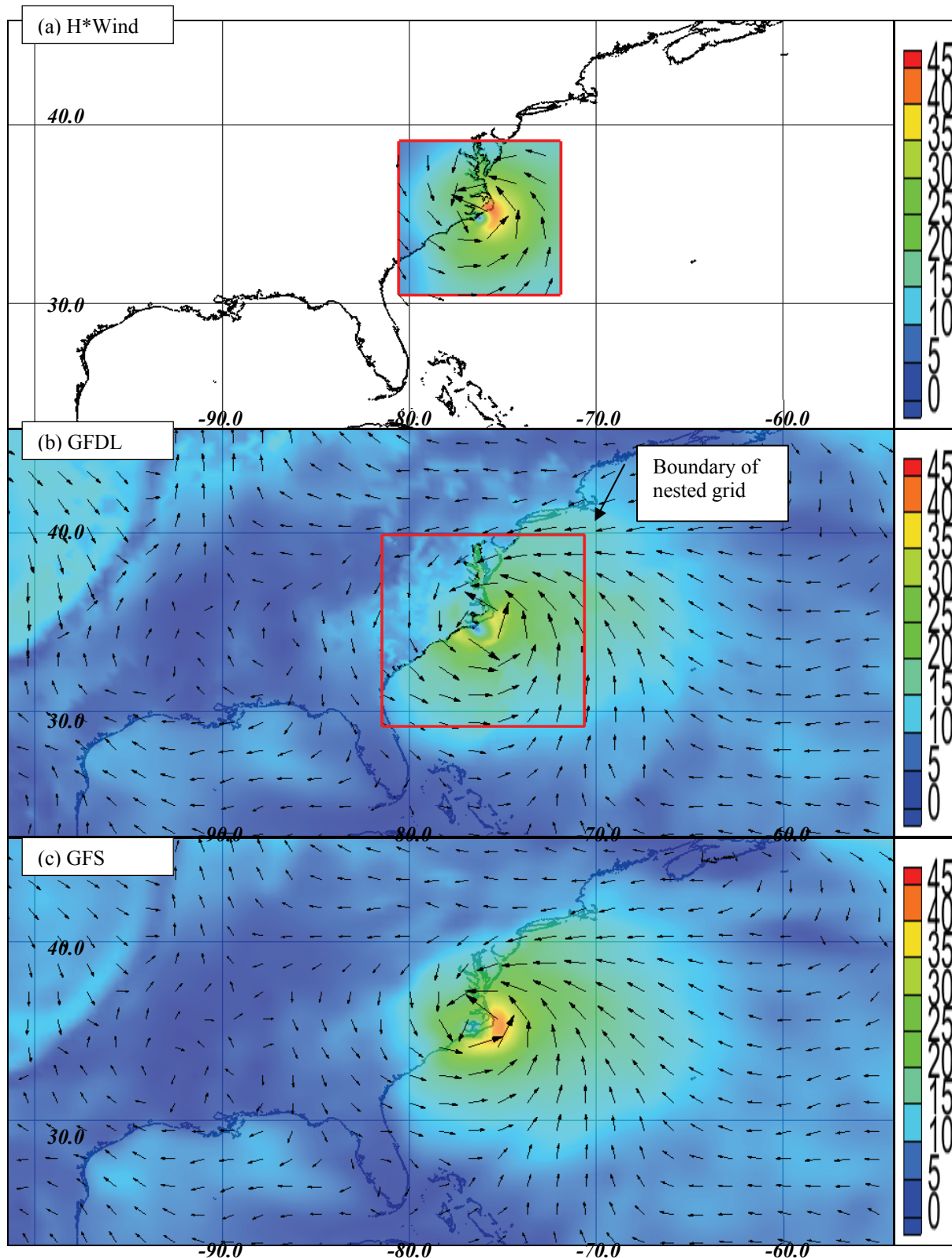


**Figure 10. Wind speed (m/s) from meteorological models on September 18 2003 before Hurricane Isabel made land fall on the North Carolina's Outer Banks from H\*Wind (a), GFDL (b), and GFS (c). Red box in the GFDL panel shows the boundary of its nested grid.**

In developing meteorological forcing for storm surge models and comparing these winds to observations, it is necessary to transform the winds to a common framework. Wind time averaging lengths are not standardized, as various observation platforms can report a 1 minute, 2 minute, or 10 minute averaged wind. For example, H\*Wind provides 1-minute sustained winds (applying an adjustment value of 1.11 for determining 1 minute peak winds from 10 minute averaged winds) to conform with advisories and warnings issued to the public by NHC. Powell et al. (1996b) report that adjustments to convert sampling height and averaging period to a common framework are accurate to within 10%; however, comparison of observations taken with different techniques can lead to errors of 15% to 40%. Therefore all reported observations and model output were adjusted to a 10 minute average. Data from H\*Wind were adjusted by 1.11 to convert from a 1 minute to 10 minute average.

Wind observations are generally taken from an unobstructed 10 m platform and drag coefficient relationships are also defined at a 10 m height. Therefore meteorological forcing or observations should also be adjusted to the 10 m reference height if not so provided (meteorological models in this study provide the 10 m reference height wind). The USACE's *Coastal Engineering Manual* provides formulae for the elevation correction of wind collection height (Resio et al., 2006). Failure to correct the height will lead to errors due to (among other things) the parabolic nature of the boundary layer. Therefore, all model output was selected to be at the 10 m level, and all observations were adjusted to the 10 m height for comparison.

#### **4.4. Adjustment of Wind Forcing Interval**

The meteorological models have different intervals for updating their output data. Simulation of Hurricane Isabel from GFDL provides hourly output from a 6-hr forecast cycle. GFS provides a 6-hr updates for its analytical wind and 6-hr intervals in its forecast wind up to 96 hours. H\*Wind has 3- or 6-hr updates depending on the NHC advisory (if the NHC issues a hurricane warning and forecast advisories every three hours, H\*Wind switches to 3-hr update). In order to create consistent wind forcing time intervals, it is necessary to use an interpolation method to adjust their output data. The method chosen for temporal and spatial interpolation is an interpolation polynomial in the Lagrange form (Jeffreys and Jeffreys 1988). The interpolation polynomial in the Lagrange form is chosen because it gives a solution that has a constant slope between output data. In addition, it is the simplest way to interpolate between output data, even though it does not incorporate any physics. Therefore all model output data in space and time were adjusted to an hourly wind forcing interval using the interpolation polynomial in the Lagrange form.

#### **4.5. Blending Meteorological Models**

In order to improve the Hurricane Isabel storm surge hindcast, it is necessary to create the best available wind field. For Isabel the best available wind field is generated by blending meteorological models. This is because H\*Wind is an observations-based analysis system which has shown the most skill in capturing the characteristics of the hurricane, but it lacks far-field and post-landfall winds, and pressure throughout. By combining aspects of the other meteorological models a forcing field can be built that supersedes their qualities individually.

There are two steps in blending meteorological models. The first step is the combining wind fields spatially by blending them within an overlapping region. The blending ratio is dependent on the grid resolution; since H\*Wind has higher grid resolution than GFDL and GFS, the value of H\*Wind is used when each grid overlaps. The next step is integrating atmospheric pressure. Atmospheric pressure from GFDL is utilized because GFDL properly resolves hurricane dynamics, while H\*Wind does not provide atmospheric pressure. A resulting blended wind field is hourly interpolated onto the basin-scale CFM using the interpolation polynomial in the Lagrange form.



## **5. LATERAL BOUNDARY CONDITION**

The non-tidal lateral boundary condition for the regional CFM is provided by both the basin-scale CFM and the NCEP Atlantic Real-Time Ocean Forecast System (RTOFS). Time series of water surface elevations (WSE) from the basin-scale CFM simulation are applied to the regional CFM along the outer boundary. RTOFS is a forecast system based on the Hybrid Coordinate Ocean Model (HYCOM). Sea Surface Height (SSH), including mean dynamic topography due to temperature variations in the ocean and currents like the Gulf Stream, is provided to the regional CFM as the lateral boundary condition.

The regional CFM grid can be efficiently run for multiple scenarios. However, this grid is not able to capture the response that occurs across the larger basin without an appropriate boundary condition. Therefore, several strategies are evaluated to understand their impact on CFM model skill. The basin-scale CFM was designed to accurately capture the physical dynamics associated with the propagation of the storm surge over the basin. The regional CFM is more suitable from the point of view of model efficiency when multiple runs are needed. Therefore, incorporating the lateral boundary condition produced by the basin-scale CFM into the regional CFM is the best option to satisfy both model accuracy and efficiency. In addition, applying the lateral boundary condition obtained from RTOFS helps to understand the baroclinic effects (i.e., mean dynamic topography due to temperature variations in the ocean and baroclinic currents) for storm surge.

### **5.1. The Lateral Boundary Condition from Basin-Scale CFM**

Time-series of water surface elevation from the basin-scale CFM are used to provide the lateral boundary condition for the regional CFM. The meteorological model used to create the lateral boundary condition is the GFS model. Six-hour interval meteorological forcing is interpolated on the basin-scale CFM grid. The hourly interpolation approach using the interpolation polynomial in the Lagrange form (see Section 4.4) is not used because RTOFS uses a 6-hr interval of GFS meteorological forcing in their simulation of Hurricane Isabel, and it is important to make a uniform comparison of techniques. Computed time series of water surface elevation is forced every hour at each grid node along the coastal boundary of the regional CFM.

### **5.2. Real-Time Ocean Forecast System**

RTOFS (Spindler et al., 2006; more information is available at <http://polar.ncep.noaa.gov/ofs/>) is an operational high resolution (eddy resolving) ocean forecast system for the NWS that provides short-term forecasts (approximately 1-week) of the Atlantic Basin, including both deep and coastal waters. The system provides nowcasts and forecasts of sea level, currents, temperature and salinity. Figure 11 illustrates the grid and bathymetry of RTOFS.

RTOFS is an ocean forecast system based on HYCOM (Bleck 2002). HYCOM is the result of collaborative efforts among the University of Miami, the Naval Research Laboratory, and the Los Alamos National Laboratory as part of the multi-institutional HYCOM Consortium for Data-

Assimilative Ocean Modeling. The goal is to develop and evaluate a data-assimilative hybrid isopycnal-sigma-pressure coordinate ocean model. RTOFS uses curvilinear coordinates in the horizontal (1200 x 1684 points) and hybrid vertical coordinates in the vertical (21 isopycnal and 5 z-level for a total 26 vertical coordinates).

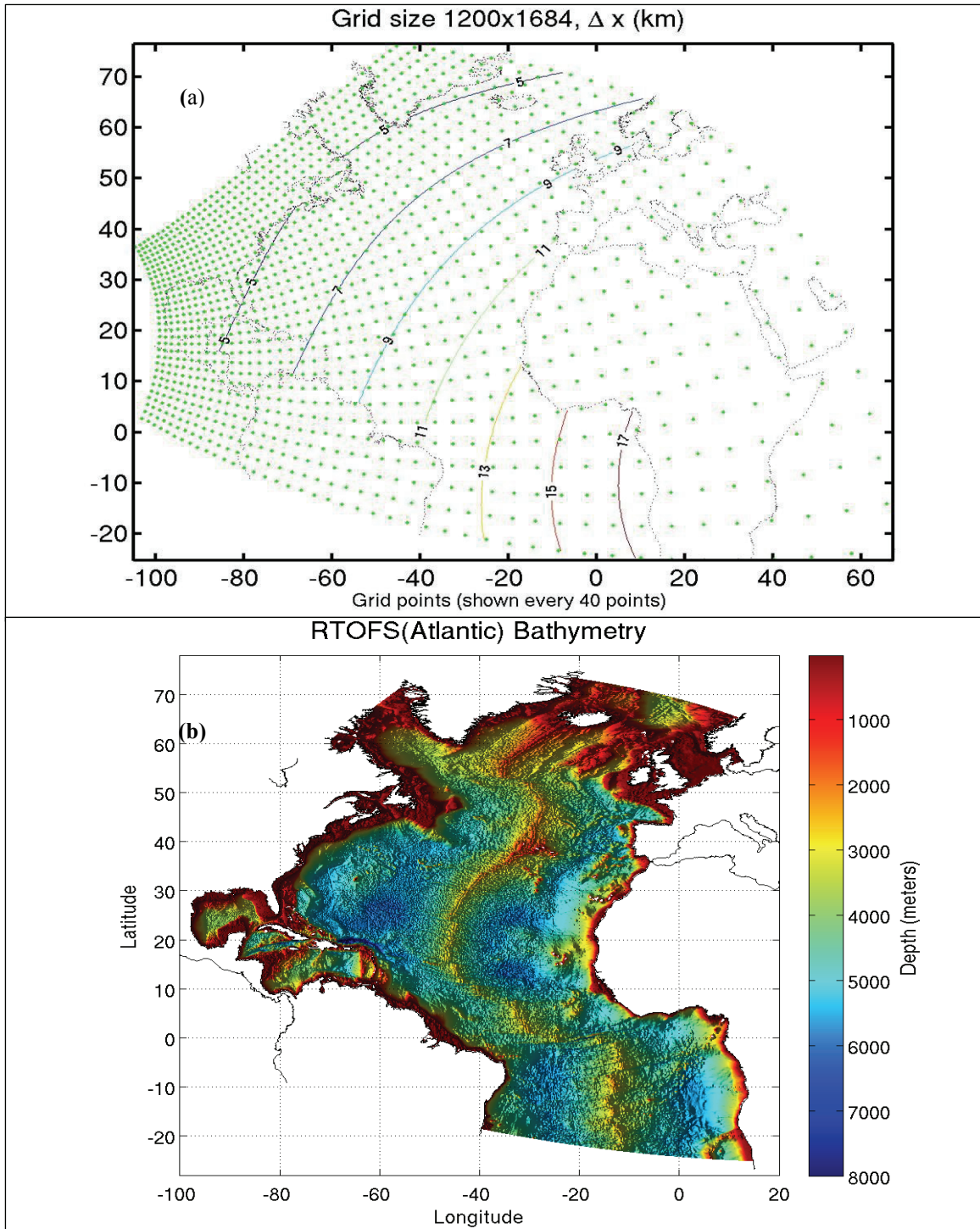


**Figure 11. RTOFS orthogonal grid with approximate grid spacing contours (a) and bathymetry (b).**

### 5.3. The Lateral Boundary Condition from RTOFS

SSH from RTOFS is tested as the lateral boundary condition for the regional CFM. In order to investigate the baroclinic effects in the boundary forcing, two cases of the lateral boundary conditions are applied. The first lateral boundary condition is with a SSH which includes the mean dynamic topography due to temperature variations in the ocean and large-scale currents, the tidal signal, and the ocean surface response to meteorological forcing. The second lateral boundary condition is a SSH without the mean dynamic topography, calculated by filtering to remove the 14 day linear mean value in the SSH. Each SSH is hourly-interpolated onto each node along the open boundary of the regional CFM.

Figure 12 shows an example of the lateral boundary condition, including tidal forcing (harmonic tidal constituents, see Section 3.4), at the sample location (see Figure 6); 1) tide, 2) the basin-scale, 3) RTOFS, and 4) detrended RTOFS. This figure clearly describes sub-tidal effects and the height of mean dynamic topography in the deviation of the mean of the blue line from the others.

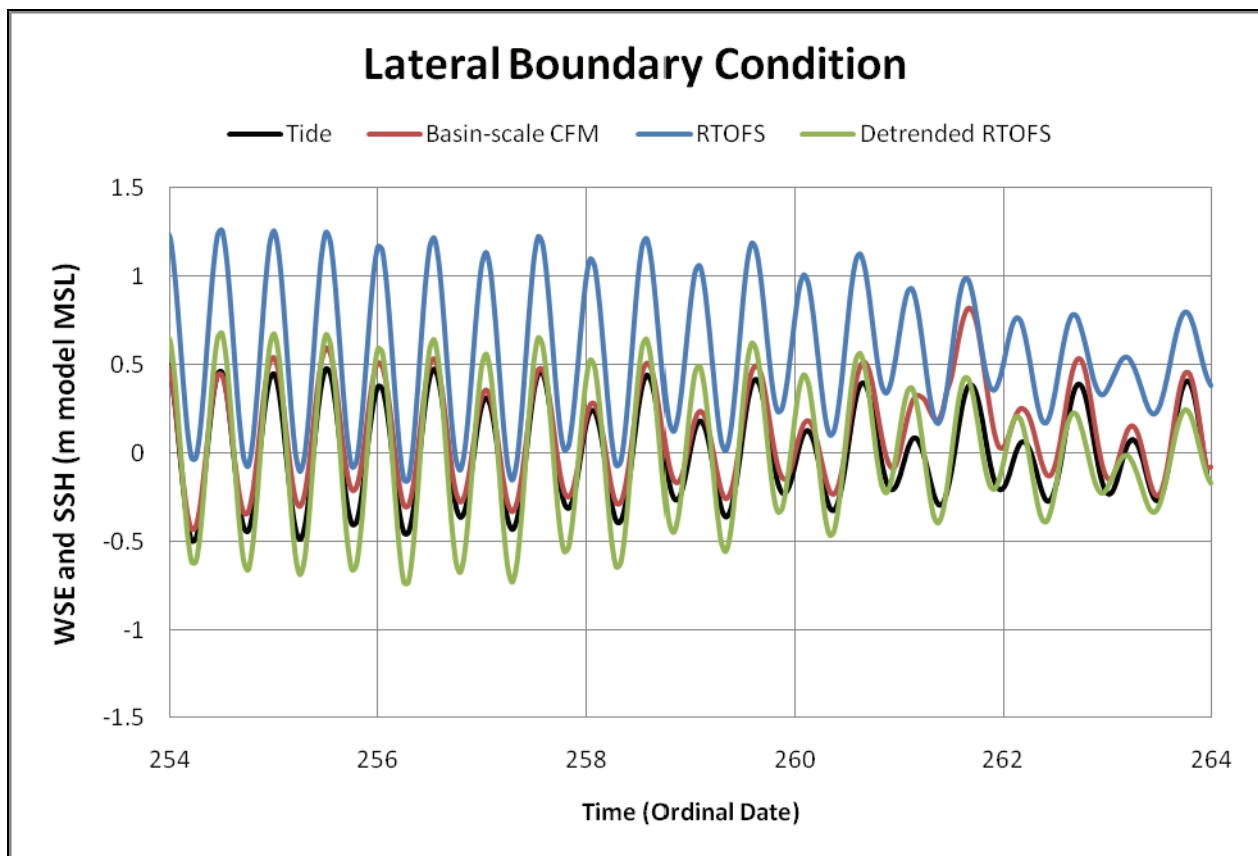


**Figure 12. The lateral boundary condition at the sample location along outer boundary of the regional CFM (see Figure 6); 1) Tide (black), 2) the basin-scale CFM (red), 3) RTOFS (blue), and 4) detrended RTOFS (green).**



## 6. RESULTS AND DISCUSSION

As a part of the Hurricane Isabel hindcast, model evaluations are carried out in several ways. First, model-generated Hurricane Isabel wind fields over the basin-scale CFM domain are compared with NDBC data. Second, time series of observed water surface elevation from NOS are used for the validation of the modeled storm surge. Third, FEMA CHWMs are used to assess the inundation predicted by the basin-scale CFM. In addition, validation of the lateral boundary condition is investigated using the regional CFM. Skill assessment, including Mean Error (ME), Root Mean Square Error (RMSE), Standard Deviation (SD), and peak difference in amplitude and phase, is performed to evaluate model accuracy.

### 6.1. Validation of Hurricane Isabel Wind Fields

The quality of the wind fields from meteorological models is assessed in two ways. First, time series of wind speed and direction applied to the basin-scale CFM are compared with NDBC continuous wind data (see Table 1 and Figure 3). Second, the wind fields in the basin-scale CFM are used to evaluate the intensity of Hurricane Isabel. In order to maintain consistency while comparing the meteorological forcing, H\*Wind is adjusted to a 10 minute averaged value and all wind data are a 10 m height. In addition, to be consistent with hourly wind intervals from GFDL, hourly H\*Wind and GFS wind fields are generated using the interpolation polynomial in the Lagrange form. Table 5 shows the detail of wind fields for Hurricane Isabel as applied to the basin-scale CFM.

**Table 5. Wind fields for Hurricane Isabel interpolation onto the basin-scale CFM.**

Model	Grid	Time	Comment
H*Wind	1000 km by 1000 km square domain with resolution of 6 km	3-6 hour interval (1730 UTC September 11 to 1630 UTC September 18)	Hourly increments using the interpolation polynomial in the Lagrange form
GFDL	2 nested grids with resolutions of 9 and 55 km	Hourly output from 6 hour forecast cycle (0000 UTC September 7 to 1200 UTC September 18)	Continues using forecast wind after last cycle at 1200 UTC September 18
GFS	Approximately 50 km grid	6 hour output (0000 UTC September 7 to 0000 UTC September 21)	Hourly increments using the interpolation polynomial in the Lagrange form

NDBC continuous wind data are used to validate wind speed and direction in the basin-scale CFM domain. NDBC continuous wind data is averaged over 10 minutes and adjusted to 10 m height. Wind direction is also a 10-min average value, measured in degrees clockwise from true North. The comparisons of wind speed and direction provided by meteorological models against NDBC continuous wind data at observation locations (see Table 1 and Figure 4) are shown in Figures 13 through 17. In the figures, any undefined value outside the H\*Wind domain is set to be zero, and time is displayed in ordinal date (from September 11 to September 21 2003).

At buoy locations 41001 and 41014 (Figures 13 and 14), all models capture the wind direction sufficiently as Isabel approaches landfall. GFDL has good agreement with observations in both wind speed and direction. GFS overestimates wind speed since GFS can't resolve the hurricane dynamics in the absence of a high resolution nested grid, and for Isabel it overestimated the size of the storm (Tolman et al., 2003). At buoy location 41002 (Figure 15), located on the left side of the hurricane Isabel track, timing of maximum wind speed from all models is delayed approximately six hours. At the land location of DUCN7, maximum peak winds from H\*Wind and GFS show good agreement with observations; however, GFDL is lower than the observations by approximately 10 m/s due to an underestimated storm size (Figures 16). The reason for this underestimation is that GFDL used the forecasted wind after 1200 UTC September 18, just prior to landfall. At CLKN7, located near the hurricane landfall point, all models match up well with the observations in both wind speed and direction (Figure 17).

The wind fields in the basin-scale CFM are examined visually for comparing the intensity of Hurricane Isabel. Wind and atmospheric pressure fields were linearly interpolated onto the basin-scale CFM grid. Figures 18 and 19 show every 6-hour interval from 0000 UTC September 17 to 1800 UTC September 18. Figures 20 and 21 illustrate every 3-hour interval from 1200 UTC September 18 to 2100 UTC September 18 as Isabel makes landfall. H\*Wind doesn't provide wind data after Hurricane Isabel made landfall as shown in Figures 20 and 21.

While Isabel is a Category 3 hurricane (1200 UTC September 17), the GFDL generally captures the structure of the wind field well, but wind speeds are generally lower than those from H\*Wind (Figure 18). The GFS wind speeds are stronger than H\*Wind and GFDL, but the GFS has similar structure of the wind field as H\*Wind. Through September 17 (Figures 18 and 19), wind speed from all models are gradually weakened. Since the model wind fields are interpolated onto the basin-scale CFM grid, the hurricane eye is extended due to coarser spatial resolution in the deep ocean. As Isabel approaches the coastline (where model grid has more resolution), all models capture the eye of the hurricane clearly (Figure 19 and 20); however, the 6-hour temporal interpolation in the GFS produces an irregular hurricane eye (Figure 20). The GFDL wind speed intensities are realistic (see Figures 13 – 17), but the spatial extent of its wind field is generally smaller than H\*Wind. In addition, since the GFDL uses long term forecast data after 1200 UTC September 18, the hurricane eye in the GFDL is gradually located to the left of the best available hurricane track. During this period, the GFS wind field shows better representation of the size of Isabel; however, the GFS overestimates wind speed.

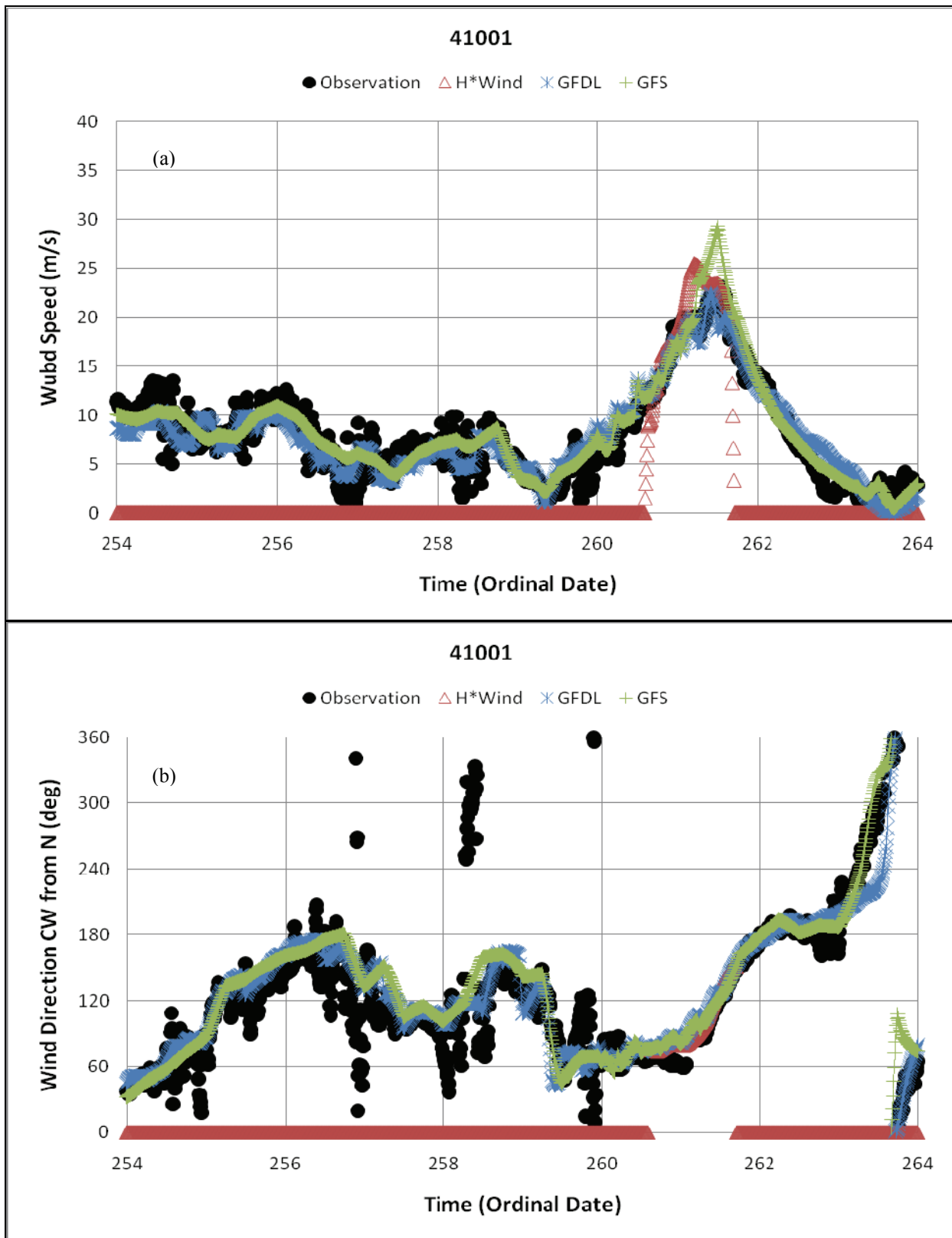


**Figure 13.** The comparison of wind speed (a) and direction (b) provided by H\*Wind (red triangle), GFDL (blue asterisk), and GFS (green cross) with observation of NDBC continuous wind data (black dot) at NDBC location 41001.

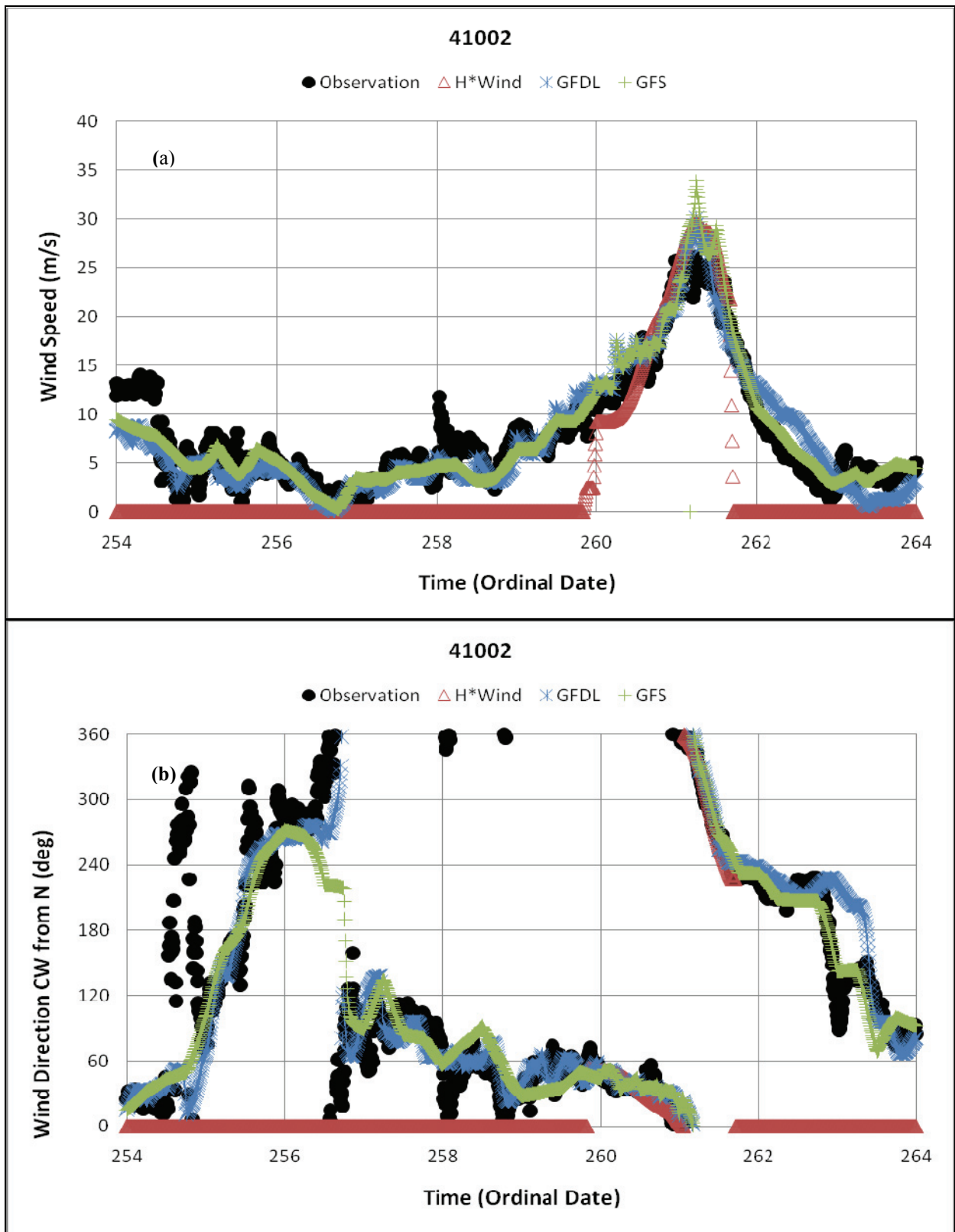


**Figure 14.** The comparison of wind speed (a) and direction (b) provided by H\*Wind (red triangle), GFDL (blue asterisk), and GFS (green cross) with observation of NDBC continuous wind data (black dot) at NDBC location 41002.

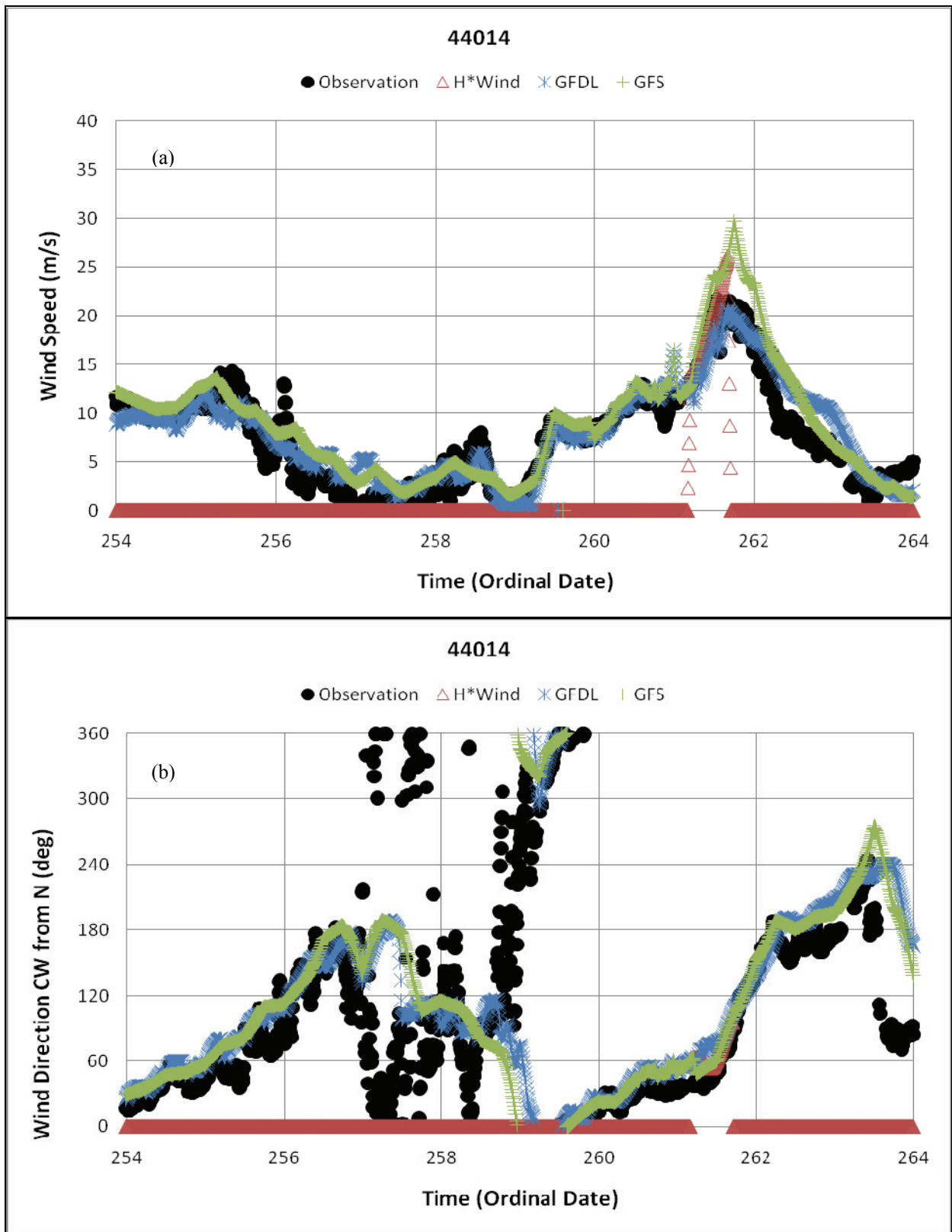


**Figure 15.** The comparison of wind speed (a) and direction (b) provided by H\*Wind (red triangle), GFDL (blue asterisk), and GFS (green cross) with observation of NDBC continuous wind data (black dot) at NDBC location 44014.

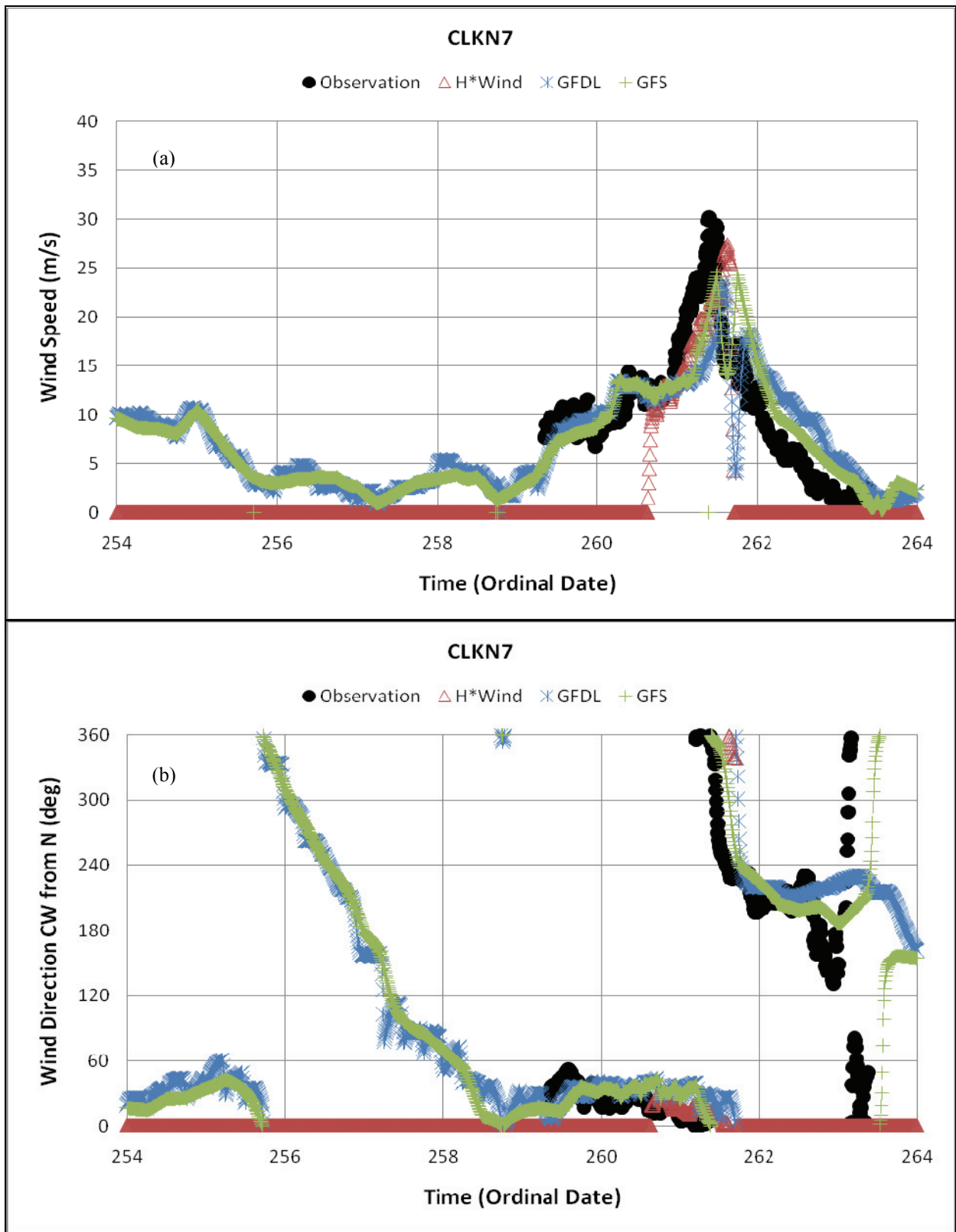


**Figure 16.** The comparison of wind speed (a) and direction (b) provided by H\*Wind (red triangle), GFDL (blue asterisk), and GFS (green cross) with observation of NDBC continuous wind data (black dot) at NDBC location DUCN7.

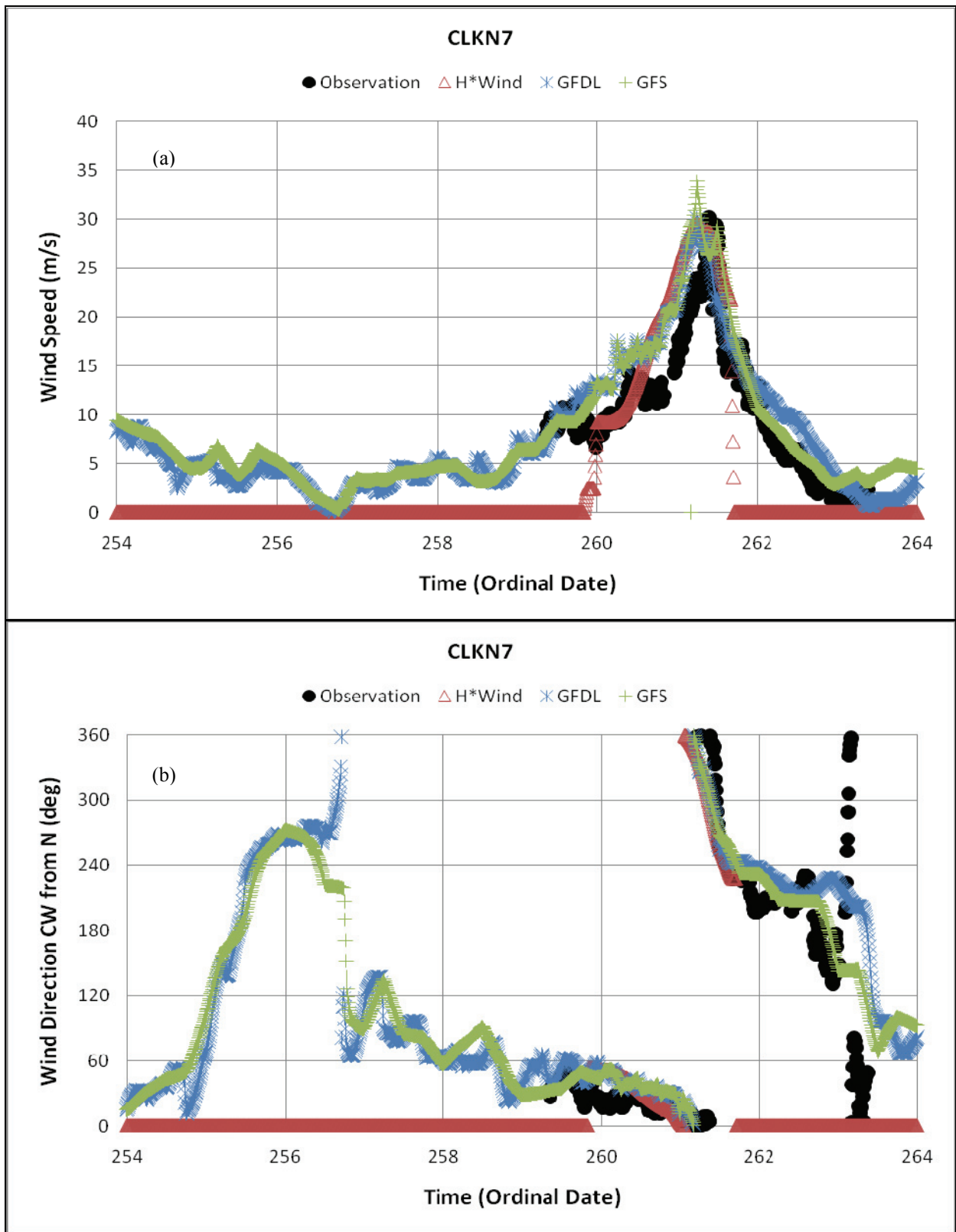


Figure 17. The comparison of wind speed (a) and direction (b) provided by H\*Wind (red triangle), GFDL (blue asterisk), and GFS (green cross) with observation of NDBC continuous wind data (black dot) at NDBC location CLKN7.

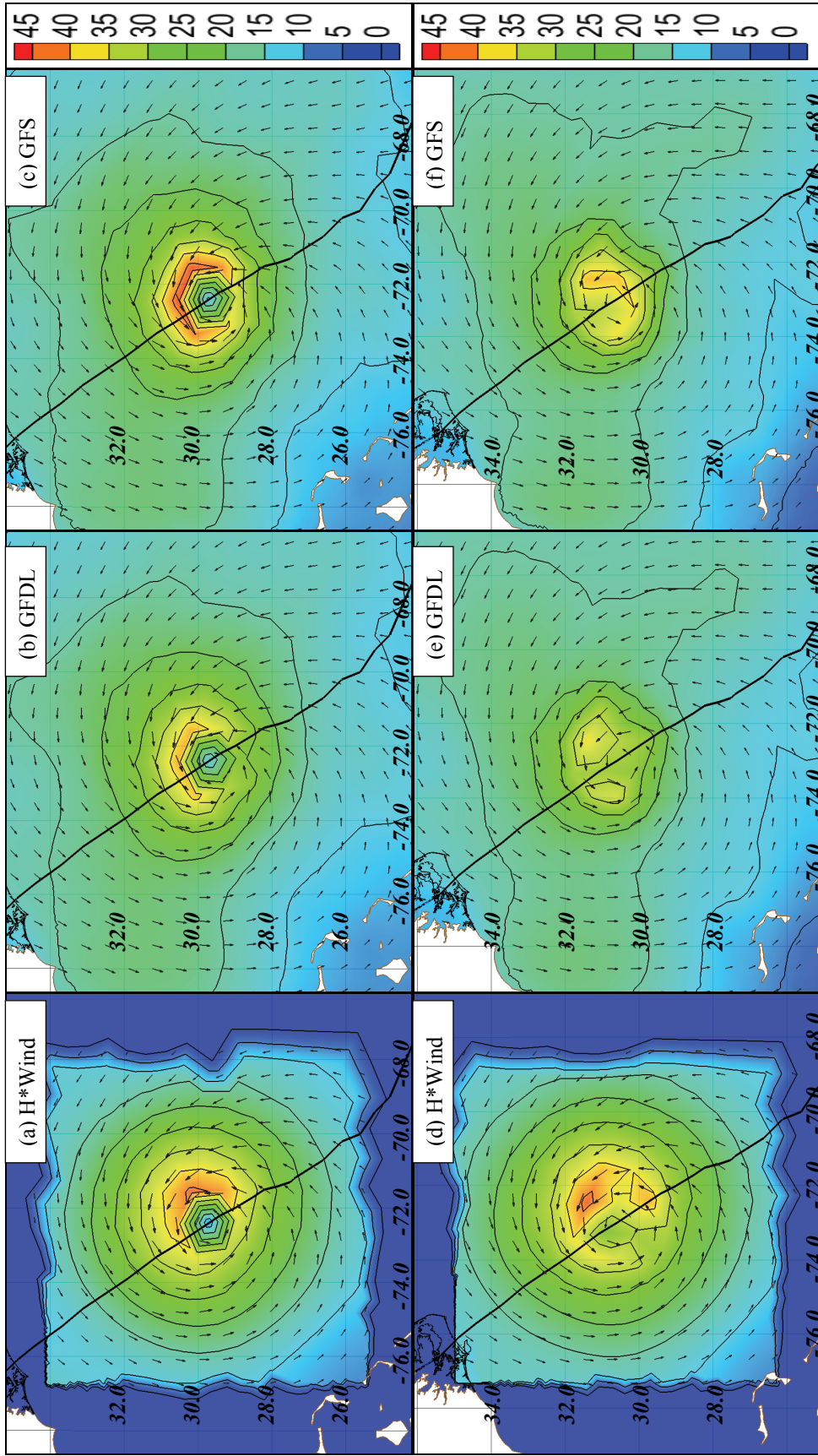


Figure 18. Track of Isabel (solid black line) and wind speeds at 10 m height in  $\text{ms}^{-1}$  for Isabel: H\*Wind (a), GFDL (b), and GFS (c) at 1800 UTC September 17, and H\*Wind (d), GFDL (e), and GFS (f) at 1200 UTC September 17.

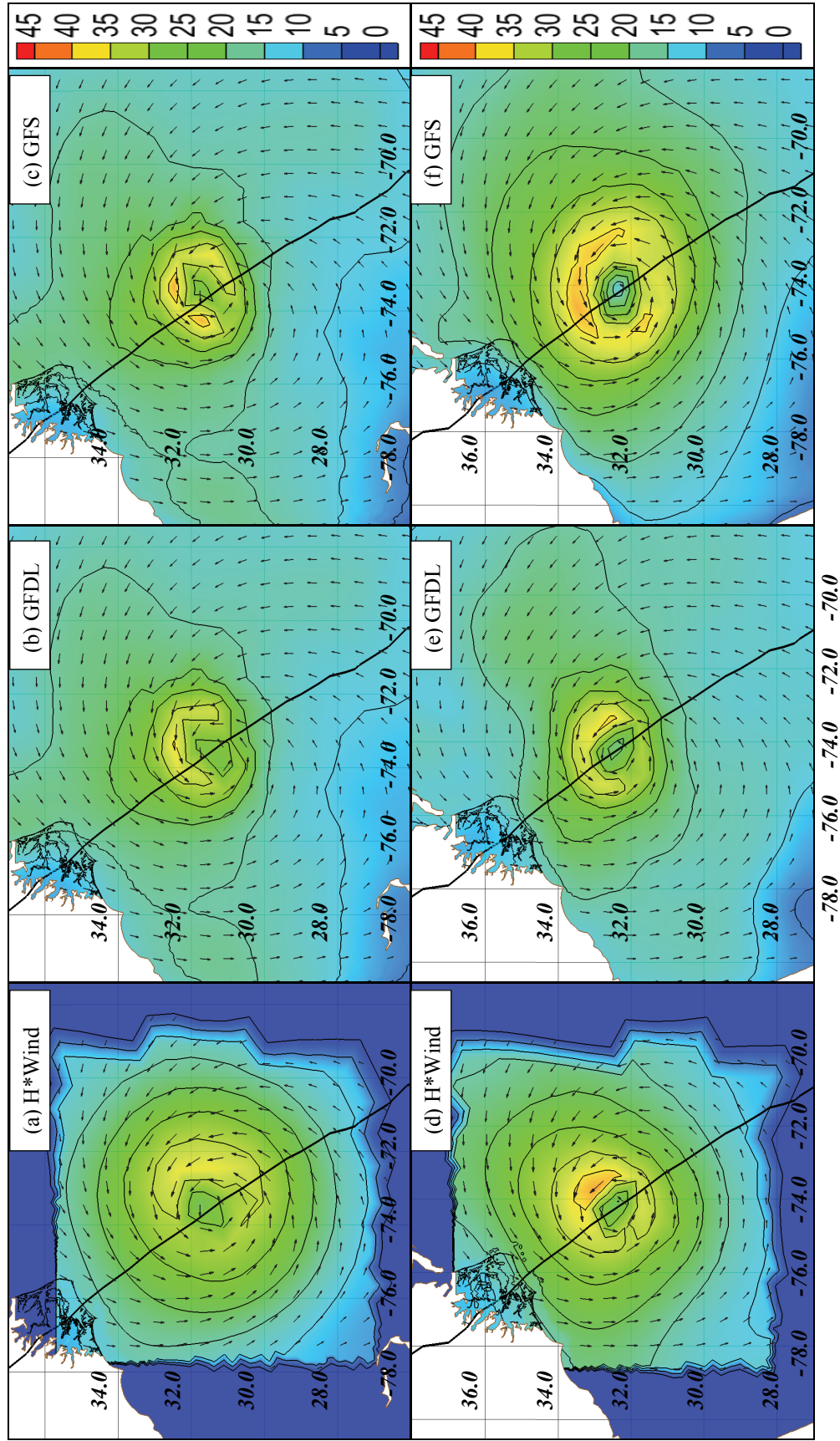


Figure 19. Track of Isabel (solid black line) and wind speeds at 10 m height in  $\text{ms}^{-1}$  for Isabel: H\*Wind (a), GFDL (b), and GFS (c) at 0000 UTC September 18, and H\*Wind (d), GFDL (e), and GFS (f) at 0600 UTC September 18.

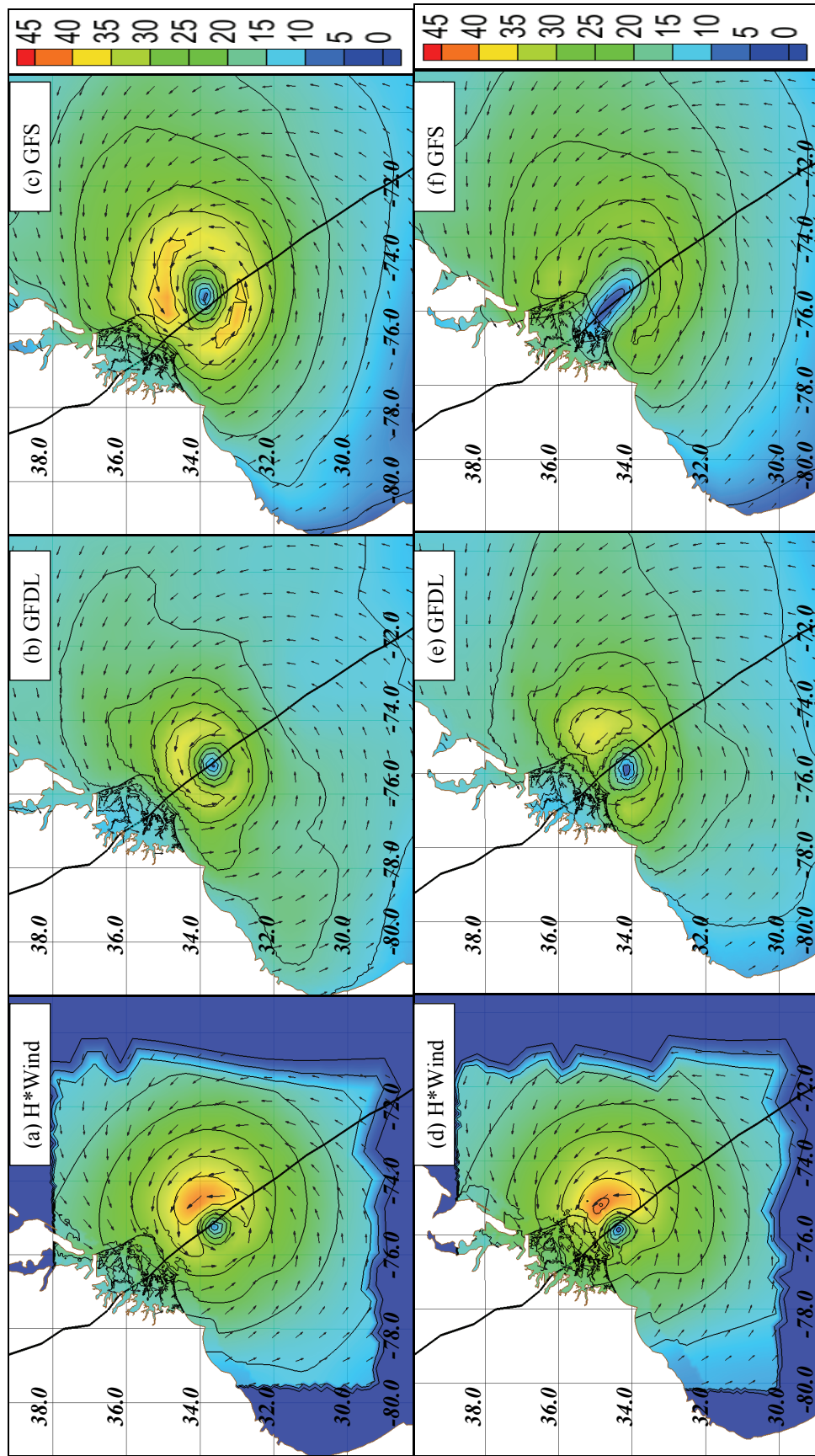


Figure 20. Track of Isabel (solid black line) and wind speeds at 10 m height in  $\text{ms}^{-1}$  for Isabel: H\*Wind (a), GFDL (b), and GFS (c) at 1200 UTC September 18, and H\*Wind (d), GFDL (e), and GFS (f) at 1500 UTC September 18.

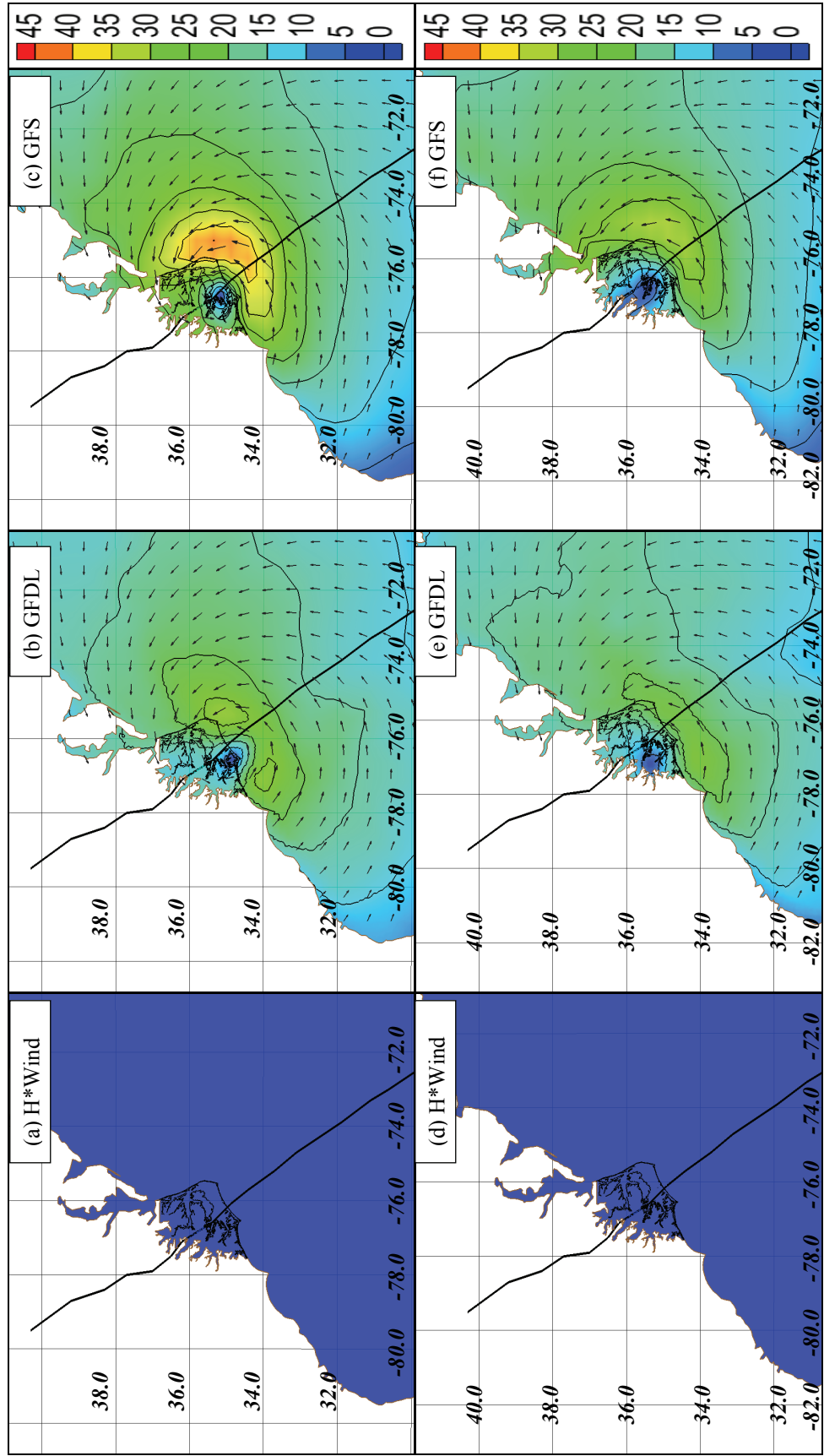
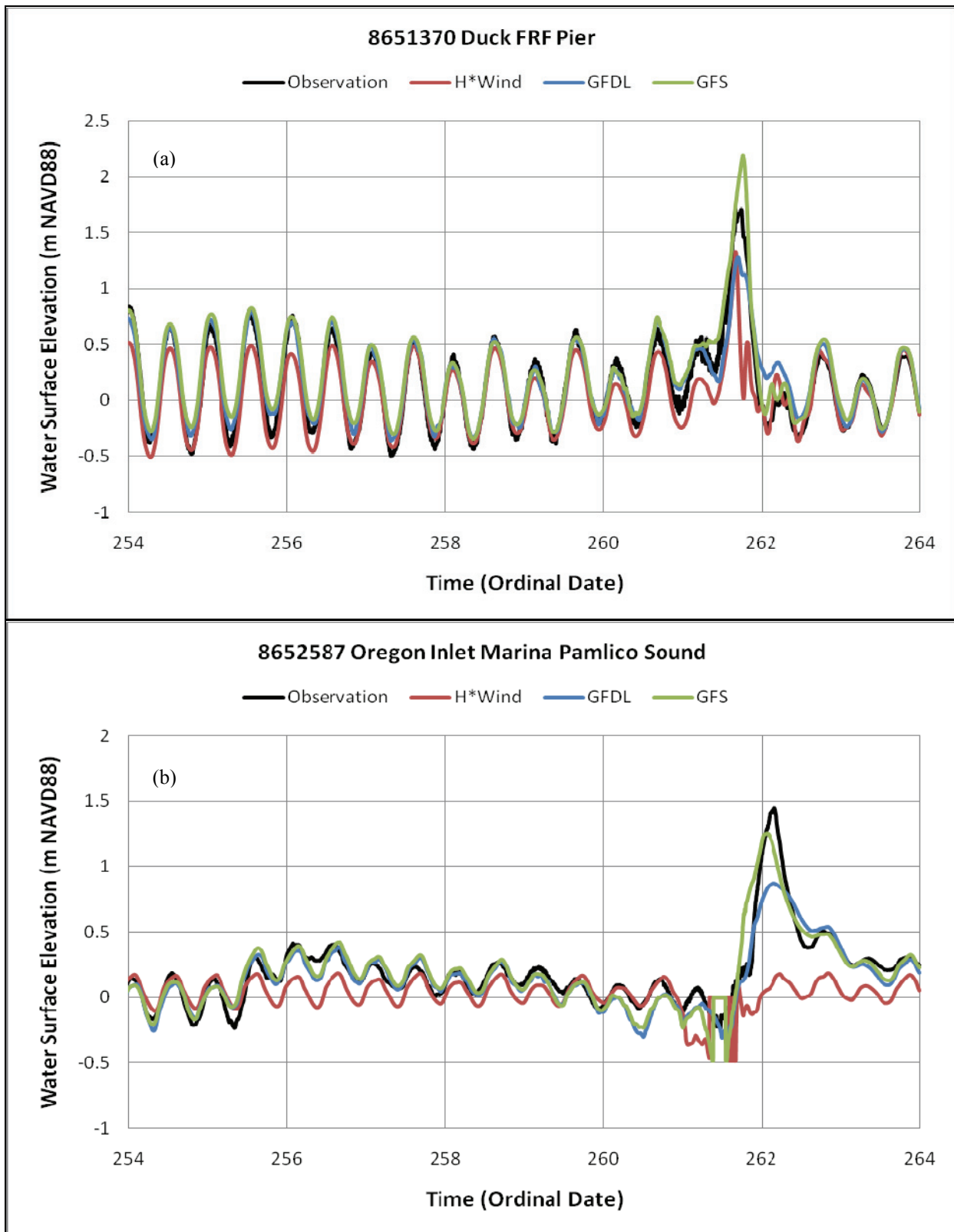


Figure 21. Track of Isabel (solid black line) and wind speeds at 10 m height in  $\text{ms}^{-1}$  for Isabel: H\*Wind (a), GFDL (b), and GFS (c) at 1800 UTC September 18, and H\*Wind (d), GFDL (e), and GFS (f) at 2100 UTC September 18.

## 6.2. Validation of Water Surface Elevation

Time series of water surface elevation are compared with observed water surface elevation at NOS tide gauge stations (see Table 2 and Figure 4). Simulations are run for 14 days, from 0000 UTC September 7 to 0000 UTC September 21, with a 4 day hyperbolic tangent ramping function and a 2 second time step. Time series of water surface elevation are saved at 6-min intervals from 254 to 264 in ordinal date (September 10 to 21). Comparison figures are shown in Figure 22 and 23. Boundary condition forcing is specified by harmonic constants for 5 tidal constituents from Schwiderski's global tidal model (Schwiderski 1980) as used in Luettich et al. (1994). The eddy viscosity coefficient is set to  $5.0 \text{ m}^2/\text{s}$ , and a hybrid quadratic bottom friction formulation is specified which applies a traditional quadratic function. A non-dimensional friction coefficient of 0.0025 in water deeper than 0.50 m is applied, and this coefficient increases exponentially in water shallower than 0.50 m to represent the increased friction during overland inundation (see Appendix B.3)

As shown in Figure 22a, the peak surge as well as the time of arrival of the surge compare very well with the observations at the Duck Field Research Facility (FRF) Pier. Peak surge from H\*Wind is lower than observations because of the absence of the inverted barometer effect. The Oregon Inlet Marina station (Figure 22b) is located inside of Pamlico Sound and just north of the inlet. The tidal signal is relatively small at this location compared to the Atlantic side. After Isabel made landfall, the wind turned from east/southeast to south and southwest and drove the water in Pamlico Sound up against the east side of the sound, causing a water level rise at the Oregon Inlet Marina station. GFDL and GFS both capture this water level rise in the Pamlico Sound. Since H\*Wind does not provide wind data after Isabel made landfall, there is no surge inside the sound as the storm passes, but only the tidal signal. At the Cape Hatteras Fishing Pier (Figure 23a) the tide gauge was destroyed before the peak storm surge arrived, so it is not possible to capture the peak surge. Storm surge from each model starts lower than the observations but does capture the rate of rise of the water. At the Beaufort Duke Marine Lab located inside Beaufort Inlet (Figure 23b), the GFDL results in the best match with the observations.



**Figure 22. The comparison of water surface elevations provided by H\*Wind (red), GFDL (blue), and GFS (green) with observations (black) at Duck FRF Pier (a) and Oregon Inlet Marine Pamlico Sound (b).**

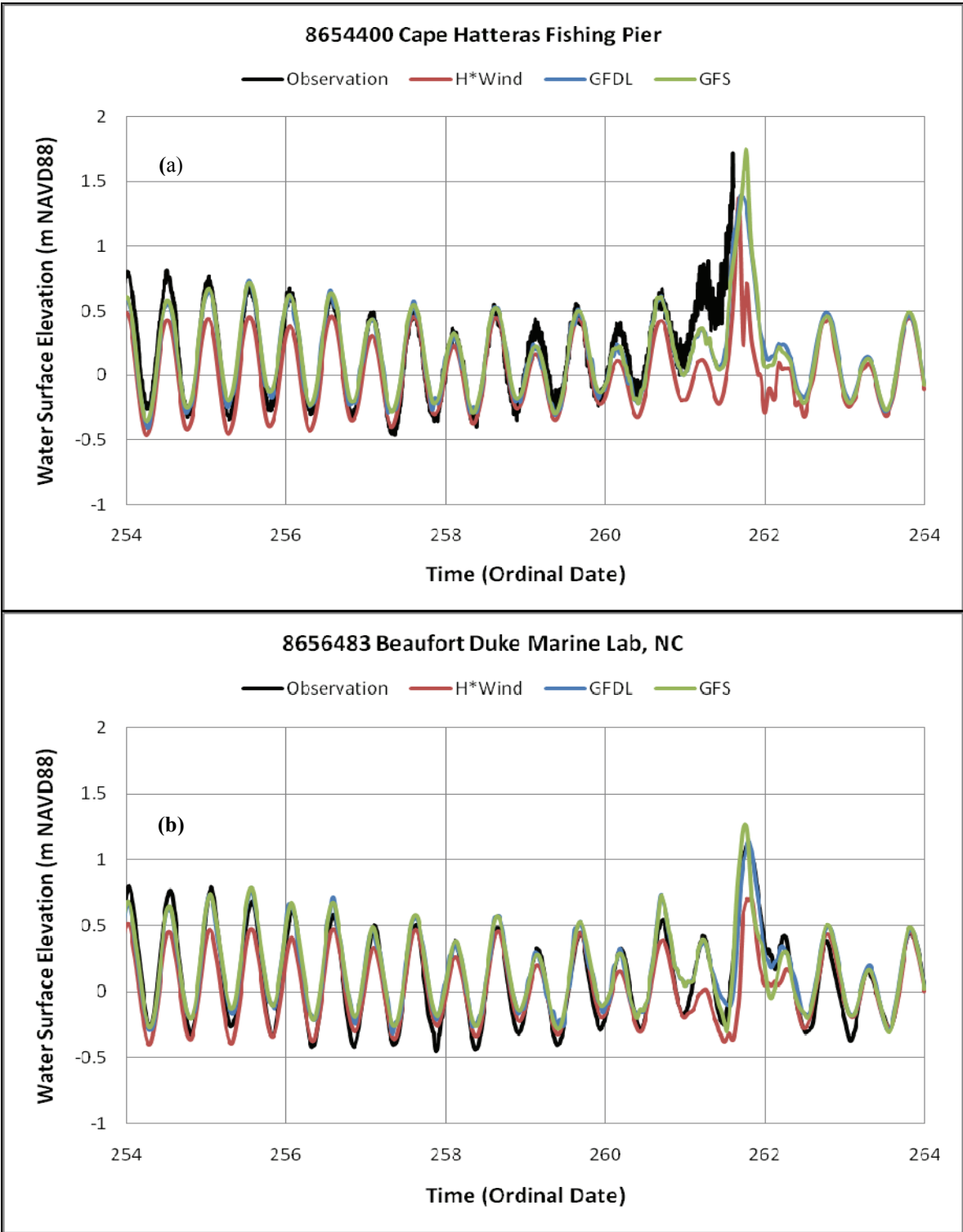


Figure 23. The comparison of water surface elevations provided by H\*Wind (red), GFDL (blue), and GFS (green) with observations (black) at Cape Hatteras Fishing Pier (a) and Beaufort Duke Marine Lab (b).

### 6.3. Validation of High Water Marks

According to the FEMA report, the highest storm surge occurred across the lower reaches of the Neuse and Pamlico Rivers. On the Neuse River, the highest surge was between Clubfoot Creek and Adams Creek where water rose to 3.2 m above NAVD 88. Significant flooding was reported in the Harlowe area in Craven Country and in the Town of Oriental in Eastern Pamlico County. Water levels rose 1.80 and 2.10 m on the Pamlico River, causing flooding in the City of Washington, NC.

Figure 24 illustrates the spatial distribution of maximum storm surge in the basin-scale CFM along with plots of 160 FEMA CHWM values; Figures 24 (a-c) show the entire basin-scale CFM domain and (d-f) show an enlargement of the west side of Pamlico Sound, including the Neuse and Pamlico Rivers. Figure 24 includes results driven by each meteorological model; from left to right, H\*Wind, GFDL and GFS, respectively. H\*Wind produces strong onshore wind effects and higher maximum peak surge than GFDL and GFS around the Pamlico-Neuse region. However, the missing wind after landfall, blowing from west/southwest to east/northeast, causes lower surge and no water rise inside Pamlico and Albemarle Sounds (see Figure 22b at Oregon Inlet Marina, Pamlico Sound). GFDL and GFS result in a similar distribution throughout the domain; however GFDL produces lower maximum peak surge because of a smaller storm in its forecast after 1200 UTC September 18.

Maximum storm surges from each run are compared to FEMA CHWMs (see Table A.1 and Figure 5). A total of 166 locations are surveyed by FEMA in October 2003. The 160 model/data pairs of values, excluding 6 locations due to undefined values, are subtracted from each other (i.e. modeled HWMs minus FEMA CHWMs) and a histogram of the differences are created as shown in Figures 25 and 26. The sample number of HWMs was limited to those flooded by each simulation. In H\*Wind, the HWM errors have a mean of -0.73 m NAVD 88 across 99 marks. HWM errors from GFDL and GFS have a mean of -0.63 m NAVD 88 across 100 marks and -0.63 m NAVD 88 across 102 marks, respectively. These error characteristics are depicted in the legend of Figures 25 and 26. As can be seen, most of the errors are negative, which means that FEMA CHWMs are larger than the model results. This is partially due to the fact that the FEMA CHWMs have a wave-induced contribution included in the storm surge value that is not included in our model.

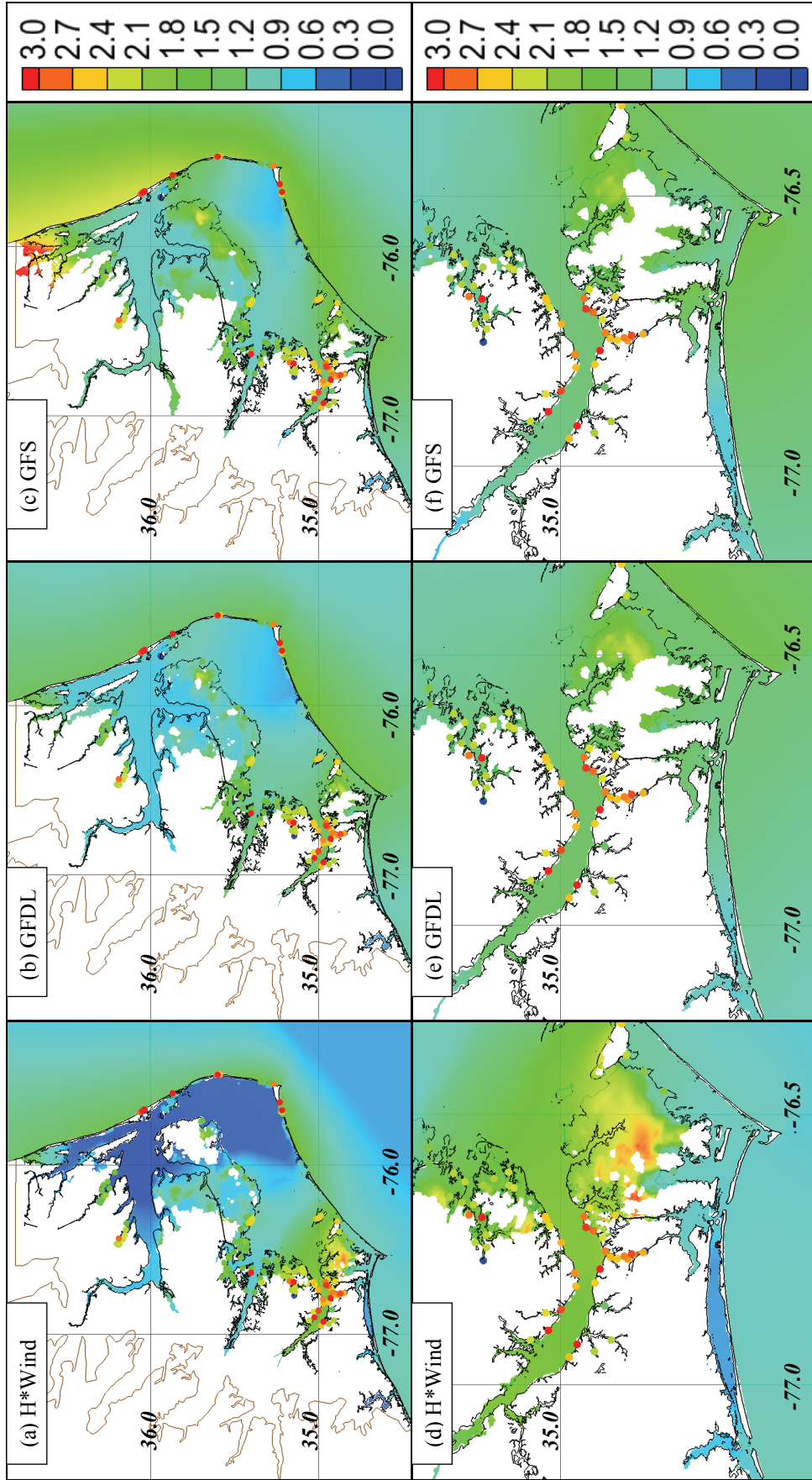
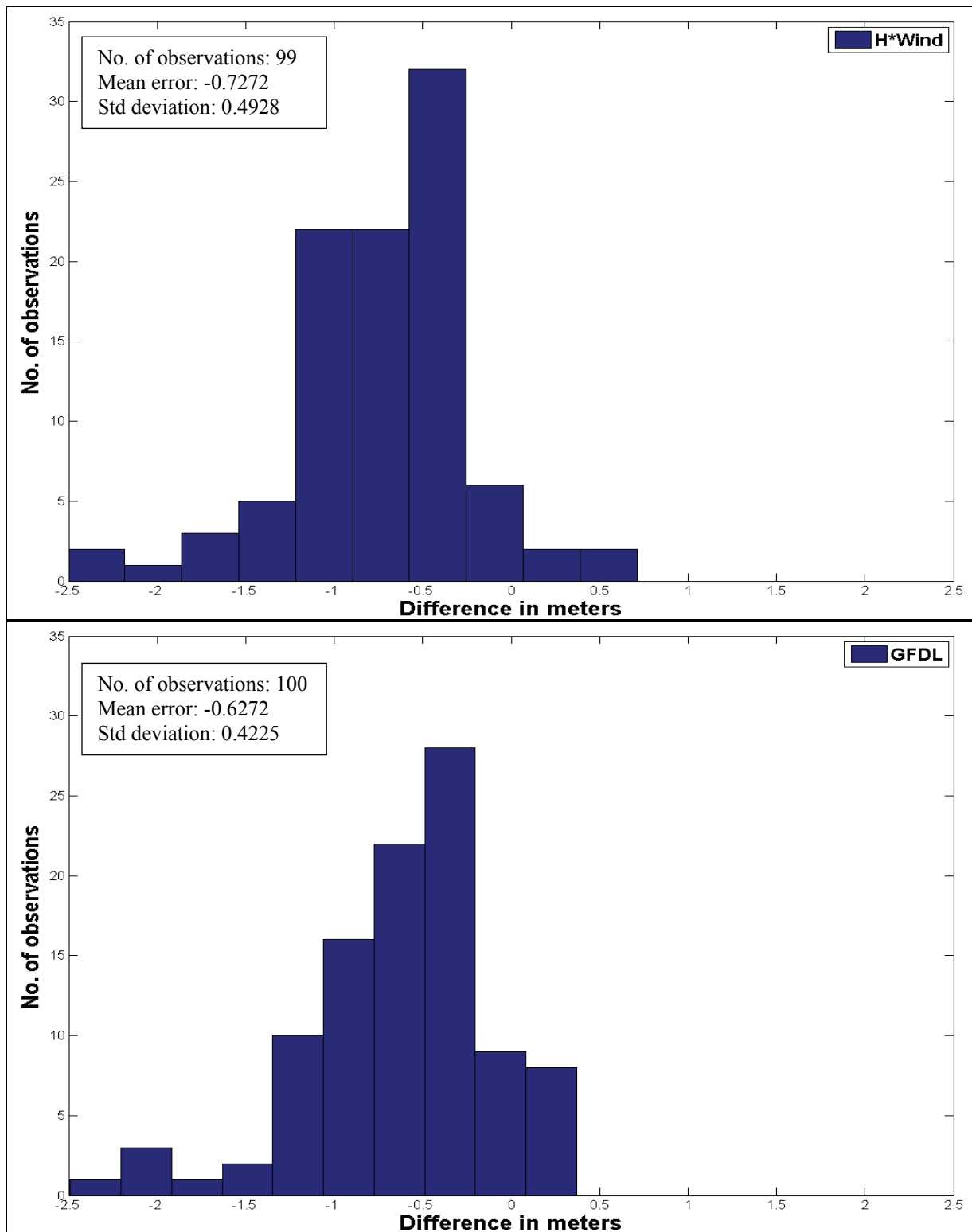
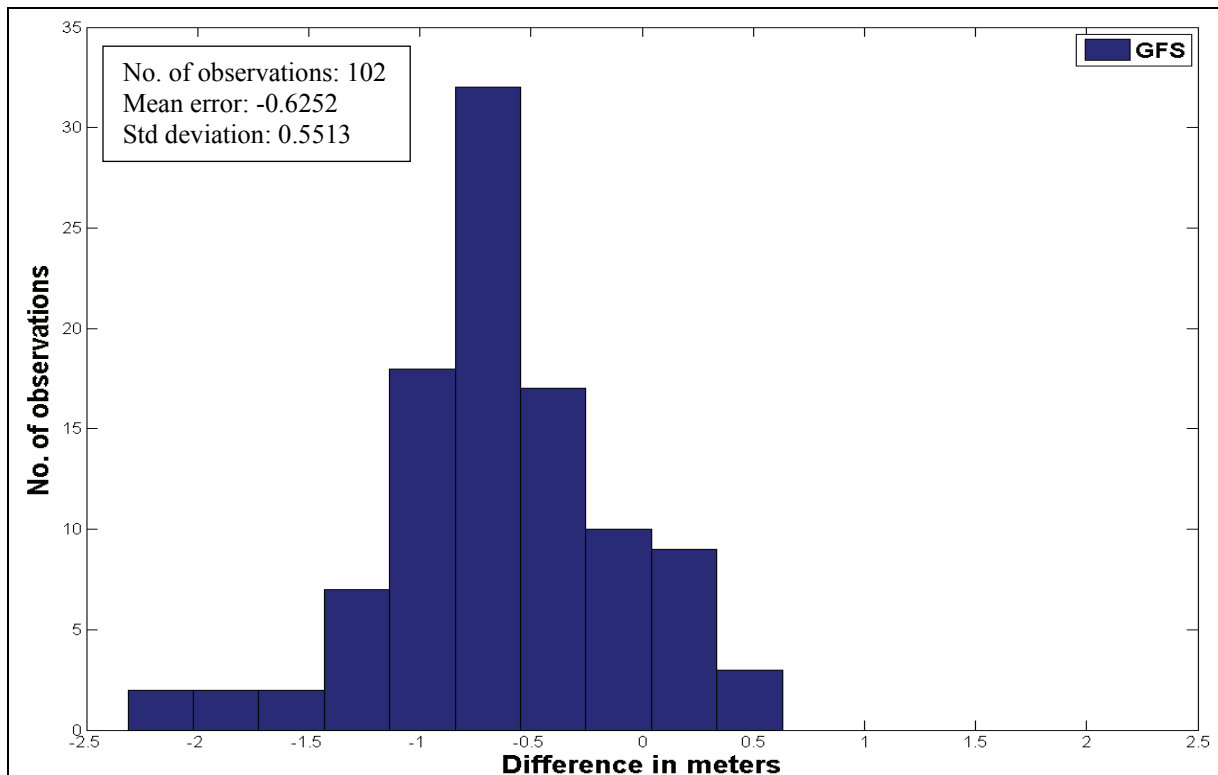


Figure 24. The distribution of maximum storm surge (m NAVD 88) in the basin-scale CFM from each meteorological model (from left to right H\*Wind, GFDL, and GFS); circles denote FEMA CHWMs; (a) – (c) illustrates the entire North Carolina sound system, and (d) – (f) show the enlargement of west side of Palmico Sound including the Neuse and Pamlico Rivers.



**Figure 25. The HWMs from H\*Wind (a) and GFDL (b) forcing minus observed FEMA HWMs for Hurricane Isabel (excluding marks that were not flooded in each simulation).**



**Figure 26. The HWMs from GFS forcing minus observed FEMA HWMs for Hurricane Isabel (excluding marks that were not flooded in the simulation).**

#### **6.4. Validation of Blended Meteorological Models**

The blended wind field is built by combining meteorological models to create the best available wind field (see Section 4.5). Figures 27 through 31 illustrate the comparison of blended model wind speeds and directions with the NDBC continuous wind data. The advantage of the blended wind field is that it combines the strong peak winds in the H\*Wind model with the far-field and post-landfall winds of the GFDL and GFS models. Additionally, the blending adds the pressure field from GFDL, which H\*Wind lacks.

Figures 32 and 33 show the comparison of time series of water surface elevation between the model and observations at NOS tide gauge stations. These plots indicate the advantages of the blended meteorological forcing. First, the pre-storm and post-landfall water levels are improved over those from the H\*Wind forcing due to the additional wind fields at those times. Second, the peak surge corresponds to the H\*Wind forcing, which provided the best peak across the North Carolina coast and sound system.

The distribution of maximum peak storm surge and plots of FEMA CHWM values are illustrated in Figure 34. Figure 35 illustrates the difference of HWMs (in m NAVD 88) between the blended model and FEMA CHWMs. HWM error has a mean of -0.40 m at 123 marks, which is a significant improvement over any of the individual meteorological model runs.

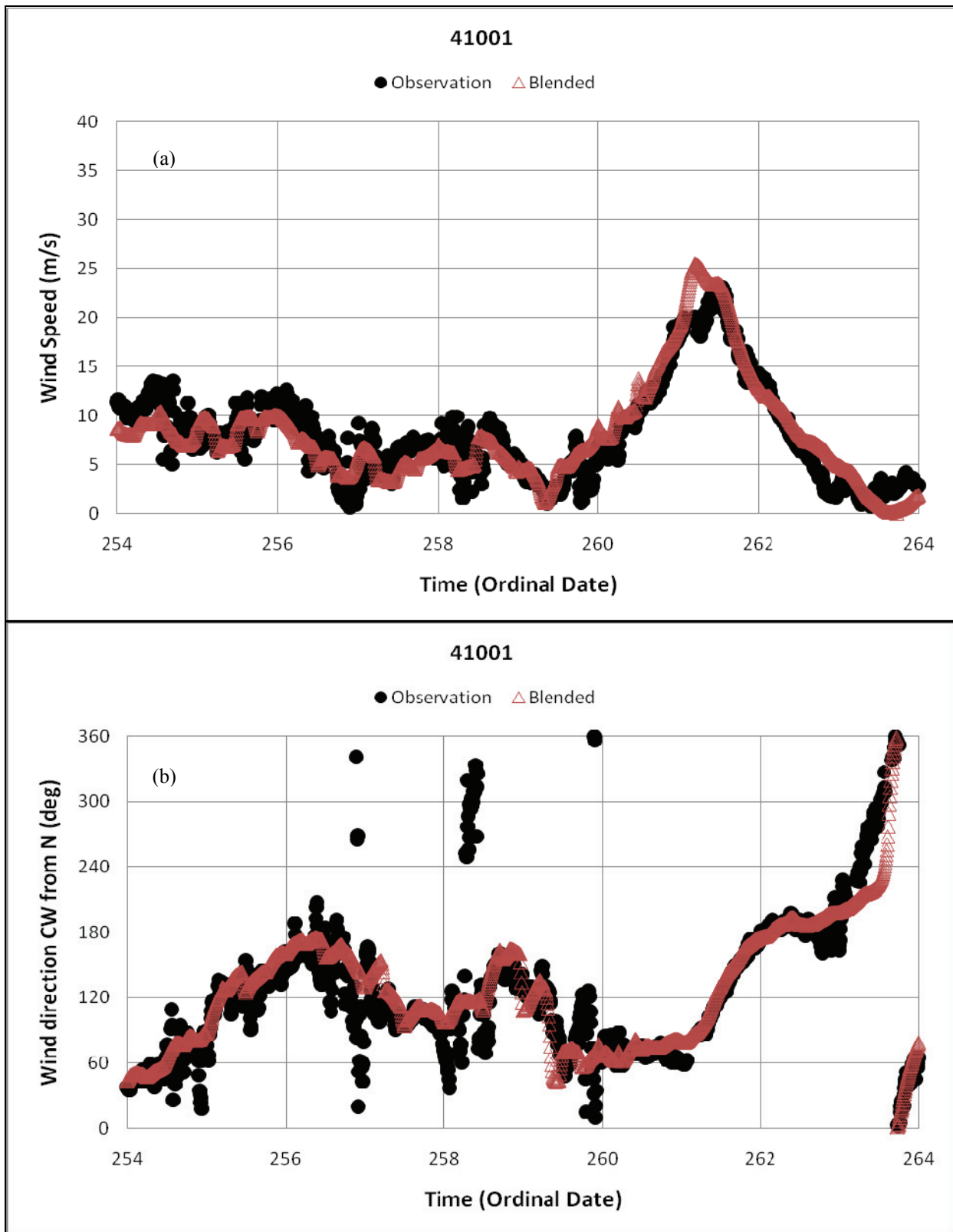


**Figure 27. The comparison of wind speed (a) and direction (b) provided by the blended models (red asterisk) with observations of NDBC continuous wind data (black dot) at NDBC location 41001.**

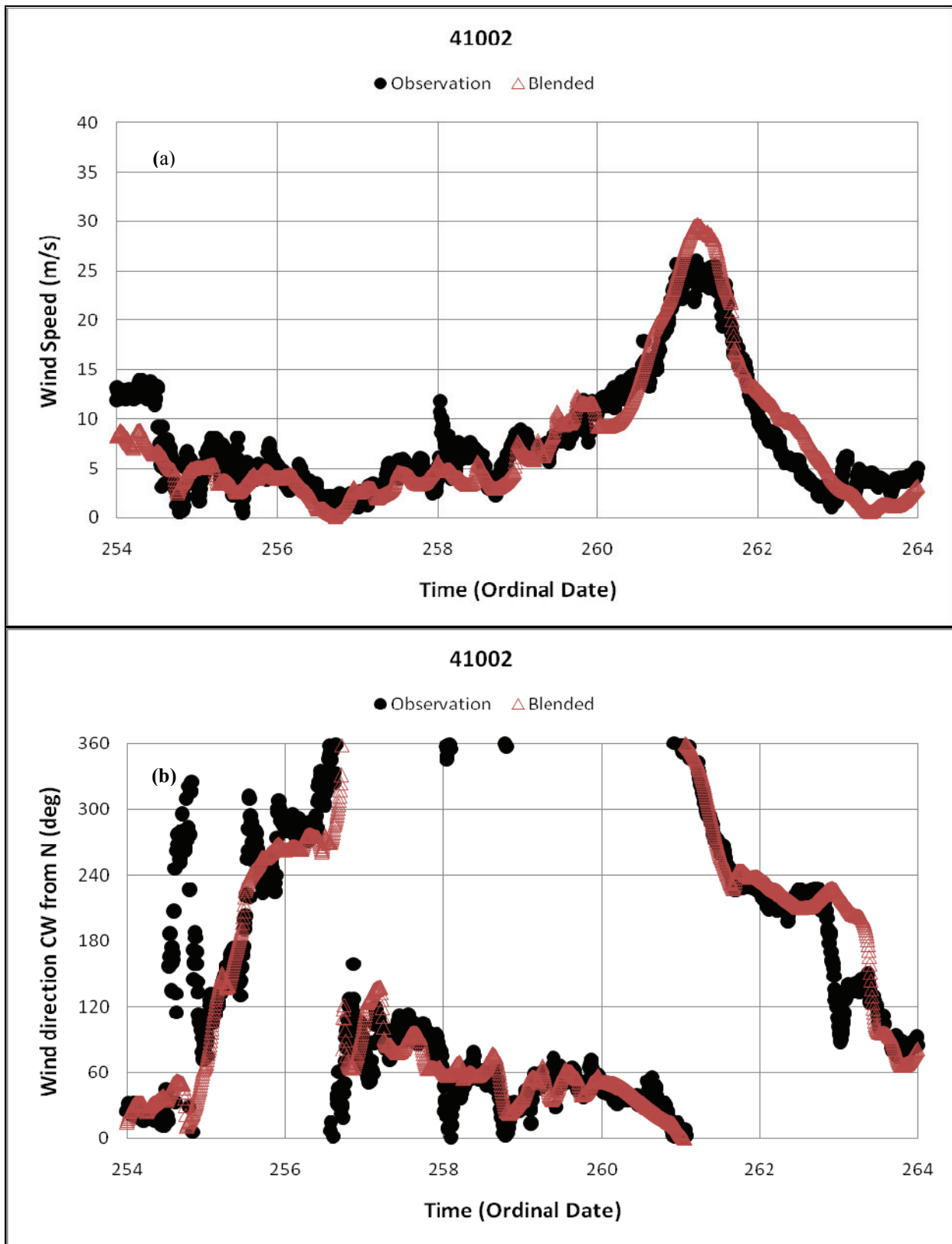


**Figure 28.** The comparison of wind speed (a) and direction (b) provided by the blended models (red asterisk) with observations of NDBC continuous wind data (black dot) at NDBC location 41002.

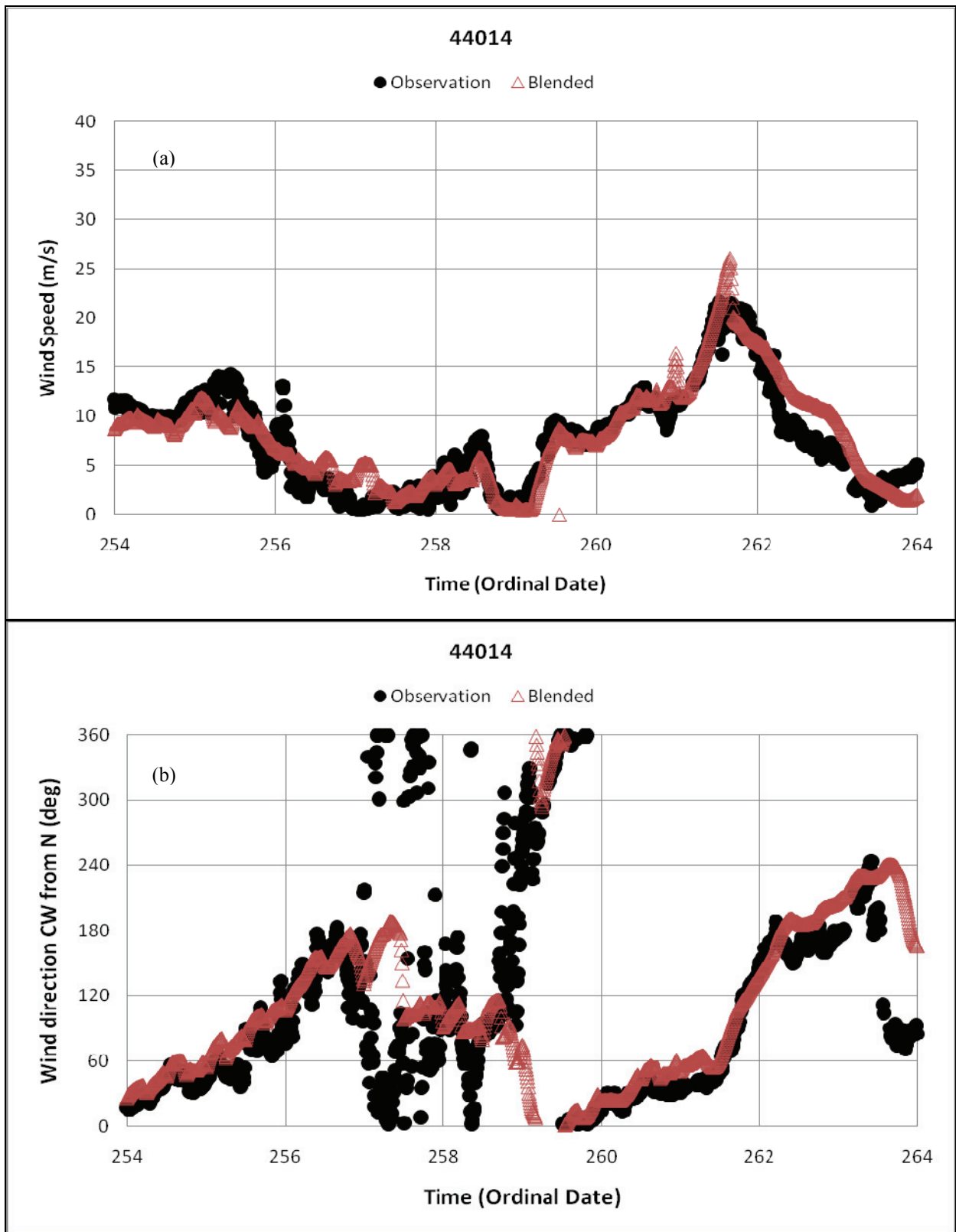


**Figure 29.** The comparison of wind speed (a) and direction (b) provided by the blended models (red asterisk) with observations of NDBC continuous wind data (black dot) at NDBC location 44014.

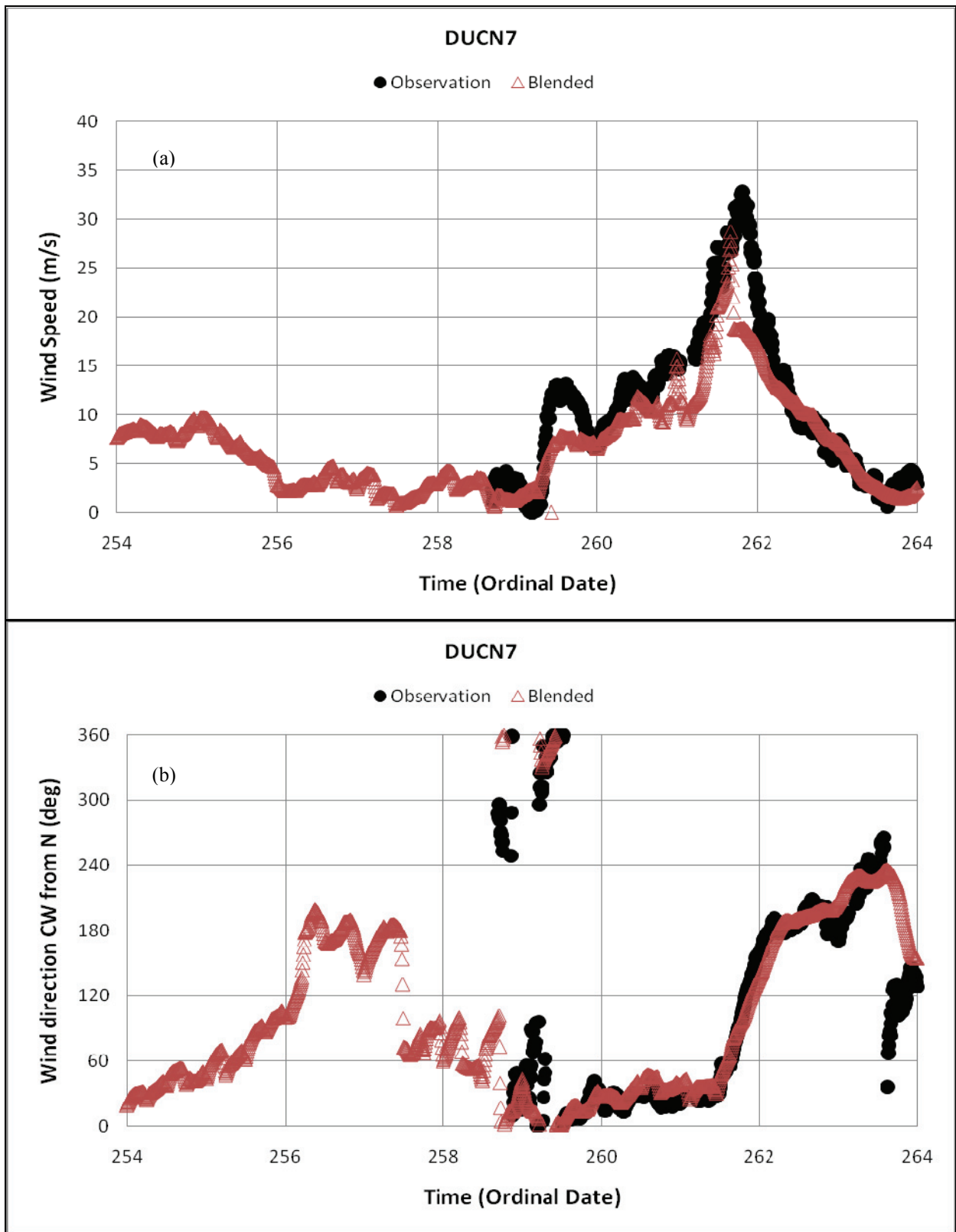


**Figure 30.** The comparison of wind speed (a) and direction (b) provided by the blended models (red asterisk) with observations of NDBC continuous wind data (black dot) at NDBC location DUCN7.

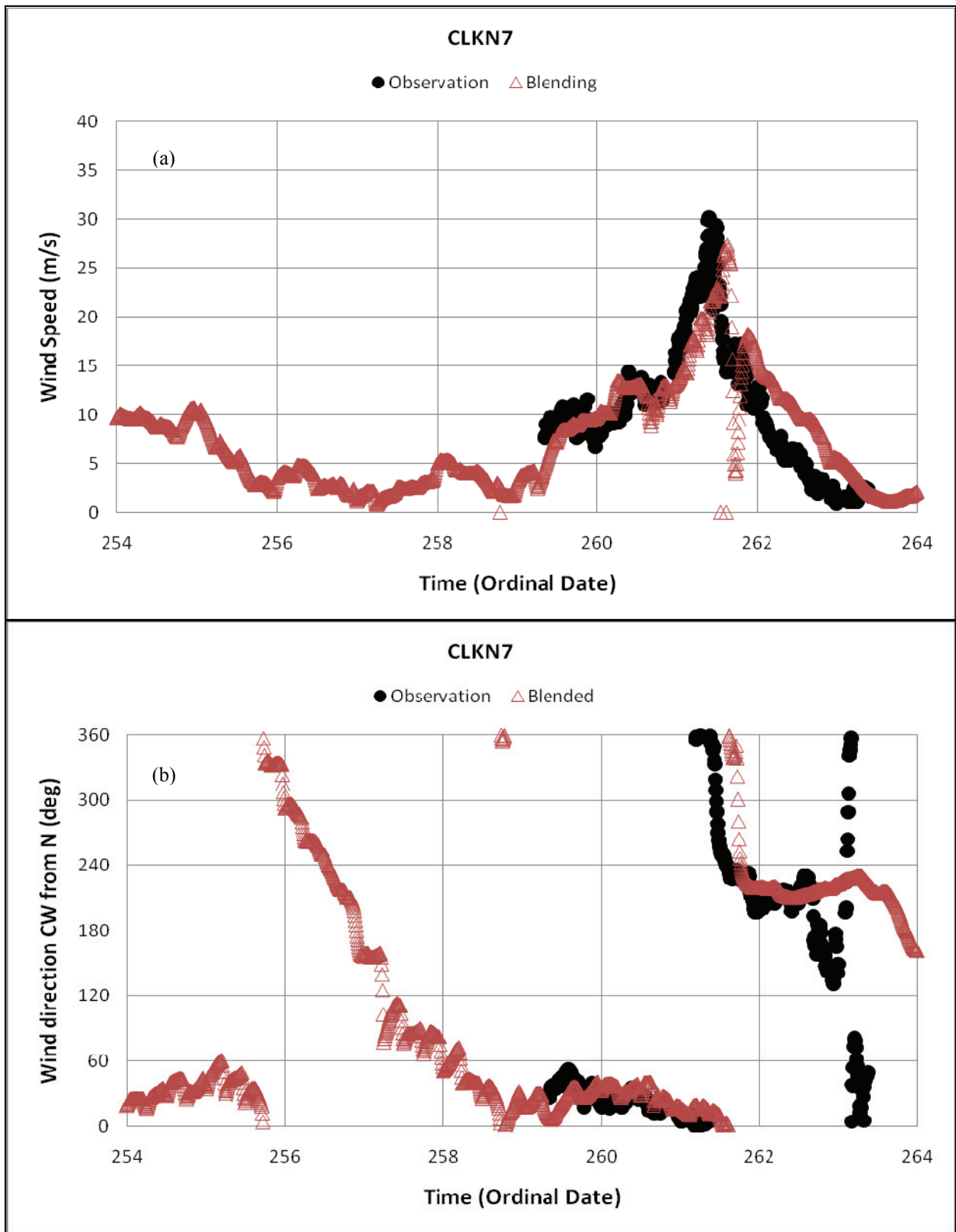


**Figure 31.** The comparison of wind speed (a) and direction (b) provided by the blended models (red asterisk) with observations of NDBC continuous wind data (black dot) at NDBC location CLKN7.

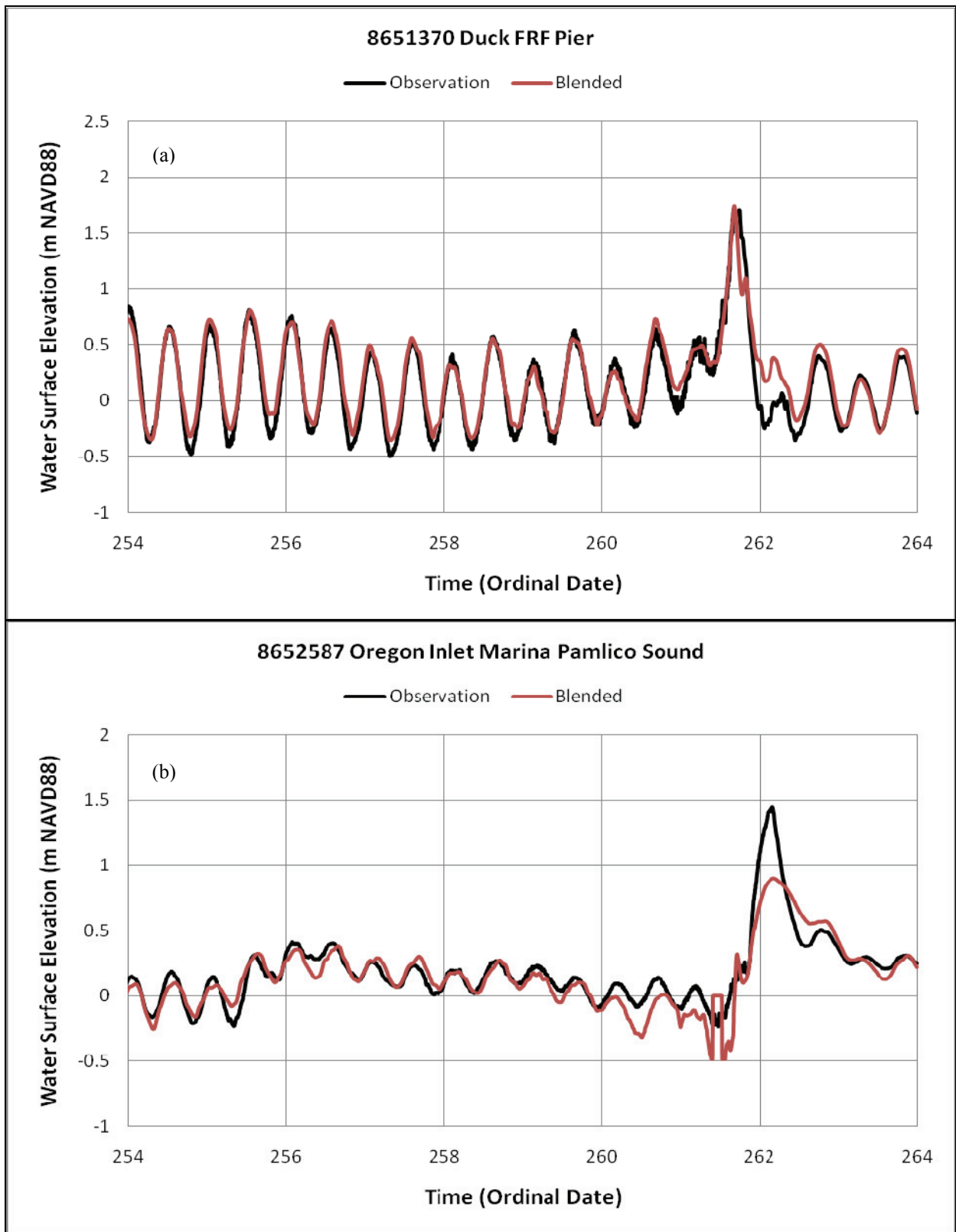


**Figure 32. The comparison of water surface elevations provided by the blended meteorological forcing (red) against observations (black) at Duck FRF Pier (a) and Oregon Inlet Marine Pamlico Sound (b).**

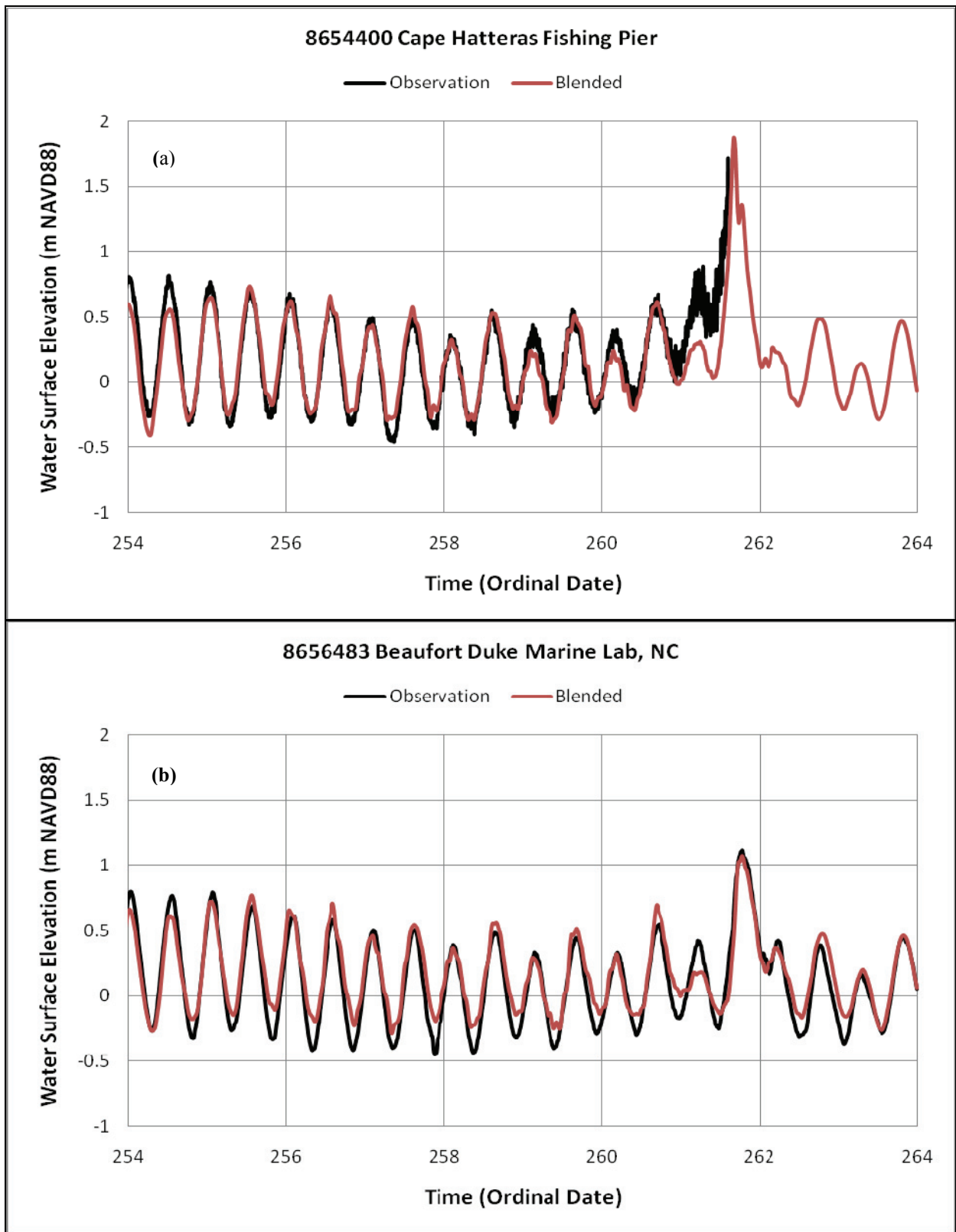


**Figure 33. The comparison of water surface elevations provided by the blended meteorological forcing (red) against observations (black) at Cape Hatteras Fishing Pier (a) and Beaufort Duke Marine Lab (b).**

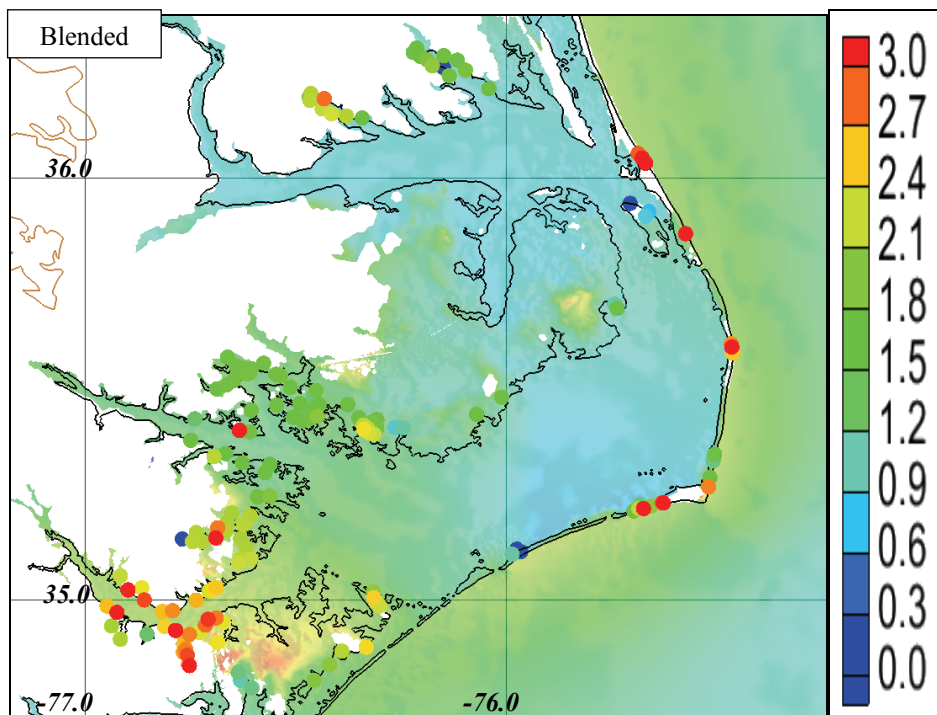


**Figure 34. The distribution of maximum storm surge (m NAVD88) in the North Carolina sound system from the blended meteorological forcing; circles denote FEMA CHWMs.**

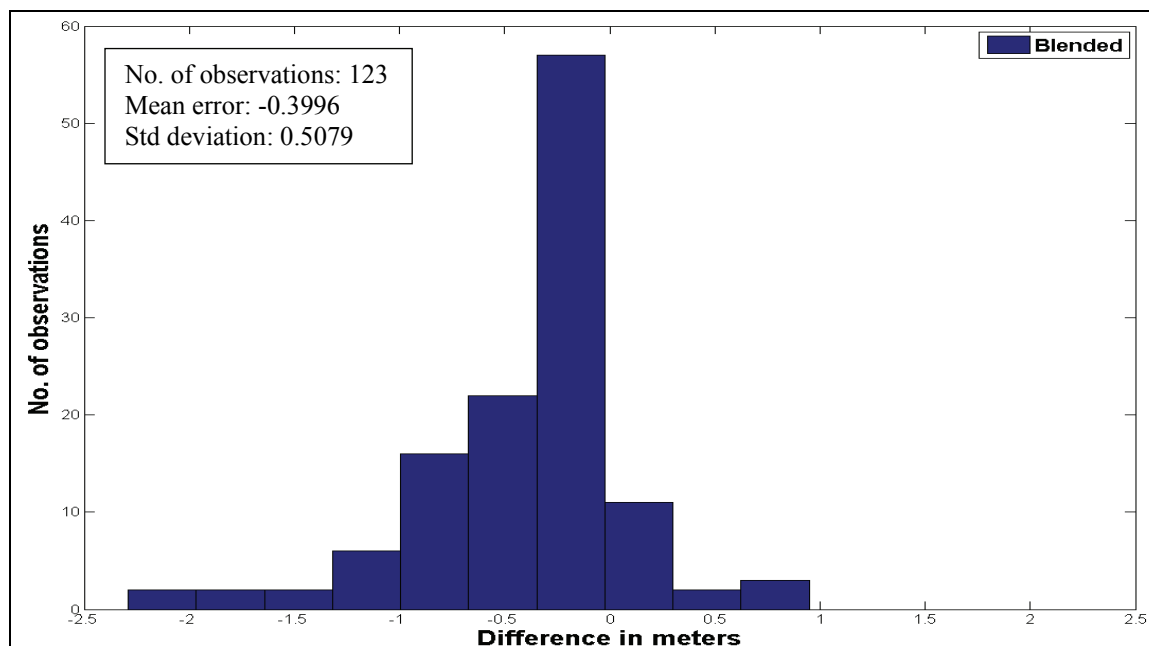


**Figure 35. The HWMs from the blended meteorological forcing minus observed FEMA HWMs for Hurricane Isabel (excluding marks that were not flooded in the simulation).**

## 6.5. Validation of Lateral Boundary Conditions

Three types of the lateral boundary condition are provided to the regional CFM at each node along the open ocean boundary: 1) periodic tidal forcing using harmonic tidal constituents derived from the East Coast 2001 (EC2001) database (Mukai et al., 2001); 2) barotropic water level time series using WSE obtained from the basin-scale CFM; and 3) baroclinic water level time series using SSH from RTOFS. With RTOFS SSH, two cases of the lateral boundary condition are applied here. The first case is SSH including the mean dynamic sea surface topography caused by baroclinic effects along with the barotropic signal. The second case is SSH without mean dynamic topography, obtained by filtering to remove the 14 day mean linear trend (detrending) in the SSH. Furthermore, subtidal water surface elevation, obtained by detiding the water surface elevation, is compared with detided observations. Since RTOFS uses 6-hour interval GFS forcing for its meteorological forcing, all of these simulations employ the same GFS forcing to make consistent comparisons.

Time series of water surface elevation are compared with the observations at four NOS tide gauge stations. Figures 36 and 37 show the comparison of time series of water surface elevation forced by three different types of the lateral boundary condition: 1) Tide (harmonic tidal constituents), 2) WSE provided by the basin-scale CFM, and 3) SSH from RTOFS. The simple tidal forcing is shown to underpredict the storm surge due to the lack of surge build-up on the shelf outside the regional CFM. By providing the lateral boundary condition from the basin-scale CFM the peak surge is improved at all locations. The lateral boundary condition provided by RTOFS results in a deviation of the modeled tidal signal in both amplitude and phase prior to the peak surge; RTOFS generates too large of a tidal signal whose phase slightly leads the observed time. More importantly, the lateral boundary condition from RTOFS does not do a better job in forcing the storm surge than the simple tidal forcing as they underpredict the surge by a similar amount.

Figures 38 and 39 illustrate the comparison of time series of water surface elevation forced by 1) the basin-scale CFM, 2) RTOFS, and 3) detrended RTOFS. By detrending, the long term mean primarily driven by baroclinic effects is removed, leaving the barotropic signal similar to the basin-scale CFM. The tidal signal and peak surge are significantly improved at Oregon Inlet Marina, Pamlico Sound; however, smaller improvements are recognized at other locations as well. In general, the error in the mean water level is improved but the under-predicted peak surge is not improved. These comparisons show that the basin-scale CFM provides better lateral boundary conditions than either RTOFS condition.

Figures 40 and 41 show the comparison of subtidal water surface elevation forced by 1) the basin-scale CFM, 2) RTOFS, and 3) detrended RTOFS, along with the observations at NOS tide gauge stations. Subtidal signals are calculated by subtracting the actual observations from NOS tidal predictions. It is clear that removing baroclinic effects from the RTOFS forcing results in noticeable improvements in the subtidal signal, but that the basin-scale CFM barotropic model does the best job of representing the ocean's meteorological response to the hurricane.

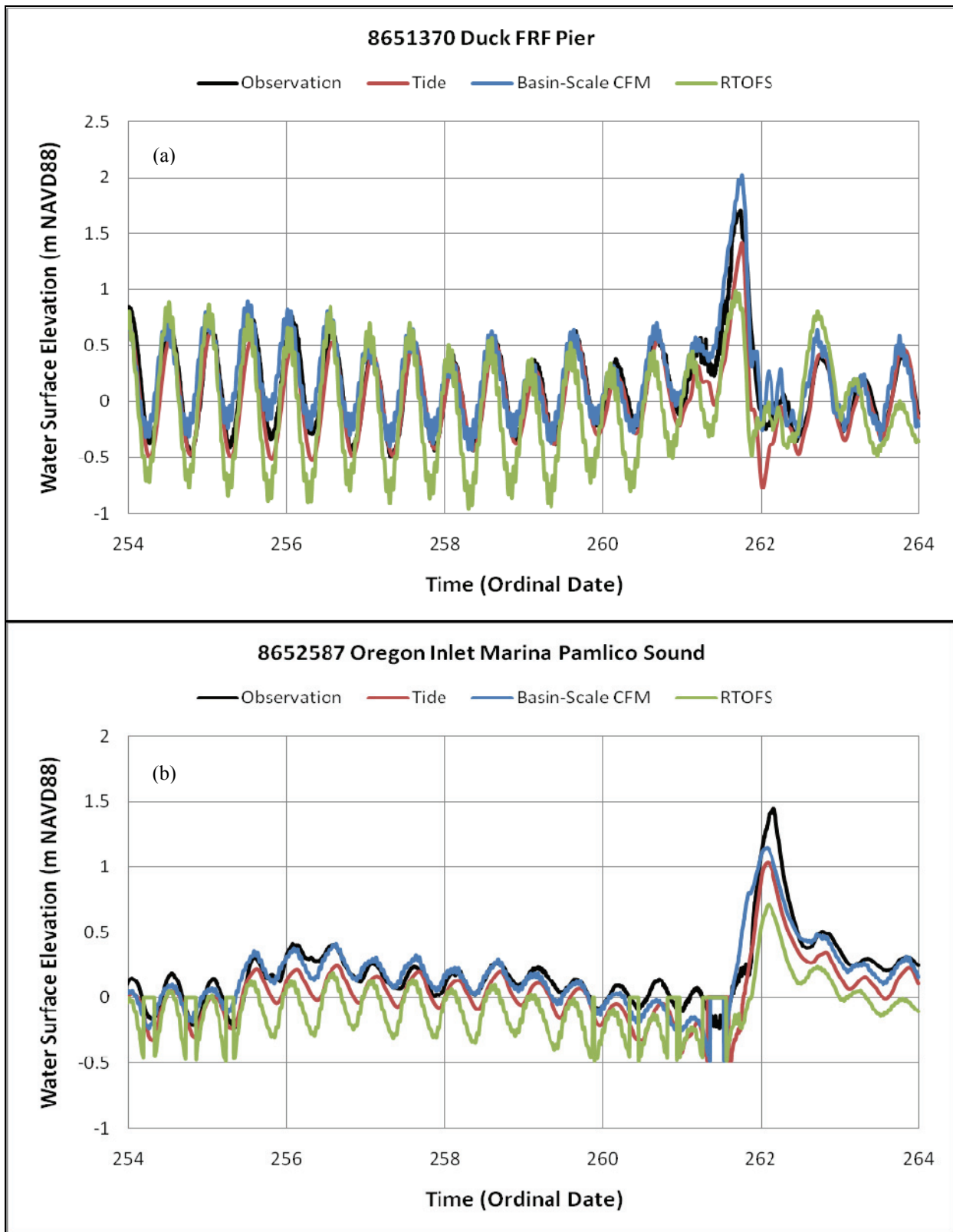


**Figure 36. The comparison of water surface elevations forced by tide (red), basin-scale CFM (blue), and RTOFS (green) lateral boundary conditions with observations (black) at Duck FRF Pier (a) and Oregon Inlet Marine Pamlico Sound (b).**

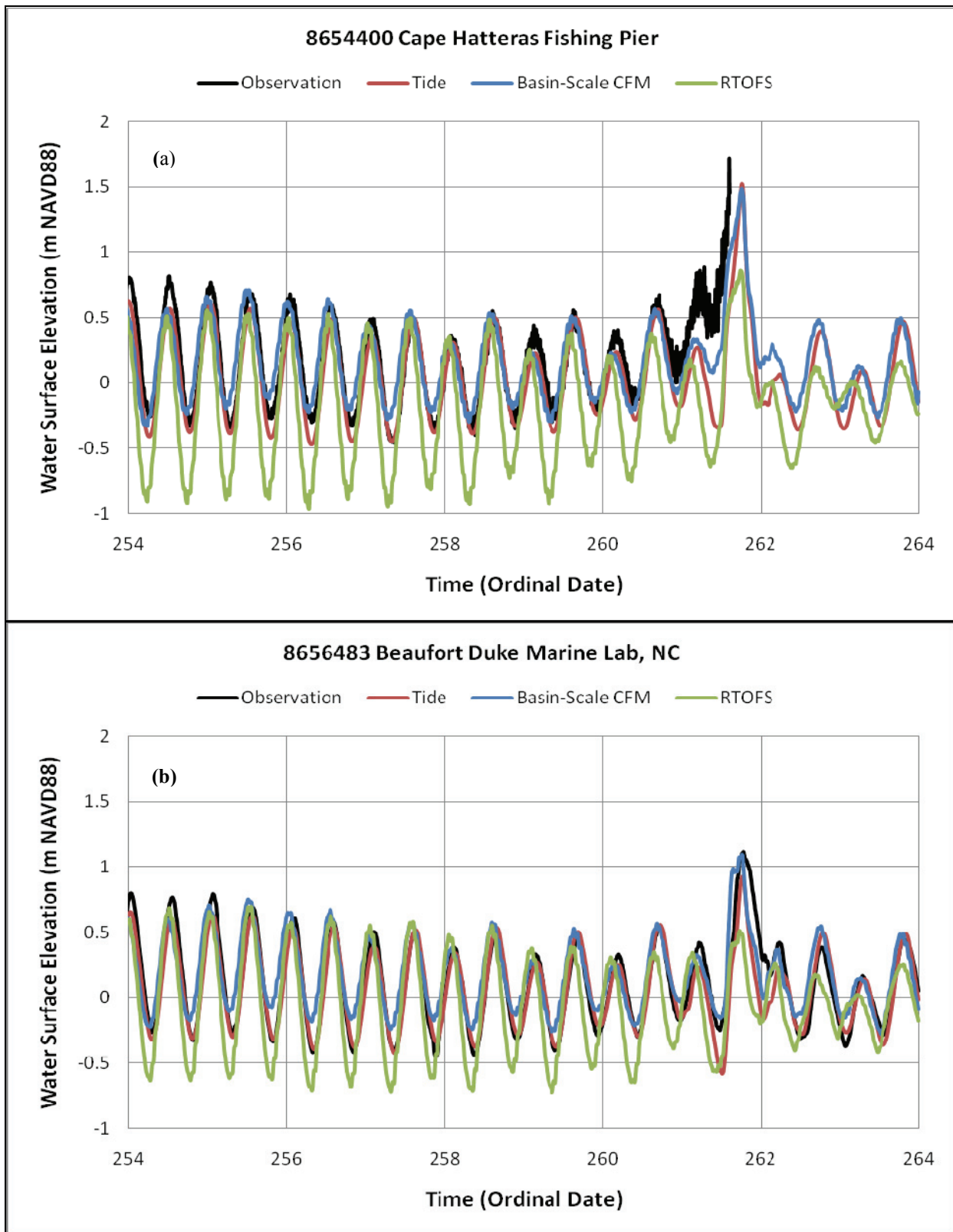


**Figure 37. The comparison of water surface elevations forced by tide (red), basin-scale CFM (blue), and RTOFS (green) lateral boundary conditions with observations (black) at Cape Hatteras Fishing Pier (a) and Beaufort Duke Marine Lab (b).**

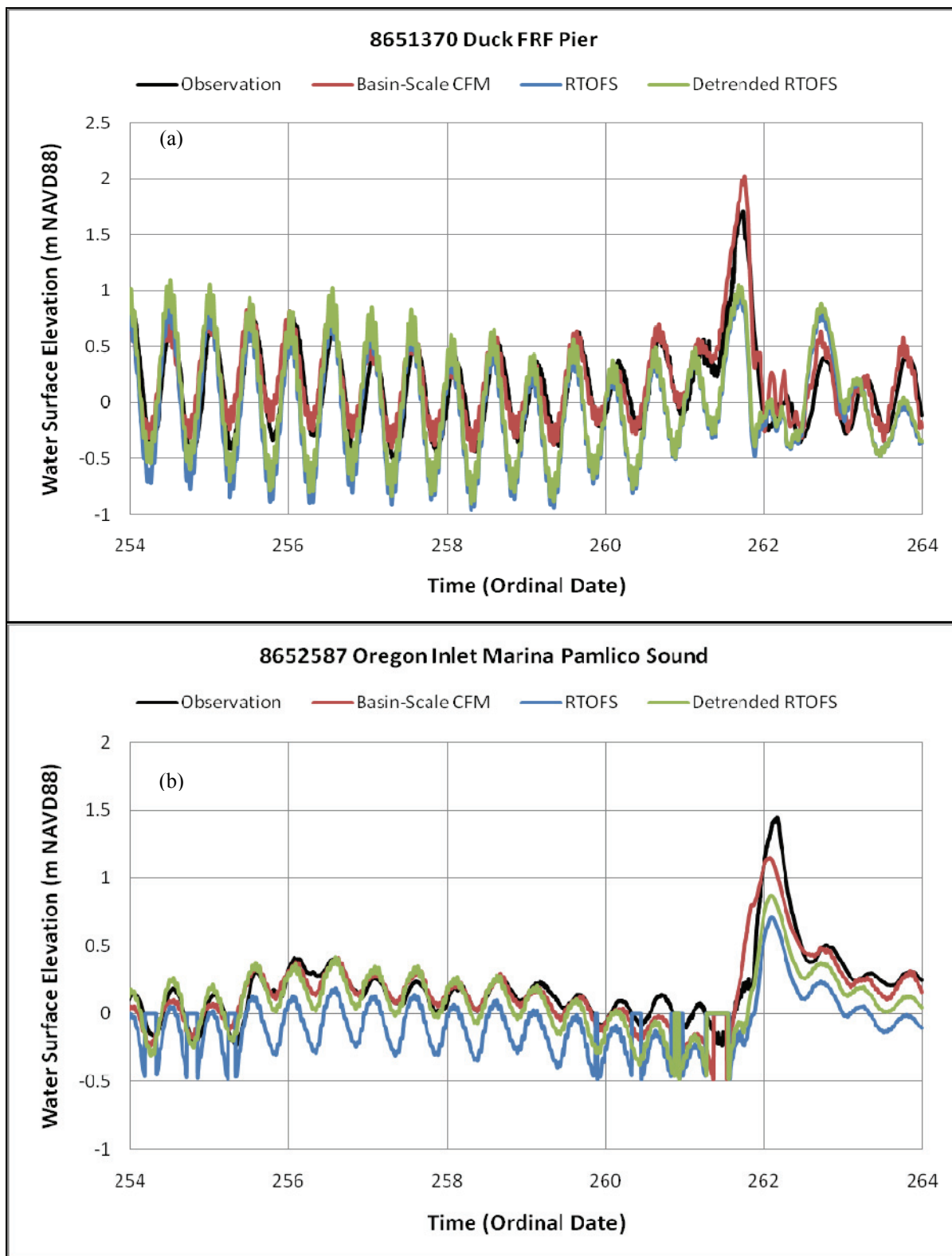


**Figure 38. The comparison of water surface elevations forced by basin-scale CFM (red), RTOFS (blue), and detrended RTOFS (green) lateral boundary conditions with observations (black) at Duck FRF Pier (a) and Oregon Inlet Marine Pamlico Sound (b).**

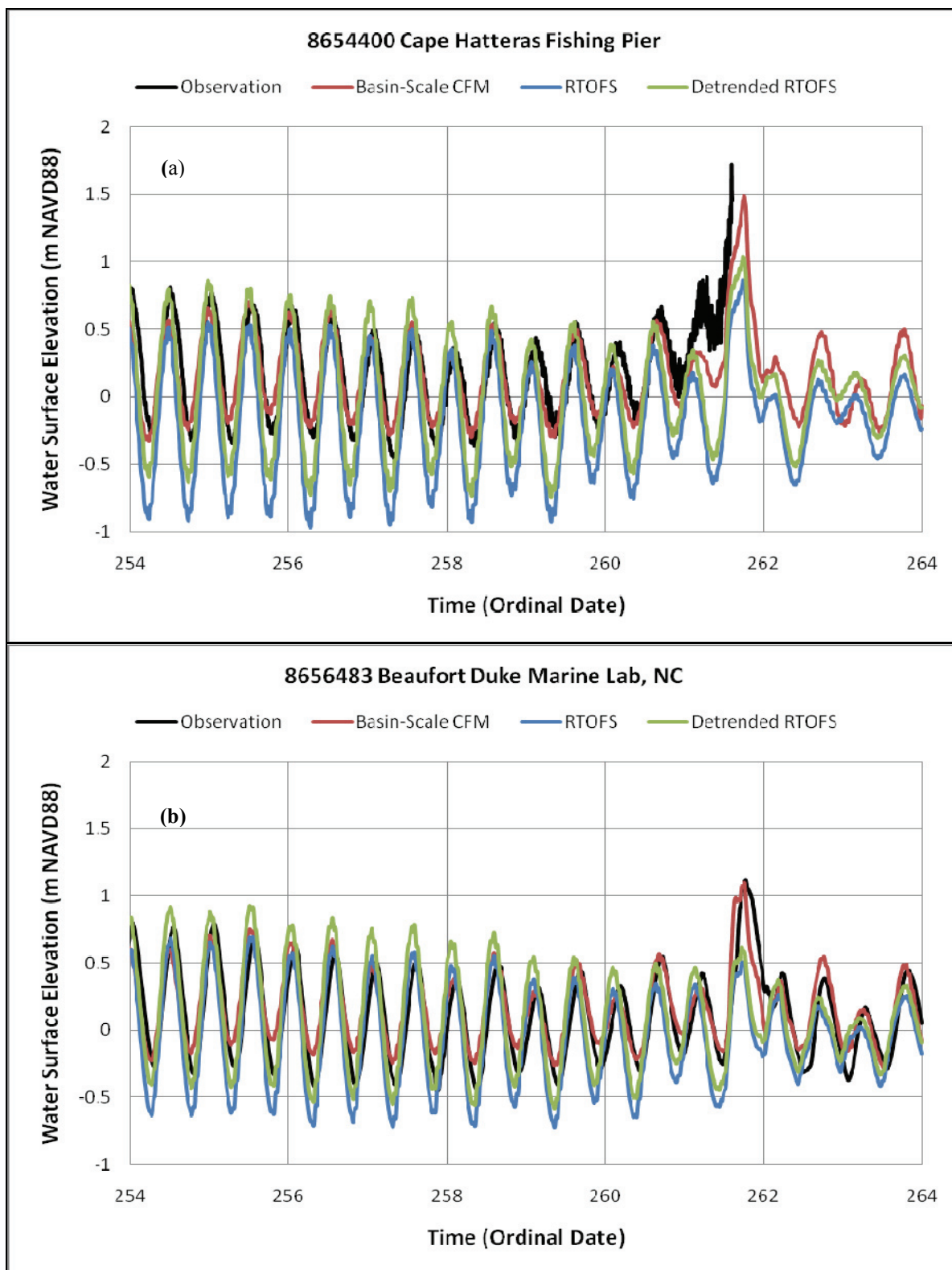


**Figure 39.** The comparison of water surface elevations forced by basin-scale CFM (red), RTOFS (blue), and detrended RTOFS (green) lateral boundary conditions with observations (black) at Cape Hatteras Fishing Pier (a) and Beaufort Duke Marine Lab (b).

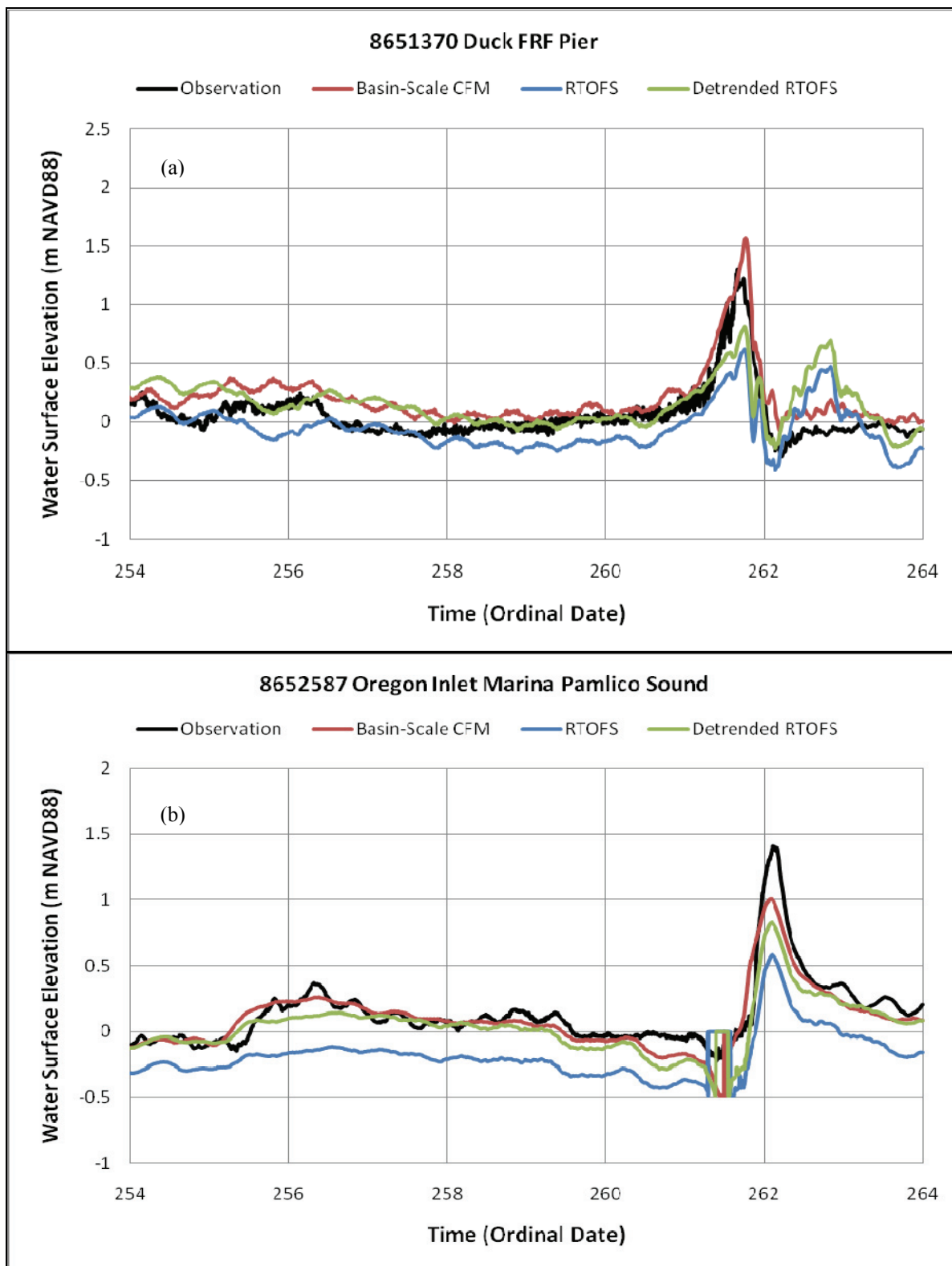


**Figure 40.** The comparison of subtidal water surface elevation forced by basin-scale CFM (red), RTOFS (blue), and detrended RTOFS (green) lateral boundary conditions with observations (black) at Duck FRF Pier (a) and Oregon Inlet Marine Pamlico Sound (b).

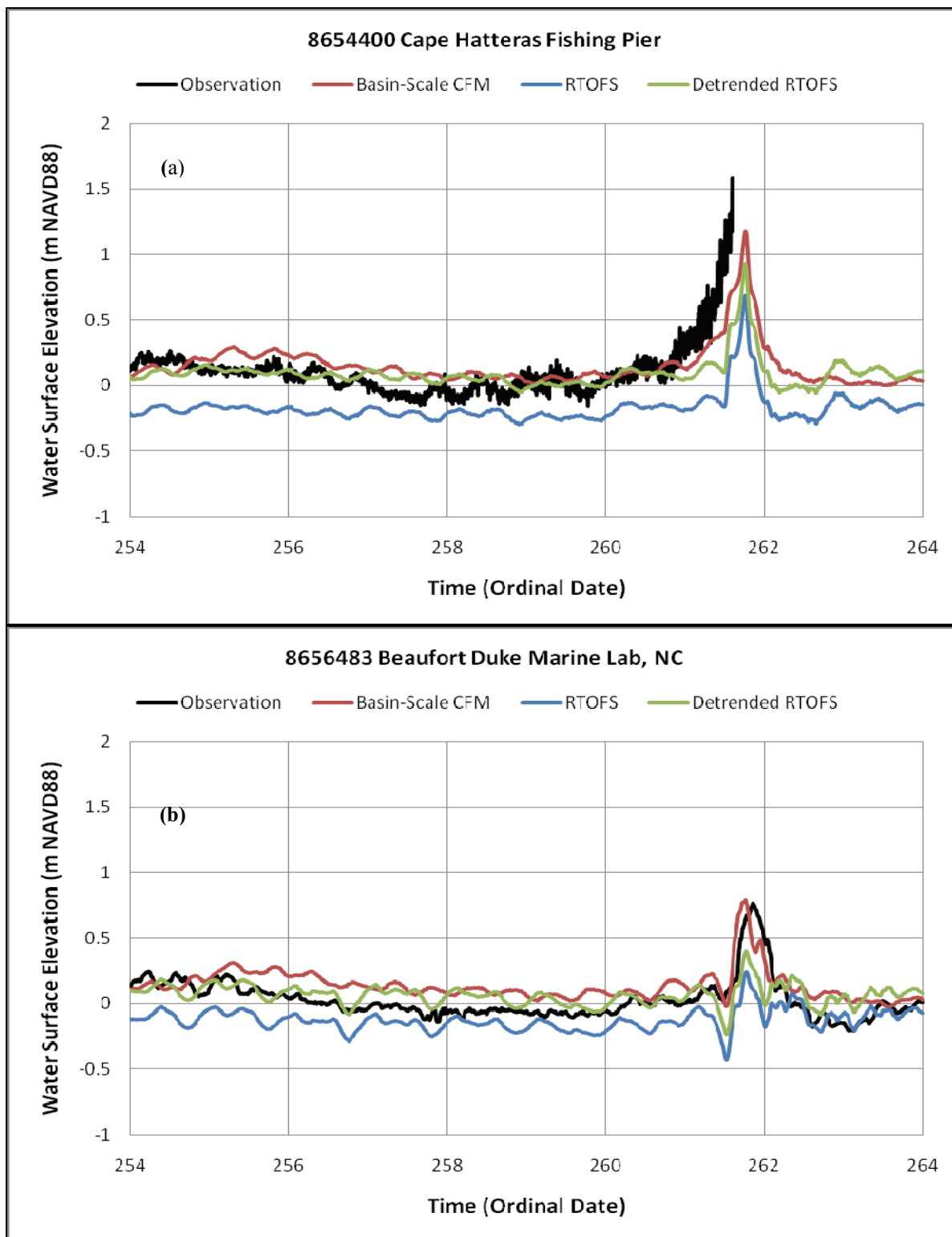


**Figure 41. The comparison of subtidal water surface elevation forced by basin-scale CFM (red), RTOFS (blue), and detrended RTOFS (green) lateral boundary conditions with observations (black) at Cape Hatteras Fishing Pier (a) and Beaufort Duke Marine Lab (b).**

## 6.6. Skill Assessment

Skill assessment is an objective measurement of the performance of a model when systematically compared with observations. NOS skill assessment criteria were created for evaluating the performance of operational nowcast/forecast circulation models (Hess et al., 2003), and a software package was subsequently developed to evaluate these criteria using standard file formats output from the models (Zhang et al., 2006). The software can compute the skill assessment automatically using files containing observations, predictions, and nowcast/forecast model results. A standard suite of skill assessment statistics is defined in Table 6 (Hess et al., 2003). In addition, peak differences (model peak minus observed peak) of amplitude (in meters) and phase (in minutes) are added to the skill assessment.

**Table 6. Skill assessment statistics**

Variable	Explanation
Error	The error is defined as the predicted value, $p$ , minus the reference (observed or astronomical tide value), $r$ : $e_i = p_i - r_i$ .
SM	Series Mean. The mean value of a series $y$ . Calculated as $\bar{y} = \frac{1}{N} \sum_{i=1}^N y_i$
RMSE	Root Mean Square Error. Calculated as $RMSE = \sqrt{\frac{1}{N} \sum_{i=1}^N e_i^2}$
SD	Standard Deviation. Calculated as $SD = \sqrt{\frac{1}{N} \sum_{i=1}^N (e_i - \bar{e})^2}$

## 6.7. Water Surface Elevation Skill Assessment

Skill assessment statistics are calculated for each model hindcast simulation (each meteorological forcing and lateral boundary condition forcing). Hurricane Isabel hindcast simulations are made from September 7 to September 21 2003, and time series of water surface elevation are saved in six minute intervals at locations where observations are available (see Table 2 and Figure 5). The last 10 days (September 10 to September 21 2003) in the simulation period are used for calculating skill assessment statistics. Due to failure of the Cape Hatteras Fishing Pier water level gauge, no peak difference could be computed and only the last 8 days (September 10 to September 18 2003) at this location are used for calculating skill assessment statistics. Filtering of values in a time series is common to remove short period variations and noise; however, filtering does not apply for these calculations in order to capture the peak surge.

The standard suite of statistics for hindcast simulations of the basin-scale CFM using different meteorological forcing are presented in Table 7. The RMSE at the four NOS tide gauges ranges from 0.11 m to 0.29 m. The H\*Wind forced simulation consistently has the highest RMSE because of its poor performance before and after the main storm winds. The GFS, GFDL, and blended forcings tend to have similar RMSE except at station 8656483 (Beaufort Duke Marine

Lab), where a larger RMSE reflects that the blended forcing does not do as well as GFDL and GFS before the main surge event.

Comparisons of peak storm surge heights and times of occurrence in both observations and simulations are shown in Table 8. The last two columns in Table 8 are peak difference in amplitude and phase, which is calculated by gauge peak minus model peak. The peak difference in amplitude and phase at the three NOS tide gauges range from -1.26 m and -108 minutes at Oregon Inlet Marina to 0.47 m and +120 minutes at Duck, FRF Pier. GFS produces approximately a two-hour peak difference in phase at two NOS tide gauge locations because the model is leading the data due to the overpredicted size of the storm. This might also be caused by the interpolated error in creating hourly meteorological forcing from the GFS' 6-hour update interval. These results clearly show an advantage in the blended forcing which almost uniformly has the smallest errors in peak height and timing.

The standard suite of statistics for the hindcast simulations of the regional CFM using different lateral boundary condition forcings are presented in Table 9. The RMSE indicates two things. First, it is seen that both RTOFS boundary conditions perform worse than either the tidal or the basin-scale CFM forcings, although detrending RTOFS to remove the baroclinic variability does help. Second, the basin-scale CFM is most consistent in minimizing RSME. Comparison of the peak storm surge heights and times of occurrence in both observations and simulations is shown in Table 10. Peak difference in amplitude ranges from -0.74 m at Oregon Inlet Marine to 0.31 m at Duck, FRF Pier. Lateral boundary conditions from the detrended RTOFS improve all values in comparison with RTOFS at the four NOS tide gauges, which indicates that the primarily baroclinic long term trend does not improve a barotropic storm surge prediction. The basin-scale CFM domain is shown to minimize error, particularly in the peak surge amplitude.

**Table 7. Skill assessment statistics of different meteorological forcings in the basin-scale CFM.**

NOS Station ID	Meteorological Forcing	SM	RMSE	SD
		(m)	(m)	(m)
8651370	H*Wind	-0.122	0.204	0.163
	GFDL	0.036	0.130	0.125
	GFS	0.082	0.126	0.095
	Blended	0.046	0.123	0.114
8652587	H*Wind	-0.122	0.286	0.259
	GFDL	-0.036	0.108	0.102
	GFS	-0.023	0.111	0.109
	Blended	-0.013	0.111	0.110
8654400	H*Wind	-0.171	0.241	0.169
	GFDL	-0.036	0.146	0.142
	GFS	-0.031	0.150	0.147
	Blended	-0.037	0.149	0.144
8656483	H*Wind	-0.092	0.182	0.156
	GFDL	0.054	0.111	0.097
	GFS	0.060	0.123	0.108
	Blended	0.048	0.181	0.175

**Table 8. The comparison of peak storm surge heights and times of occurrence in both observations and simulations in the basin-scale CFM.**

NOS Station ID	Gauge Peak	Time of Gauge Peak	Meteorological Forcing	Model Peak	Time of Model Peak	Peak Difference	
	(m NAVD 88)			(UTC)		(m NAVD 88)	(min)
8651370	1.716	9/18/2003 16:06	H*Wind	1.330	9/18/03 16:06	-0.386	0
			GFDL	1.283	9/18/03 16:54	-0.433	48
			GFS	2.189	9/18/03 18:06	0.473	120
8652587	1.439	9/19/2003 3:48	Blended	1.748	9/18/03 16:18	0.032	12
			H*Wind	0.186	9/19/03 5:18	-1.264	90
			GFDL	0.875	9/19/03 3:48	-0.575	0
			GFS	1.253	9/19/03 2:00	-0.197	-108
			Blended	0.988	9/19/03 3:24	-0.462	-24
			H*Wind	1.376	9/18/03 16:06		
8654400	N/A	N/A	GFDL	1.394	9/18/03 16:48	N/A*	N/A
			GFS	1.746	9/18/03 18:18		
			Blended	1.895	9/18/03 16:12		
8656483	1.121	9/18/2003 18:42	H*Wind	0.710	9/18/03 19:36	-0.412	54
			GFDL	1.147	9/18/03 19:06	0.026	24
			GFS	1.271	9/18/03 18:06	0.150	-36
			Blended	1.108	9/18/03 18:42	-0.013	0

\* N/A indicates no data was available for this analysis.

**Table 9. Skill assessment statistics of different lateral boundary condition forcings in the regional CFM.**

<b>NOS Station ID</b>	<b>L.B.C. Forcing</b>	<b>SM (m)</b>	<b>RMSE (m)</b>	<b>SD (m)</b>
8651370	Tide	-0.131	0.191	0.140
	Basin-Scale CFM	0.062	0.193	0.183
	RTOFS	-0.218	0.374	0.304
	Detrended RTOFS	-0.122	0.335	0.312
8652587	Tide	-0.147	0.182	0.106
	Basin-Scale CFM	-0.028	0.116	0.112
	RTOFS	-0.240	0.301	0.182
	Detrended RTOFS	-0.096	0.172	0.142
8654400	Tide	-0.140	0.222	0.172
	Basin-Scale CFM	-0.030	0.197	0.195
	RTOFS	-0.387	0.481	0.286
	Detrended RTOFS	-0.150	0.327	0.290
8656483	Tide	-0.040	0.115	0.108
	Basin-Scale CFM	0.059	0.184	0.175
	RTOFS	-0.165	0.291	0.240
	Detrended RTOFS	-0.007	0.249	0.249

**Table 10. The comparison of peak storm surge heights and times of occurrence in both observations and simulations in the regional CFM.**

NOS Station ID	Gauge Peak (m NAVD88)	Time of Gauge Peak (UTC)	L.B.C. Forcing	Model Peak (m NAVD88)	Time of Model Peak (UTC)	Peak Difference	
						Amplitude (m NAVD88)	Phase (min)
8651370	1.716	9/18/2003 16:06	Tide	1.198	9/18/03 18:18	-0.518	126
			Basin-Scale CFM	2.022	9/18/03 18:18	0.306	126
			RTOFS	0.985	9/18/03 17:24	-0.731	78
8652587	1.439	9/19/2003 3:48	Detrended RTOFS	1.100	9/18/03 17:18	-0.616	72
			Tide	0.931	9/19/03 2:06	-0.519	-102
			Basin-Scale CFM	1.147	9/19/03 2:00	-0.303	-108
			RTOFS	0.711	9/19/03 2:18	-0.739	-90
8654400	N/A	N/A	Detrended RTOFS	0.874	9/19/03 2:18	-0.576	-90
			Tide	1.343	9/18/03 18:18		
			Basin-Scale CFM	1.485	9/18/03 18:12	N/A	N/A
			RTOFS	0.860	9/18/03 18:00		
			Detrended RTOFS	1.041	9/18/03 18:00		
8656483	1.121	9/18/2003 18:42	Tide	0.871	9/18/03 18:24	-0.250	-18
			Basin-Scale CFM	1.100	9/18/03 18:24	-0.022	-18
			RTOFS	0.536	9/18/03 17:42	-0.585	-60
			Detrended RTOFS	0.623	9/18/03 17:36	-0.499	-66

\* N/A indicates no data was available for this analysis.



## 7. SUMMARY AND CONCLUSIONS

NOS has been partnering with the NWS in a storm surge project to couple a coastal finite element model with operational weather prediction models. The goal is to improve storm surge simulations over that available from the models independently by combining their different capabilities. NOAA's NWS develops and implements atmosphere and ocean models used for forecast guidance at NCEP's Environmental Modeling Center (EMC). These numerical modeling applications include widely used, large scale atmosphere and ocean models. This suite of developmental and operational models includes meteorological (e.g., the GFDL) and general ocean circulation (e.g., the RTOFS) models which capture hurricane activity.

The CFM (basin-scale and regional) has been developed to predict the impact of storm surge flooding by utilizing a DEM which has a continuous bathy/topo dataset relative to a single referenced datum (i.e., NAVD 88). The 15 m contour was chosen as the landward boundary, since this will allow the CFM to model severe storm surge conditions. Mesh size within sounds ranged between several hundred meters to nearly two kilometers, and rivers were discretized ranging from many nodes across to a pair of elements only 50 m in size.

Wind field comparisons of NDBC observations with H\*Wind, GFDL, and GFS models were performed for Hurricane Isabel. Wind field comparisons considered wind speed and direction at three NDBC buoy locations and two NDBC land locations along the North Carolina coast. Each of the models performed favorably to the observations at all locations; however, there were discrepancies at the time of maximum wind for most of the locations. Blending meteorological models produced the best available wind field in comparison to observations at most of the locations.

Comparison of time series of water surface elevation with observations showed that both versions of the CFM produce reasonable results regardless of meteorological forcing. However, one exception was for H\*Wind at the Oregon Inlet Marina. Because H\*Wind did not provide wind data after landfall, both CFMs did not capture water rise generated inside Pamlico Sound. Blended meteorological forcing resulted in the best performance in maximum peak heights and times of occurrence at most NOS tide gauge locations. Comparison of 160 FEMA CHWMs in North Carolina yielded storm surge model errors of high water marks with a majority of model values within plus or minus 20 percent of FEMA CHWMs.

Applying two cases of lateral boundary conditions from RTOFS indicated that removing the mean dynamic topography improved time series of water surface elevation at all of NOS tide gauge locations. Also, detided time series of water surface elevation produced similar conclusions. These results implied that the mean dynamic topography primarily caused by baroclinicity did not have an effect on the storm surge.

SM, RMSE, and SD in time series of water surface elevation and peak difference in amplitude and phase of peak water level are calculated to evaluate model performances. Considering the total skill assessment, the blended meteorological forcing produced better results than other models in the basin-scale CFM. Also, the lateral boundary condition created by the basin-scale CFM resulted in better skill assessment statistics than other lateral boundary condition forcing.

Future work may include Hurricane Isabel hindcast using the Hurricane Weather and Research Forecasting (HWRF) model (<http://www.emc.ncep.noaa.gov/HWRF/index.html/>), which recently became an operational hurricane model at NCEP. In addition, SSH generated by future versions of RTOFS will continue to be evaluated as a lateral boundary condition in order to evaluate their effectiveness.

## ACKNOWLEDGMENTS

The author would like to acknowledge CSDL's Rich Patchen, Edward Myers, and Jiangtao Xu for their support on final quality control review of this report.

## REFERENCES

- Beven, J. and H. Cobb, 2004: Tropical Cyclone Report, Hurricane Isabel, 6 – 19 September 2003. <http://www.nhc.noaa.gov/2003isabel.shtml> (accessed 22 June 2009).
- Bleck, R., 2002: An Oceanic General Circulation Model Framed in Hybrid Isopycnic-Cartesian Coordinates. **Ocean Modelling**, 4, 55-88.
- FEMA, 2003: Hurricane Isabel Rapid Response Coastal High Water Mark (CHWM) Collection. **Hazard Mitigation Technical Assistance Program, Contract No. EMW-2000-CO-0247, Task Order 272.**
- Feyen, J.C., K.W. Hess, E.A. Spargo, A. Wong, S.A. White, J. Sellars, and S.K. Gill., 2006: Development of a Continuous Bathymetric/Topographic Unstructured Coastal Flooding Model to Study Sea Level Rise in North Carolina. **Proceedings the 9th International Conference on Estuarine and Coastal Modeling**, M.L. Spaulding, editor, 338-356.
- Hess, K.W. and T.F. Gross, R.A. Schmalz, J.G.W. Kelley, III, F. Aikman, E. Wei, and M.S. Vincent, 2003: NOS Standards for Evaluating Operational Nowcast and Forecast Hydrodynamic Model Systems. **NOAA Technical Report NOS CS 17**, 46 pp.
- Hess, K.W., E.A. Spargo, A. Wong, S.A. White, and S.K. Gill, 2005: VDatum for Central Coastal North Carolina: Tidal Datums, Marine Grids, and Sea Surface Topography. **NOAA Technical Report NOS CS 21**, 45 pp.
- Jeffreys, H. and B.S. Jeffreys, 1988: Lagrange's Interpolation Formula. **Methods of Mathematical Physics, 3rd ed.**, Cambridge University Press, Cambridge, England.
- Liu, W.T., K.B. Katsaros, and J.A. Businger, 1979: Bulk Parameterizations of Air–Sea Exchanges of Heat and Water Vapor including the Molecular Constraints at the Interface. **J. Atmos. Sci.**, 36, 1722–1735.
- Luetlich, R.A., J.J. Westerink, and N.W. Scheffner, 1992: ADCIRC: An Advanced Three-Dimensional Circulation Model of Shelves, Coasts, and Estuaries, Report 1: theory and methodology of ADCIRC-2DDI and ADCIRC-3DL. **U.S. Department of the Army, Technical Report DRP-92-6.**
- Luetlich, R.A., J.J., Westerink, and J.C. Muccino, 1994: Modeling Tides in the Western North Atlantic using Unstructured Graded Grids. **Tellus**, 46(A), 178-199.

- Luettich, R.A., J.L. Hensch, C.W. Fulcher, F.E. Werner, B.O. Blanton and J.H. Churchill, 1999: Barotropic Tidal and Wind Driven Larval Transport in the vicinity of a Barrier Island Inlet, **Fisheries Oceanography**, 8(Suppl. 2), 190-209.
- Luettich, R.A. and J.J. Westerink, 2004: Formulation and Numerical Implementation of the 2D/3D ADCIRC Finite Element Model version 44.XX. [http://adcirc.org/adcirc\\_theory\\_2004\\_12\\_08.pdf](http://adcirc.org/adcirc_theory_2004_12_08.pdf) (accessed 22 June 2009).
- Mukai, A.M., J.J. Westerink, R.A. Luettich, Jr., and D. Mark 2001: Eastcoast 2001, A Tidal Constituent Database for Western North Atlantic, Gulf of Mexico and Caribbean Sea. **U.S. Army Corps of Engineers Report ERDC/CHL TR 02-42**, 196pp.
- NOAA, USACE, and FEMA 2005: Hurricane Isabel Assessment: Review of Hurricane Evacuation Study Products and Other Aspects of the National Hurricane Mitigation and Preparedness Program (NHMPP) in the Context of the Hurricane Isabel Response. **Hurricane Planning and Impact Assessment Reports**, NOAA Coastal Services Center, Charleston, SC.
- Powell, M.D., S.H. Houston, and T.A. Reinhold, 1996a: Hurricane Andrew's Landfall in South Florida Part I: Standardizing Measurements for Documentation of Surface Wind Fields. **Weather Forecast.**, 11, 304-328.
- Powell, M.D., S.H. Houston, and T.A. Reinhold, 1996b: Hurricane Andrew's Landfall in South Florida Part II: Surface Wind Fields and Potential Real-Time Applications. **Weather Forecast.**, 11, 329-349.
- Powell, M.D. and T.A. Reinhold, 2007: Tropical Cyclone Destructive Potential by Integrated Kinetic Energy. **Bull. Amer. Meteo. Soc.**, 87, 513-526.
- Reid R.O., 1990: Tides and Storm Surge. **Handbook of Coastal and Ocean Engineering**, 533-590. Gulf Publishing Company, Houston TX.
- Resio, D., S. Bratos, and E. Thompson, 2006: Meteorology and Wave Climate. **Coastal Engineering Manual**, Part II, Hydrodynamics, Chapter II-2, Engineer Manual 1110-2-1100, Vincent, L., and Demirbilek, Z. (editors), U.S. Army Corps of Engineers, Washington, DC.
- Schureman, P., 1958: Manual of Harmonic Analysis and Prediction of Tides. **U.S. Department of Commerce Coast and Geodetic Survey Special Publication No. 98**, 317pp
- Schwiderski, E.W., 1980: On Charting Global Ocean Tide. **Reviews of Geophysics and Space Physics**, 18(1), 243-268.
- Shaffer, W., 2007: Personal Communication.
- Spargo, E.A. and J.W. Woolard, 2005: VDatum for the Calcasieu River from Lake Charles to the Gulf of Mexico, Louisiana: Tidal Datum Modeling and Population of the Grid. **NOAA Technical Report NOS CS 19**, 25 pp.

- Spargo, E.A., K.H. Hess, and S.A. White, 2006: VDatum for the San Juan Islands and the Strait of Juan de Fuca with Updates for Puget Sound: Tidal Datum Modeling and Population of the Grids. **NOAA Technical Report NOS CS 25**, 50 pp.
- Spindler, T., I. Rivin, L. Burroughs and C. Lozano, 2006: NOAA Real-Time Ocean Forecasting System RTOFS – (Atlantic). **NOAA/NWS/NCEP Technical Procedure Bulletin MMAB 2006-02**.
- Tolman, H. L., J. H. G. M. Alves and Y. Y. Chao, 2004: A Review of Operational Forecasting of Wind Generated Waves by Hurricane Isabel at NCEP. **NOAA / NWS / NCEP / MMAB Technical Note Nr. 235**, 45 pp.
- Westerink, J.J., R.A. Luettich, J.C. Feyen, J.H. Atkinson, C.N. Dawson, M.D. Powell, J.P. Dunion, H.J. Roberts, E.J. Kubatko, and H. Pourtaheri, 2008: A Basin- to Channel-Scale Unstructured Grid Hurricane Storm Surge Model Applied to Southern Louisiana. **Monthly Weather Review**. Volume 136, 833-864.
- White S.A. and J. Sellars., 2004: Creation of the Digital Elevation Model for the North Carolina Sea Level Rise Project. **Unpublished Report**, National Geodetic Survey, NOAA, Silver Spring, MD.
- Zhang A., K.H. Hess, E. Wei, and E.P. Myers, 2006: Implementation of Model Skill Assessment Software for Water Level and Currents. **NOAA Technical Report NOS CS 24**, 61 pp.



## APPENDIX A. FEMA Coastal High Water Marks

Table A.1. FEMA CHWMs in the study area (An undefined value is identified as 999).

No.	Latitude	Longitude	Flood Elevation [m NAVD88]	Historical Mark
1	35.534	-76.615	1.7	ISA-03-1011
2	35.537	-76.610	1.7	ISA-03-1012
3	35.549	-76.628	1.7	ISA-03-1013
4	35.552	-76.641	1.7	ISA-03-1014
5	35.548	-76.607	1.6	ISA-03-1015
6	35.560	-76.576	1.6	ISA-03-1016
7	35.534	-76.547	1.6	ISA-03-1017
8	35.531	-76.536	1.7	ISA-03-1018
9	35.519	-76.648	1.6	ISA-03-1019
10	35.509	-76.664	1.6	ISA-03-1020
11	35.499	-76.687	1.5	ISA-03-1021
12	35.574	-76.662	1.6	ISA-03-1022
13	35.339	-76.694	2.1	ISA-03-1109
14	35.346	-76.667	1.3	ISA-03-1110
15	35.324	-76.627	1.5	ISA-03-1111
16	35.377	-76.749	1.5	ISA-03-1112
17	35.428	-76.740	1.2	ISA-03-1113
18	35.397	-76.609	1.7	ISA-03-1114
19	35.401	-76.634	3.0	ISA-03-1115
20	35.402	-76.633	1.6	ISA-03-1116
21	35.448	-76.606	1.6	ISA-03-1117
22	36.212	-76.041	1.3	Floyd-0001
23	36.290	-76.148	1.7	Floyd-0002
24	36.212	-76.041	0.9	ISA-03-0001
25	36.255	-76.097	1.7	ISA-03-0002
26	36.279	-76.116	1.3	ISA-03-0003
27	36.290	-76.148	1.0	ISA-03-0004
28	35.004	-76.314	2.4	ISA-03-0623
29	34.993	-76.309	2.2	ISA-03-0624
30	34.808	-76.457	1.8	ISA-03-0625
31	34.846	-76.755	2.5	ISA-03-0702
32	34.827	-76.637	1.1	ISA-03-0721
33	34.808	-76.631	0.9	ISA-03-0722
34	34.790	-76.604	1.1	ISA-03-0723
35	35.018	-76.315	1.9	ISA-03-1122
36	34.984	-76.300	2.2	ISA-03-1123
37	34.886	-76.332	2.3	ISA-03-1124
38	34.877	-76.390	2.1	ISA-03-1125
39	34.845	-76.420	1.9	ISA-03-1126
40	34.843	-76.753	999	ISA-03-NF06
41	34.868	-76.758	2.8	ISA-03-0700
42	34.894	-76.766	2.4	ISA-03-0703
43	34.907	-76.763	2.4	ISA-03-0704
44	34.881	-76.762	2.6	ISA-03-0705
45	34.921	-76.728	2.2	ISA-03-0706
46	34.939	-76.715	2.7	ISA-03-0707
47	34.899	-76.686	2.3	ISA-03-0708
48	34.917	-76.752	2.6	ISA-03-0709

49	34.953	-76.708	2.9	ISA-03-0710
50	34.956	-76.689	2.7	ISA-03-0711
51	34.946	-76.672	2.3	ISA-03-0712
52	34.875	-76.767	2.5	ISA-03-0713
53	34.926	-76.785	3.7	ISA-03-0714
54	34.936	-76.811	2.4	ISA-03-0715
55	34.918	-76.853	1.2	ISA-03-0716
56	34.906	-76.916	2.0	ISA-03-0717
57	34.937	-76.938	2.0	ISA-03-0718
58	34.969	-76.925	3.1	ISA-03-0719
59	34.984	-76.948	2.4	ISA-03-0720
60	35.267	-75.519	2.6	ISA-03-0400
61	35.229	-75.629	2.7	ISA-03-0401
62	35.229	-75.626	3.1	ISA-03-0402
63	35.222	-75.654	1.9	ISA-03-0403
64	35.585	-75.462	2.4	ISA-03-0404
65	35.599	-75.464	3.8	ISA-03-0405
66	35.216	-75.674	3.2	ISA-03-0406
67	35.209	-75.696	1.6	ISA-03-0407
68	35.216	-75.685	2.1	ISA-03-0408
69	35.224	-75.682	1.1	ISA-03-0409
70	35.606	-75.465	2.6	ISA-03-0410
71	35.329	-75.508	1.1	ISA-03-0500
72	35.289	-75.516	1.5	ISA-03-0501
73	35.344	-75.504	1.3	ISA-03-0502
74	36.034	-75.668	3.9	ISA-03-0503
75	36.047	-75.677	4.9	ISA-03-0504
76	36.057	-75.686	2.7	ISA-03-0505
77	35.909	-75.669	0.7	ISA-03-0506
78	35.920	-75.661	0.6	ISA-03-0507
79	35.867	-75.573	3.7	ISA-03-0508
80	35.700	-75.742	0.9	ISA-03-0509
81	35.690	-75.737	1.3	ISA-03-0511
82	35.939	-75.705	999	ISA-03-NF07
83	35.107	-75.986	0.9	ISA-03-0622
84	35.406	-76.329	2.1	ISA-03-1000
85	35.421	-76.317	1.7	ISA-03-1001
86	35.406	-76.307	1.6	ISA-03-1002
87	35.408	-76.264	0.8	ISA-03-1003
88	35.391	-76.314	2.2	ISA-03-1004
89	35.407	-76.245	0.9	ISA-03-1005
90	35.427	-76.307	1.3	ISA-03-1006
91	35.403	-76.338	2.3	ISA-03-1007
92	35.395	-76.326	2.2	ISA-03-1008
93	35.413	-76.339	2.1	ISA-03-1009
94	35.431	-76.350	1.5	ISA-03-1010
95	35.465	-76.490	1.3	ISA-03-1023
96	35.481	-76.459	1.1	ISA-03-1024
97	35.449	-76.459	1.3	ISA-03-1025
98	35.434	-76.449	1.9	ISA-03-1026
99	35.429	-76.466	1.7	ISA-03-1027
100	35.424	-76.483	1.4	ISA-03-1028
101	35.495	-76.452	1.6	ISA-03-1029
102	35.503	-76.512	1.5	ISA-03-1030
103	35.448	-76.487	1.2	ISA-03-1031

104	35.432	-76.506	1.5	ISA-03-1032
105	35.461	-76.545	1.6	ISA-03-1033
106	35.463	-76.444	1.5	ISA-03-1034
107	35.462	-76.376	1.4	ISA-03-1035
108	35.480	-76.011	1.3	ISA-03-1222
109	35.439	-76.070	1.4	ISA 03-1223
110	35.113	-75.965	999	ISA-03-NF48
111	35.119	-75.974	999	ISA-03-NF49
112	34.973	-76.792	2.6	ISA-03-0611
113	34.971	-76.817	2.4	ISA-03-0612
114	34.999	-76.860	2.8	ISA-03-0613
115	35.027	-76.866	2.3	ISA-03-0614
116	35.022	-76.898	3.0	ISA-03-0615
117	35.022	-76.899	3.0	ISA-03-0616
118	35.056	-76.916	2.1	ISA-03-0617
119	34.998	-76.736	2.5	ISA-03-0800
120	35.020	-76.706	2.2	ISA-03-0801
121	35.028	-76.689	2.4	ISA-03-0802
122	35.087	-76.636	2.2	ISA-03-0803
123	35.095	-76.631	2.1	ISA-03-0804
124	35.096	-76.606	2.1	ISA-03-0805
125	35.124	-76.618	2.0	ISA-03-0806
126	35.144	-76.631	2.0	ISA-03-0807
127	35.161	-76.666	2.0	ISA-03-0808
128	35.146	-76.690	2.1	ISA-03-0809
129	35.146	-76.690	3.0	ISA-03-0810
130	35.138	-76.723	2.0	ISA-03-0811
131	35.137	-76.745	2.1	ISA-03-0812
132	35.158	-76.736	2.0	ISA-03-0814
133	35.183	-76.663	2.0	ISA-03-0815
134	35.170	-76.685	2.7	ISA-03-0816
135	35.205	-76.652	2.0	ISA-03-0817
136	35.177	-76.624	2.1	ISA-03-0818
137	35.198	-76.608	2.0	ISA-03-0819
138	35.243	-76.591	1.7	ISA-03-0820
139	35.245	-76.562	1.8	ISA-03-0821
140	35.320	-76.561	1.4	ISA-03-1118
141	35.301	-76.573	1.3	ISA-03-1119
142	35.245	-76.561	1.8	ISA-03-1120
143	35.025	-76.695	2.3	ISA-03-1121
144	35.143	-76.769	999	ISA-03-NF50
145	36.308	-76.213	1.3	Floyd-0003
146	36.308	-76.213	1.4	Floyd-0004
147	36.280	-76.189	1.8	Floyd-0005
148	36.266	-76.175	1.9	Floyd-0006
149	36.242	-76.135	1.7	Floyd-0007
150	36.297	-76.221	1.2	ISA-03-0005
151	36.308	-76.212	1.0	ISA-03-0006
152	36.287	-76.203	1.5	ISA-03-0007
153	36.280	-76.189	1.3	ISA-03-0008
154	36.267	-76.176	1.2	ISA-03-0009
155	36.267	-76.176	1.6	ISA-03-0010
156	36.242	-76.135	1.6	ISA-03-0011
157	36.261	-76.149	999	ISA-03-NF51
158	36.142	-76.342	1.4	ISA-03-0012

159	36.147	-76.380	2.0	ISA-03-0013
160	36.188	-76.432	2.7	ISA-03-0014
161	36.200	-76.464	2.0	ISA-03-0015
162	36.191	-76.468	1.7	ISA-03-0016
163	36.183	-76.466	2.1	ISA-03-0017
164	36.163	-76.437	2.1	ISA-03-0018
165	36.152	-76.414	2.2	ISA-03-0019
166	35.942	-76.349	1.3	ISA-03-1219

## APPENDIX B. HYDRODYNAMIC MODEL PARAMETERS

### B.1. Wind Stress

The wind speeds provided by meteorological models are used to generate wind stress conditions in the ADCIRC model (Luettich and Westerink, 2004). In order to correlate wind speed to wind stress, ADCIRC employs the following formulation,

$$\begin{aligned}\tau_{sx} &= C_d \rho_{air} |W| W_x, \\ \tau_{sy} &= C_d \rho_{air} |W| W_y,\end{aligned}$$

where  $\rho_{air}$  is air density,  $C_d$  is frictional drag coefficient defined  $(0.75 + 0.067 \cdot W) \times 10^{-3}$  as developed by Garrett (1977),  $|W|$  is the magnitude of wind velocity and  $W_x$  and  $W_y$  are components of wind velocity in the  $x$  and  $y$  direction. All wind velocities are taken at the 10 m height above the mean water level.

### B.2. Atmospheric Pressure Gradient

The ADCIRC model converts a pressure gradient to an equivalent water column height through the transformation  $p / \rho_w g$ , where  $p$  is the pressure gradient,  $\rho_w$  is density of sea water, and  $g$  is acceleration due to gravity.

### B.3. ADCIRC Input File (fort.15)

A typical model control file for the hurricane simulations is presented below. Further details on model parameter settings can be found within this abbreviated file.

```
Basin-Scale CFM: 14-day Run    ! 32 CHARACTER ALPHANUMERIC RUN DESCRIPTION
V47.22                        ! 24 CHARACTER ALPHANUMERIC RUN IDENTIFICATION
1                              ! NFOVER - NONFATAL ERROR OVERRIDE OPTION
1                              ! NABOUT - ABBREVIATED OUTPUT OPTION PARAMETER
1                              ! NSCREEN - OUTPUT TO UNIT 6 PARAMETER
0                              ! IHOT - HOT START OPTION PARAMETER
2                              ! ICS - COORDINATE SYSTEM OPTION PARAMETER
0                              ! IM - MODEL RUN TYPE: 0=2DDI, 1=3DL(VS), 2=3DL(DSS)
2                              ! NOLIBF - NONLINEAR BOTTOM FRICTION OPTION
2                              ! NOLIFA - OPTION TO INCLUDE FINITE AMPLITUDE TERMS
1                              ! NOLICA - OPTION TO INCLUDE CONVECTIVE ACCELERA
1                              ! NOLICAT - OPTION TO CONSIDER TIME DERIVATIVE
0                              ! NWP - VARIABLE BOTTOM FRICTION AND LATERAL VISCO
1                              ! NCOR - VARIABLE CORIOLIS IN SPACE OPTION
1                              ! NTIP - TIDAL POTENTIAL OPTION PARAMETER
-5                             ! NWS - WIND STRESS AND BAROMETRIC PRESSURE OPTION
1                              ! NRAMP - RAMP FUNCTION OPTION
9.81000                       ! G - ACCELERATION DUE TO GRAVITY - DETERMINES
-3                             ! TAU0 - WEIGHTING FACTOR IN GWCE
```

```

0.005 0.2          ! TAU0FULLDOMAINMIN, TAU0FULLDOMAINMAX
2.00000           ! DT - TIME STEP (IN SECONDS)
0.00000           ! STATIM - STARTING SIMULATION TIME IN DAYS
0.00000           ! REFTIME - REFERENCE TIME (IN DAYS)
3600              ! WTIMINC - METEOROLOGICAL WIND TIME INTERVAL
14.00000          ! RNDAY - TOTAL LENGTH OF SIMULATION (IN DAYS)
4.00000           ! DRAMP - DURATION OF RAMP FUNCTION (IN DAYS)
0.350000 0.300000 0.350000 ! TIME WEIGHTING FACTORS FOR THE GWCE EQUATION
0.010000 0 0 0.010000 ! H0, NODEDRYMIN, NODEWETMIN, VELMIN - MINIMUM
-79.000000 35.000000 ! SLAM0, SFEA0 - LONGITUDE AND LATITUDE
0.002500 1.00 10.00 0.333330 ! FFACTORMIN, HBREAK, FTHETA, FGAMMA - BOTTOM FRIC
5.000000          ! EVM - SPATIALLY CONSTANT HORIZONTAL EDDY VISCO
0.000000          ! CORI - CONSTANT CORIOLIS COEFFICIENT
5                 ! NTIF - NUMBER OF TIDAL POTENTIAL CONSTITUENTS
K1                ! TIPOTAG - NAME OF TIDAL POTENTIAL CONSTITUENT
0.14156500 0.000072921158358 0.736 1.077 249.170 ! TPK, AMIGT, ETRF, FFT, FACET - CONST
O1                ! TIPOTAG - NAME OF TIDAL POTENTIAL CONSTITUENT
0.10051400 0.000067597744151 0.695 1.125 215.130 ! TPK, AMIGT, ETRF, FFT, FACET - CONST
M2                ! TIPOTAG - NAME OF TIDAL POTENTIAL CONSTITUENT
0.24233400 0.000140518902509 0.693 0.978 101.610 ! TPK, AMIGT, ETRF, FFT, FACET - CONST
S2                ! TIPOTAG - NAME OF TIDAL POTENTIAL CONSTITUENT
0.11284100 0.000145444104333 0.693 1.000 0.000 ! TPK, AMIGT, ETRF, FFT, FACET - CONST
N2                ! TIPOTAG - NAME OF TIDAL POTENTIAL CONSTITUENT
0.04639800 0.000137879699487 0.693 0.979 40.750 ! TPK, AMIGT, ETRF, FFT, FACET - CONST
5                 ! NBFR - NUMBER OF PERIODIC FORCING FREQUENCIES
K1                ! BOUNTAG - FORCING CONSTITUENT NAME
0.000072921158358 1.077 249.170
O1                ! BOUNTAG - FORCING CONSTITUENT NAME
0.000067597744151 1.125 215.130
M2                ! BOUNTAG - FORCING CONSTITUENT NAME
0.000140518902509 0.978 101.610
S2                ! BOUNTAG - FORCING CONSTITUENT NAME
0.000145444104333 1.000 0.000
N2                ! BOUNTAG - FORCING CONSTITUENT NAME
0.000137879699487 0.979 40.750
K1                ! EALPHA - FORCING CONSTITUENT NAME AGAIN
0.095800 241.020 ! EMO, EFA
0.095800 241.020 ! EMO, EFA
:
:
This portion of the input has been eliminated
:
:
0.087300 85.720 ! EMO, EFA
0.087300 85.720 ! EMO, EFA
O1                ! EALPHA - FORCING CONSTITUENT NAME AGAIN
0.081900 230.730 ! EMO, EFA
0.081900 230.730 ! EMO, EFA
:
:
This portion of the input has been eliminated
:
:
0.061000 331.610 ! EMO, EFA
0.061000 331.610 ! EMO, EFA
M2                ! EALPHA - FORCING CONSTITUENT NAME AGAIN
0.461400 220.790 ! EMO, EFA
0.461400 220.790 ! EMO, EFA
:
:
This portion of the input has been eliminated

```

```

:
0.502300 345.330      ! EMO, EFA
0.502300 345.330      ! EMO, EFA
S2                    ! EALPHA - FORCING CONSTITUENT NAME AGAIN
0.162700 267.410      ! EMO, EFA
0.162700 267.410      ! EMO, EFA
:
:
This portion of the input has been eliminated
:
:
0.136100 17.760       ! EMO, EFA
0.136100 17.760       ! EMO, EFA
N2                    ! EALPHA - FORCING CONSTITUENT NAME AGAIN
0.100300 196.500      ! EMO, EFA
0.100300 196.500      ! EMO, EFA
:
:
This portion of the input has been eliminated
:
:
0.117200 323.680      ! EMO, EFA
0.117200 323.680      ! EMO, EFA
110                   ! ANGINN - MINIMUM ANGLE FOR TANGENTIAL FLOW
-1 0.000000 14.000000 180 ! NOUTE, TOUTSE, TOUTFE, NSPOOLE - FORT 61 OPTIONS
170                   ! NSTAE - NUMBER OF ELEVATION RECORDING STATIONS,
-75.739410 36.183532  ! 8651370 Duck, FRF, Pier, NC
-75.551568 35.790577  ! 8652587 Oregon Inlet Marine, Pamlico Sound, NC
-75.634436 35.215867  ! 8654400 Cape Hatteras Fishing Pier, NC
-76.670699 34.719819  ! 8656483 Beaufort Duke Marine Lab, NC
-76.614700 35.534300  ! 5.60 FEMA CHWMs
-76.609800 35.537400  ! 5.50 FEMA CHWMs
:
:
This portion of the input has been eliminated
:
:
-76.414300 36.151500  ! 7.20 FEMA CHWMs
-76.349200 35.941700  ! 4.20 FEMA CHWMs
0 0.000000 20.000000 180 ! NOUTV, TOUTSV, TOUTFV, NSPOOLV - FORT 62 OPTIONS
0                       ! NSTAV - NUMBER OF ELEVATION RECORDING STATIONS, -1
0.000000 14.000000 300 ! NOUTM, TOUTSM, TOUTFM, NSPOOLM - METEOROLOGICAL
5                       ! NSTAM - NUMBER OF ELEVATION RECORDING STATIONS,
-75.750000 36.180000  ! DUCN7
-74.840000 36.610000  ! 44014
-72.660000 34.680000  ! 41001
-76.520000 34.620000  ! CLKN7
-75.350000 32.310000  ! 41002
-1 9.000000 14.000000 1800 ! NOUTGE, TOUTSGE, TOUTFGE, NSPOOLGE - (UNIT 63)
-1 9.000000 14.000000 1800 ! NOUTGV, TOUTSGV, TOUTFGV, NSPOOLGV - (UNIT 64)
-1 9.000000 14.000000 1800 ! NOUTGM, TOUTSGM, TOUTFGM, NSPOOLGM - (UNIT 73/74)
0                       ! NHARF - NUMBER OF FREQUENCIES IN HARMONIC ANA
0.000000 0.000000 0 0.000000 ! THAS, THAF, NHAINC, FMV - HARMONIC ANALYSIS PARA
0 0 0 0                 ! NHASE, NHASV, NHAGE, NHAGV - UNITS 51,52,53,54
0 8640                 ! NHSTAR, NHSINC - HOT START FILE GENERATION PARA
1 0 0.000001 25       ! ITITER, ISLDIA, CONVCR, ITMAX - ALGEBRAIC SOLUTION

```